AtHaspin, a putative histone H3-specific kinase in *Arabidopsis thaliana*?

Dissertation

zur Erlangung des akademischen Grades

doctor rerum naturalium (Dr. rer. nat.)

vorgelegt der
Mathematisch-Naturwissenschaftlich-Technischen Fakultät
(mathematisch-naturwissenschaftlicher Bereich)
der Martin-Luther-Universität Halle-Wittenberg

von Frau Raheleh Karimi Ashtiyani
geb. am 16.09.1979 in Teheran, Iran

HALLE (SAALE)

ACKNOWLEDGMENT

I am very grateful to my supervisor Dr. Andreas Houben for giving me the opportunity to work in his group (Chromosome Structure and Function), continuous support and guidance, permanent encouragement and invaluable effort in correcting this thesis.

I thank Dr. Twan Rutten for the great help with the confocal microscopy and Dr. Annegret Tewes for help in preparing transformed tobacco plants.

Many thank to Prof. Dr. Gerd Jurgens for giving me the opportunity to work in his Lab.

I would like to appreciate our group technicians Oda Weiss, Katrin Kumke and Margit Hantschmann for their perfect technical assistance.

Many Thanks to Richard Pickering for helpful suggestion and valuable help in correcting my thesis.
Thanks to members of CSF group specially Dr. Dimitri Demidov for their helpful discussions and creating the nice scientific atmosphere in the lab.

Special thank also to Ali for continuous support, encouragement and helpful suggestions.

با نهایت سپاس و درود این پایان نامه را به مادر عزیز و مهربانم به خاطر عشق و ایثارش، به پدر بزرگوارم به خاطر صبر و همت بلندش، به برادر عزیزم، امین و به خواهر مهربانم، انسیه و به علی که بی دریغ همراه و همدل من بوده و هست تقدیم می‌کنم. چرا که هر گونه موفقیتی را در زندگی مدیون زحمات این عزیزانم.

Content

Abbreviations

ATP	adenosine tri-phosphate
BLAST	basic local alignment search tool
bp	base pair
BSA	bovine serum albumin
CDK	ayclin-dependent protein kinases
cDNA	aomplementary aeoxyribonucleic acid
CENP-A	centromere protein A
Col-0	columbia-0
DAPI	4',6-diamidino-2-phenylindole
DNA	deoxyribonucleic acid
DTT	dithiothreitol
EDTA	ethylenediaminetetraacetic acid
EF	elongation factor
ePKs	eukaryotic protein kinase superfamily
FITC	fluorescein isothiocyanate
GFP	green fluorescent protein
GTP	guanosine 5'-triphosphate
GUS	Beta-glucuronidase
h	hour
Haspin	haploid germ cell-specific nuclear protein
H3	histone H3
H4	histone H4
H2A	histone H2A
H2B	histone H2B
HCl	hydrochloride acid
Hyg	hygromycin
Kan	kanamycin
kb	kilo base
kDa	kiloDaltons

LB medium	luria-bertani broth medium
Mg	magnesium
ml	milliliter
mM	millimolar
mRNA	messenger ribonucleic acid
MS medium	Murashige and Skoog medium
NaCl	sodium chloride
NaOH	sodium hydroxide
PAT	polar auxin transport
PBS	phosphate buffered saline
PCR	polymerase chain reaction
PPT	DL-Phosphinotricin (Glufosinate ammonium)
RNA	ribonucleic acid
RNAi	RNA interference
rpm	revolutions per minute
RT	room temperature
RT-PCR	reverse transcription polymerase chain reaction
S10	serine 10
S28	serine 28
SDS	sodium dodecyl sulfate
siRNA	small interfering RNA
SSC	saline-sodium citrate
Thr3	Threonine 3
Thr11	Threonine 11
T-DNA	transferred DNA
Tris	tris(hydroxymethyl)aminomethane
UTR	untranslated region
WT	wild type
YFP	yellow fluorescent protein (microscopy)
ºC	centigrade
µl	microlitre
µg	microgram

List of figures

12

empty control vector did not result in YFP signals in the vascular system of the stem (R). In pistils, expression is detected in the vascular tissue of style and septum (G) and in the funiculus of fertilized ovules (K). YFP localisation in seed endosperm (J) and leaf epidermal cells (P) revealed that AtHaspin is a cytosolic protein. In contrast, YFP signals of empty 35S::YFP mutant plants were observed in the nucleus (arrow) of epidermal cells (O) and of root tips (L). (N) Strong signals were observed in the shoot apex region of the analysed 35S::YFP-AtHaspin seedlings. (S) Wavelength of YFP signals was validated by confocal microscopy around 527nm. (T) Western blot analysis on 35S:YFP-AtHaspin plants revealed corresponding YFP-AtHaspin protein bands (arrow)……………………………………………………………………………73

List of tables

1. Introduction

1.1. Chromatin structure

Chromatin is a complex of DNA, histones, and non-histone proteins found in the nucleus of an eukaryotic cell (Alberts et al., 2002). DNA in chromatin is compacted over 10000- fold compared to its straight form. Importantly the structure of chromatin permits localised decondensation and repackaging to facilitate the processes of replication, transcription and repair (Elgin and Workman, 2002). The structure of chromatin varies considerably as the cell progresses through the cell cycle. The changes in structure are required to allow the DNA to be used and managed, whilst minimizing the risk of damage. The cell cycle-dependent transition from decondensed interphase chromatin to condensed metaphase chromatin, and *vice versa*, is the most obvious dynamic change in the chromatin structure.

The basic unit of chromatin is the nucleosome core particle, which contains 146 bp of DNA wrapped nearly twice around an octamer of core histones. The histone octamer is composed of a central heterotetramer of histones H3 and H4, flanked by two heterodimers of H2A and H2B (Kornberg, 1974; Luger et al., 1997; Peterson and Laniel, 2004). Histones are the major proteins involved in chromatin, which are highly conserved and regulate many cellular events, including transcription, DNA replication, recombination and repair (Bottomley, 2004). Each core histone is composed of a structured domain and an unstructured amino-terminal 'tail' of 25-40 residues. Post-translational modifications of histone tails regulate transcription and chromatin structure and have a critical role in the dynamic condensation/decondensation that occurs during the cell cycle (Wu and Grunstein, 2000; Felsenfeld and Groudine, 2003; Prigent and Dimitrov, 2003).

1.2. Post transcriptional histone modifications

The core histone tails are subject to an enormous number of posttranscriptional modifications, including acetylation and methylation of lysines (K) and arginines (R), phosphorylation of

serines (S) and threonines (T), ubiquitination and sumoylation of lysines, as well as ADP-ribosylation (Grant, 2001; Zhang and Reinberg, 2001; Peterson and Laniel, 2004). These modifications of the N-terminal tails of the core histones with DNA methylation control the folding of the nucleosomal array into higher order structure and mediate signalling for cellular processes. Thus, in many ways histone tails can be viewed as complex protein-protein interaction surfaces that are regulated by numerous post-translational modifications.

The first-studied of covalent histone modification was histone acetylation (Brownell et al., 1996; Grunstein, 1997). Acetylation and methylation of different lysine (Lys) and arginine residues in histones H3 and H4 have been extensively correlated with transcriptionally active or transcriptionally repressed states of gene expression and heterochromatin formation (Richards and Elgin, 2002; Fischle et al., 2003), while phosphorylation of histone tails has been linked to chromosome condensation/segregation, activation of transcription, apoptosis and DNA damage repair (Cheung et al., 2000).

Combinations of histone modifications are thought to constitute a code, the so-called "histone code". Although histones and their modifications are highly conserved, the chromosomal distribution of individual modifications can differ along the cell cycle as well as among and between groups of eukaryotes, emphasizing the important role of histones in the biology of the nucleus and the possibility of evolutionary divergence in reading the "histone code" (reviewed in (Fuchs et al., 2006)).

1.3. Cell-cycle dependent phosphorylation of histone H3

The cell cycle-dependent transition from decondensed interphase chromatin to condensed metaphase chromatin, and *vice versa*, is the most obvious dynamic change in chromatin structure. Early observations in several eukaryotes have shown that the level of H3 phosphorylation, which is minimal in interphase, increases substantially at the beginning of the prophase and decreases again during telophase (Gurley et al., 1975; Gurtley et al., 1975; Gurley et al., 1978; Hendzel et al., 1997).

In non-plant eukaryotes consistent with the initiation of the chromatin condensation, histone H3 phosphorylation at Ser10 primarily begins in pericentromeric heterochromatin at G2 and

spreads over the whole chromosome arms, becomes maximal at condensed metaphase chromatin and diminishes during late anaphase and early telophase (Gurley et al., 1978; Hendzel et al., 1997; Van Hooser et al., 1998). In addition, Goto et al. (1999) were able to demonstrate another cell-cycle dependent phosphorylation of H3 at serine position 28 which is initiated specifically during early mitosis and correlated closely with mitotic chromosome condensation.

However, there are remarkable differences in the chromosomal distribution of phosphorylated histone H3 between animal and plant cells. In plant mitotic cells, phosphorylation of histone H3 at serine 10 (Houben et al., 1999; Kaszas and Cande, 2000; Manzanero et al., 2000) and serine 28 (Gernand et al., 2003) which starts in late prophase and becomes maximal at metaphase and disappears at telophase correlates with the position of the pericentromere. Interestingly distribution of histone H3 at serine 10 and 28 varies between two meiotic divisions. During the first division the chromosomes are highly phosphorylated throughout their entire length, while pericentromeric regions are the major sites of histone H3 phosphorylation during meiosis II and mitosis (Kaszas and Cande, 2000; Manzanero et al., 2000; Gernand et al., 2003). Surprisingly, at the same time, single chromatids resulting from equational division of univalents at anaphase I revealed no detectable phosphorylated H3 at the second meiotic division (Manzanero et al., 2000). These observations and further experiments in maize mutant defected in sister chromatid cohesion (Kaszas and Cande, 2000) revealed that in plants H3 phosphorylation is involved in maintenance of sister chromatid cohesion.

Phosphorylation of H3 at threonine 3 and 11 is restricted to the mitotic cells as well. However, their patterns are mainly different from that of serine 10 and 28 phosphorylation. In none-plant species, Thr11 and Thr3 phosphorylation is most abundant in the centromere regions, it may serve as a recognition code for centromere assembly (Tanaka, 1999; Preuss et al., 2003; Polioudaki et al., 2004; Dai and Higgins, 2005). In contrast to animal cells, in plants phosphorylation at Thr11 occurs along entire chromosome arms, and correlates with the condensation of mitotic and meiotic chromosomes (Houben et al., 2005).

Phosphorylation at Thr3 begins from prophase, as chromosomes start to condense. In late prophase stage phosphorylation dispersed along chromosome arms and it is maintained until

anaphase. However, there are remarkable differences in the chromosomal distribution of H3Thr3ph between mitosis and the first and second meiotic divisions. In contrast to the mitotic and first meiotic division where phosphorylation of H3 at Thr3 occurs along the entire length of chromosomes, at the second meiotic division phosphorylation is restricted to the pericentromeric regions (Caperta et al., 2008) (Fig. 1).

In general, in non-plant eukaryotes there is a precise spatial and temporal correlation between the cell-cycle dependent phosphorylation of H3 at serine position Ser10 and Ser28 (Goto et al., 1999) and the processes of chromosome condensation (Hendzel et al., 1997; Van Hooser et al., 1998), and phosphorylation at Thr3 and Thr11 are involved in kinetochore function ((Preuss et al., 2003; Polioudaki et al., 2004; Dai et al., 2005). However, in plants, mitotic H3 phosphorylation at both serine positions seems to be involved in sister chromatid cohesion and Thr3 and Thr11 correlates with the chromosome condensation (Houben et al., 2005; Caperta et al., 2008). In addition, to a cell cycle-related function, studies in *Chlamydomonas reinhardtii* indicate that histone H3Thr3 phosphorylation also is involved in transcription regulation and in heritable gene silencing (Casas-Mollano et al., 2008).

	DAPI	H3S28ph	H3T3ph	merge
mitosis	interphase (a)			
	prophase (b)			
	metaphase (c)			
	anaphase (d)			
meiosis	metaphase I (e)			
	metaphase II (f)			
	anaphase II (g)			

20
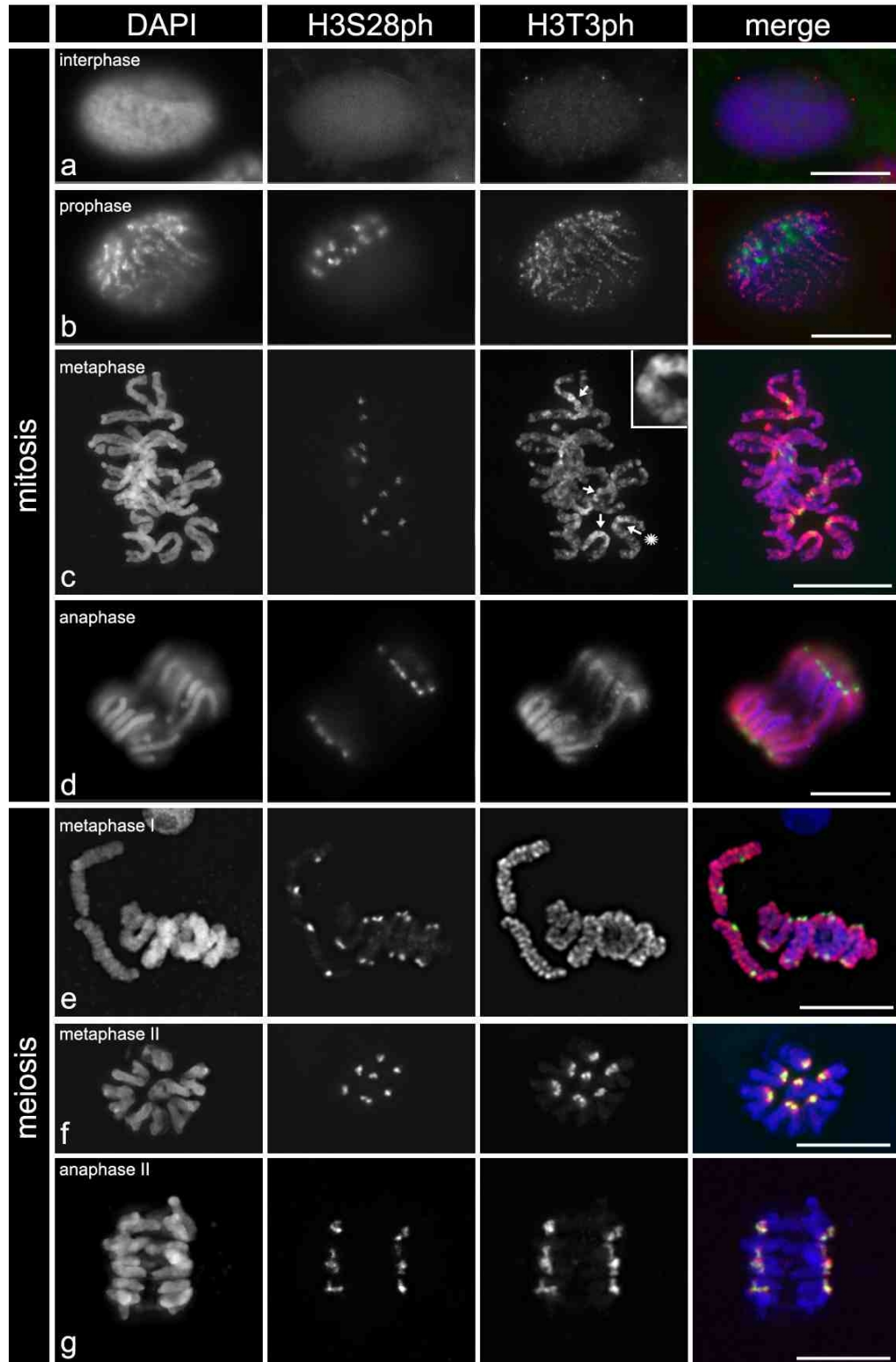
Fig. 1. Immunodetection of phosphorylated histone H3 at Thr 3 (H3T3ph, in red) and Ser 28 (H3S28ph, in green) in somatic cells (**a-d**) and meiocytes (**e-g**) of *Secale cereale.*

1.4. Protein kinases

Phosphorylation of protein on serine, threonine, and tyrosine residues is controlled by protein kinases, which are a group of enzymes that transfer a phosphate group from the donor ATP or GTP to specific serine, threonine, or tyrosine residues in specific substrate proteins (Higgins, 2001a; Ferrari, 2006). This process of reversible phosphorylation modulates the function of a huge variety of substrates, including metabolic enzymes, transcription factors, adapter molecules, and other kinases. Thus, protein kinases are critical in the activity of the eukaryotic cells, including cellular proliferation, gene expression, metabolism, motility, membrane transport, hormone responses, and apoptosis (Higgins, 2001a; Hanks, 2003).

Protein kinases can be classified into many families including prokaryotic bacteria and archaea families and eukaryotic-type protein kinase like yeast, worm, fly and human families (Leonard et al., 1998; Manning et al., 2002). The eukaryotic protein kinase superfamily (ePKs) is the most known protein kinase in eukaryotes, which consists of 250-300 amino acids as a catalytic domain, comprising 12 sub-domains (regions I-XI in Fig. 2) of highly conserved residues required for ATP binding and substrate phosphorylation. The crystal structure of a number of ePK domains revealed a common bi-lobed structure, where the smaller N-terminal lobe (regions I-V) contains conserved residues required for nucleotide binding, whereas the larger C-terminal lobe (regions V-XI) is involved in substrate binding and phosphotransfer initiation. The cleft between the lobes contains further invariant amino acids that form the active site, which accommodates ATP (Fig. 2) (Hanks and Hunter, 1995; Ferrari, 2006).

Identification and classification of the members of the ePK superfamily in different species led to the classification of 510 potentially unique human ePKs (Kostich et al., 2002), 115 distinct ePKs from budding yeast (around 2% of all genes), 434 from *Caenorhabditis elegans* (about 2.5% of all genes), 223 from *Drosophila,* (Manning et al., 2002), and 1019 from *Arabidopsis thaliana* (Wang et al., 2003). There are two main subdivisions within the superfamily of ePK: the protein-serine/threonine kinases and the protein-tyrosine kinases.
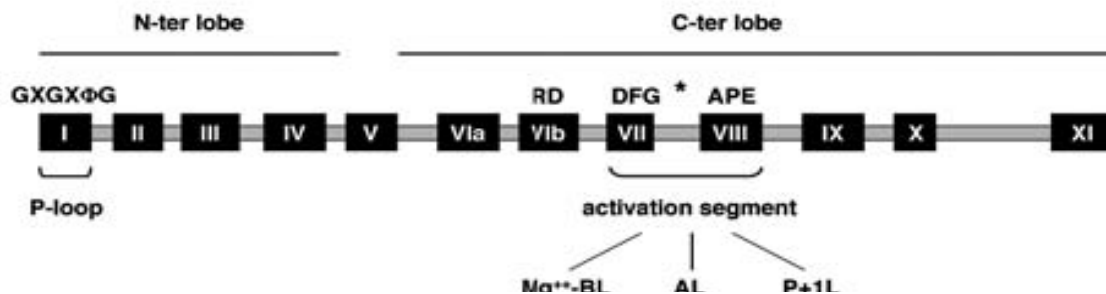
Fig. 2. Structure of a typical eukaryotic protein kinase catalytic domain. The core catalytic domain of protein kinases encompasses 12 subdomains I-IV and VI-XI, participate in the formation of the bi-lobed structure of protein kinases. Binding of Mg-ATP is largely the function of the N-terminal lobe region, while peptide-substrate binding is mediated by the C-terminal lobe (Ferrari, 2006).

1.5. Candidate protein kinases involved in cell-cycle progression

Cyclin-dependent protein kinases (CDK) are a conserved and prominent superfamily of eukaryotic serine/threonine protein kinases, which play a critical role at controlling various checkpoints of the eukaryotic cell cycle (Nigg, 1995; Morgan, 1997; Mendenhall and Hodge, 1998). In eukaryotes, CDK and cyclins form large superfamilies, so that a very large number of CDK-cyclin complexes can occur with various substrates specificity at various locations within the cell and at various time points within the cell cycle (Joubes et al., 2000). Cell-cycle events in the majority of vertebrate eukaryotes are controlled by two CDKs, known as CDK1 and CDK2, which operate primarily in M phase and S phase. Other CDKs play auxiliary cell cycle roles or are not involved in cell cycle regulation (Morgan, 1997).

In diverse plant species, there are large numbers of CDK-like proteins, which are classified into two distinct B-type groups (CycB1, CycB2) and three distinct A-type groups (CycA1, CycA2, CycA3), and three distinct D-type groups (CycD1, CycD2, CycD3) (Renaudin et al., 1996; Mironov et al., 1999). The best characterized plant CDKs belong to the A-type class. This class comprises kinases most closely related to the prototypical CDKs, animal CDK1 and CDK2, which share the conserved motif in the cyclin binding domain (Mironov et al., 1999). Experiments in plants support relevance for cell division control only for the A-type class and CYCB1 (Mironov et al., 1999).

CDKs phosphorylate hundreds of distinct proteins. These CDK substrates are phosphorylated at serine or threonine residues in a specific sequence context that is recognized by the active site of the CDK protein. Activated well understood CDK1-cycline complexes phosphorylate numerous non-histones substrates, for example nuclear lamins, microtubule-binding proteins, condensins and Golgi matrix components. Phosphorylation is important for nuclear envelope breakdown, centrosome separation, spindle assembly, chromosome condensation and Golgy fragmentation (reviewed in (Nigg, 2001)).

Additional mitotic kinases that have been studied are the members of the polo kinase family (e.g. mammalian Plk1), the Aurora family (e.g. mammalian Aurora-A, Aurora B, Aurora-C), the NIMA family (e.g. mammalian Nek2), as well as kinases implicated in mitotic checkpoints (e.g. Bub1, RubR1, TTK/ESK), mitotic exit and cytokinesis, MAP kinases. Their cellular function is to regulate cell division by phosphorylation their substrates in chromatin at the spindle apparatus and to signal the outcome of the various checkpoints (reviewed in (Nigg, 2001)).

1.5.1 Candidate kinases involved in cell cycle-dependent histone H3 phosphorylation

Histone H3 is phosphorylated during mitosis and meiosis *in vivo*, but the identities of the involved kinases remain somewhat uncertain. The best studied kinase is a member of the evolutionarily highly conserved Aurora kinase family. Mammalian Aurora B-like kinases phosphorylate histone H3 at serine 10 (Goto et al., 1999; Hsu et al., 2000; Giet and Glover, 2001; Crosio et al., 2002) and 28 (Goto et al., 1999; Goto et al., 2002) in a cell cycle-dependent manner. It is located to the kinetochores in prophase, and becomes concentrated there until the onset of anaphase before relocalising to the spindle midzone at anaphase (Carmena and Earnshaw, 2003). Consistent with this, Aurora B has both chromatin- and spindle-associated substrates and influences mitosis at a number of steps. It is involved in cytokinesis and required for phosphorylation of the centromeric histone variant CENP-A to regulate the kinetochore assembly (Zeitlin et al., 2001; Hauf et al., 2003).

Three members of plant Aurora-like kinases have been characterized for *A. thaliana* (Demidov et al., 2005; Kawabe et al., 2005), which are divided in two major sub-groups, plant Aurora α and plant Aurora β based on the evolutionary conserved catalytic domains (Demidov et al.,

2005). All three Aurora kinases could phosphorylate serine 10 in histone H3 *in vitro*, and all of them were predominantly expressed in tissues enriched with dividing cells (Demidov et al., 2005; Kawabe et al., 2005).

The cellular localisation studies using Auroras cDNAs::GFP fusion constructs derived by the 35S promoter in cultured tobacco BY-2 cells demonstrate that, in interphase cells, all three Auroras were predominantly located in the nucleus (Demidov et al., 2005; Kawabe et al., 2005). Both AtAurora1–GFP and AtAurora2–GFP fusions associated with the nuclear envelope and with the mitotic structures such as microtubule spindles, and the AtAurora1–GFP signal also appeared at the emerging cell plate during cytokinesis. AtAUR3–GFP, however, exhibited a dot-like pattern on chromosomes, probably at the centromere/kinetochore region (Demidov et al., 2005; Kawabe et al., 2005).

Treatment of BY-2 cells by Aurora inhibitor Hesperadin, indicated that, plant Aurora kinases play roles in correction of aberrant kinetochore–microtubule attachment and dissociation of cohesin during chromosome alignment and segregation (Kurihara et al., 2008; Demidov et al., 2009 (In press)).

NIMA kinase (never in mitosis) was the first described in *Aspergillus nidulans* (Osmani et al., 1991; Osmani and Ye, 1996). Studies in this filamentous fungus suggested that NIMA cooperates with CDk1(also known as Cdc2) at the G2/M transition (Ye et al., 1995) and its activity is required for phosphorylation of H3 serine 10 and chromosome condensation (De Souza et al., 2000). The mammalian genome carries at least eleven NIMA-related kinases, called Nek1–Nek11 (O'Connell et al., 2003). Of these, Nek2 represents the closest structural relative of NIMA (Fry, 2002).

A. thaliana encodes seven NIMA-related genes (AtNek1-AtNek7), *Oryza sativa* encodes six (OsNek1-OsNek6) and the genome of *Populus trichocarpa* encodes at least nine NIMA-related genes (PtNek1-PtNek9) (Cloutier et al., 2005; Vigneault et al., 2007). Ectopic expression of the poplar NIMA-related kinase 1 (PNek1) in *A. thaliana* caused morphological abnormities in flower and siliques. Expression sites of a PNek1 promoter::GUS construct in both poplar and *Arabidopsis* plants corresponded to sites of auxin production and vascular development

(Vigneault et al., 2007). In general all these results suggest a role of PNek1 in organ and tissue development and cell proliferation. In difference, recent studies (Motose et al., 2008; Sakai et al., 2008) showed that AtNek6 plays roles in the control of cellular morphogenesis by association with cortical microtubules, and interacting with Armadillo repeat-containing kinesin-related proteins (ARKs), which might promote the stabilization of endoplasmic microtubules.

The protein haspin (haploid germ cell-specific nuclear protein kinase) was recently indentified in mice and human and reported as a cell cycle-dependent serine/threonine kinase (Tanaka, 1999).

1.6. Haspin-like kinases

Most known protein kinases in eukaryotes are members of the eukaryotic protein kinases (ePKs). Despite of homology of haspin-like proteins with many ePK families they do not fall in any of the previously identified ePK families. They appear to form a unique and distinct family with a subset of previously uncategorized kinase-like proteins from a variety of species. The C-terminal kinase domain, regions VIII through XI in the haspin like proteins appear to lack some of highly conserved residues found in other ePKs, and there is a relative lack of sequence similarity to other ePKs in regions that may play a role in substrate recognition (particularly regions VIII and IX). In contrast, many of the residues that are essentially invariant in other ePKs, and known to be critical in formation the Mg^{2+} -ATP-binding and catalytic sites, are conserved in majority of haspin proteins. Haspins also do not have conserved threonine, serine or tyrosine residues in the activation loops or T-loop between regions VII and VIII. Phosphorylation of residues in this region regulates kinase activity in a number of kinase families (Higgins, 2001a).

The serine/threonine haspin kinase has been identified in mice first by Tanaka (1999). The haspin gene, Germ Cell Specific Gene 2 (Gsg2), has been localised on mouse chromosome 11 (Matsui et al., 1997). The murine haspin was specifically expressed in haploid germ cells, localised in nuclei of round spermatids, and has *in vitro* serine/threonine kinase activity (Tanaka et al., 1999). Ectopic expression of haspin by transfection of mouse cDNA into

cultured somatic cells cause cell cycle arrest at G1, suggesting its role in cell proliferation and dedifferentiation of haploid germ cells (Tanaka et al., 1999).

In 2001, human haspin was isolated and identified by hybridization of a human testicular cDNA library with a mouse haspin cDNA probe (Tanaka et al., 2001). In parallel, Higgins (2001b) identified the human haspin gene within an intron of integrin αE gene by chance while he was investigating the transcriptional complexity at this locus. Human haspin is mapped to the 17p13 region as an intron-less gene. cDNA of human and mouse haspin showed 72% similarity, at protein level 62% identity was found (Tanaka, 1999).

Human haspin transcripts are most abundantly expressed in testis germ cells as well as mouse haspin (Higgins, 2001b; Tanaka et al., 2001). However, mammalian haspin is also transcribed at lower levels in diploid cell lines and tissues like thymus, bone marrow, fetal tissues and all tested proliferated tissues (Higgins, 2001b).

Immunofluorescence detection of myc-tagged haspin and, confocal microscopy on EGFP-haspin cells, revealed that haspin protein localises exclusively in the nucleus during interphase of transfected human cell lines. In fixed mitotic cells haspin was found associated with the condensed chromosomes in prophase through anaphase (Fig. 3) (Tanaka, 1999; Dai et al., 2005). On metaphase chromosomes, it is localised along chromosome arms but concentrated at pericentromeric regions (Fig. 4) (Dai and Higgins, 2005; Dai et al., 2005). In addition to the localisation of haspin on chromosomes, it also appeared at centrosomes and spindle during mitosis (Dai et al., 2005). In general, these data revealed that mammalian haspin has cell cycle-dependent behaviour and associates with condensed chromosomes throughout mitosis. No data are available on the meiotic distribution of any haspin.

In vitro kinase assay experiments confirmed that human haspin has kinase activity and phosphorylates its own serine and threonine residues and it is required for histone H3Thr3 phosphorylation (Dai et al., 2005) as previously shown for murine haspin (Tanaka, 1999).

Further experiments using immunoprecipitates of myc-haspin from transfected cells subjected to *in vitro* kinase assays with purified histones and histone-GST proteins (containing the first 45

residues of histone H3 fused to the N terminus of GST to preserve the normal orientation of the tail) as exogenous substrates, confirmed that haspin specifically phosphorylates histone H3 *in vitro.* A series of histone H3-GST point mutations and the use of phospho-specific antibodies demonstrated the phosphorylation site as threonine 3 (Dai et al., 2005).
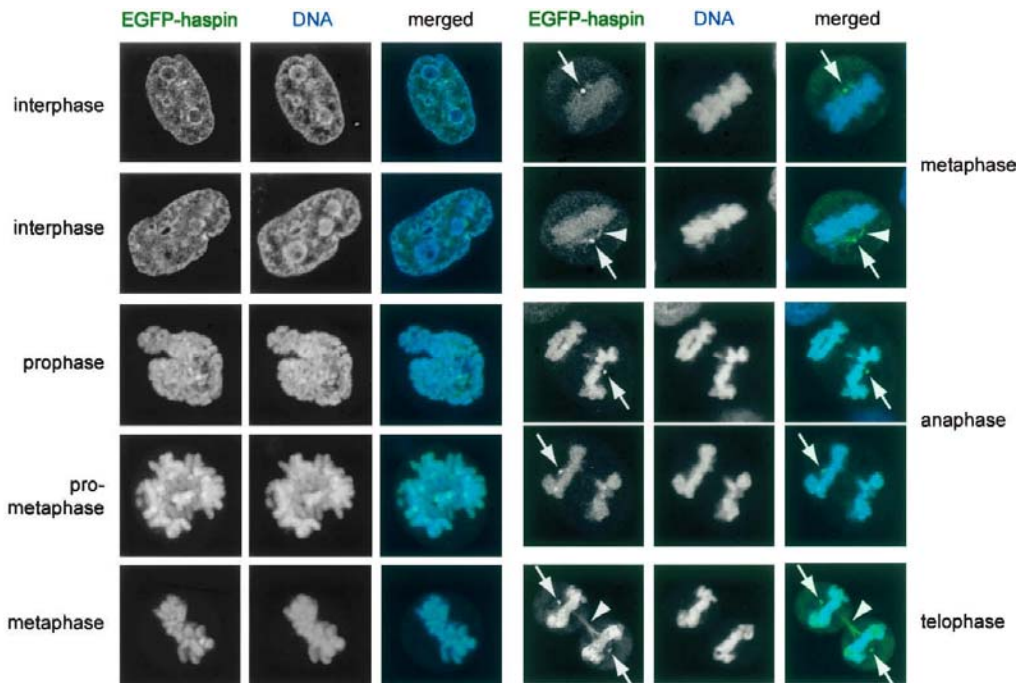
Fig. 3. Fluorescence microscopy of mammalian cell lines transfected with EGFP-haspin (Dai et al., 2005). Distribution of EGFP-haspin signals in interphase and during the different stages of mitosis. Arrows indicate the presence of haspin at the centrosomes, and arrowheads indicate haspin associated with the spindle. DNA is visualized in blue and EGFP-haspin in green.
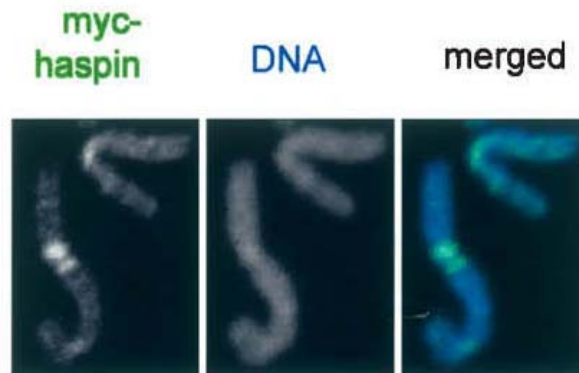
Fig. 4. Metaphase chromosomes from myc-haspin transfected HeLa cells were fixed and stained with anti-myc-FITC (in green) and DNA was visualized in blue. Haspin protein is localised at pericentromeric region (Dai et al., 2005).

To determine if haspin phosphorylates histone H3 threonine 3 *in vivo*, HeLa cells overexpressing myc-tagged haspin were generated under an inducible promoter (Dai et al., 2005). Immunoblotting experiments using anti-phospho-histone H3 antibodies showed much higher level of histone H3 threonine 3 phosphorylation compared to control cells. Overexpressing myc-haspin cells showed reduction in proliferation and a delay during mitosis (Dai and Higgins, 2005). In contrast, depletion of haspin by RNA interference (RNAi) demonstrates a dramatically reduced level of mitotic H3 threonine 3 phosphorylation and prevents normal chromosome alignment at metaphase (Fig. 5). In addition, haspin RNAi cause an accumulation of cells in prometaphase and decrease in anaphase and telophase cells (Dai et al., 2005). These data indicate that haspin is the major kinase that directly phosphorylates histone H3Thr3 during mitosis in mammals (Dai et al., 2005).

Haspin-RNAi causes an accumulation of cells with late prometaphase configurations in which partial metaphase plates are present, but many chromosomes appear stranded near the spindle poles (Dai et al., 2006). To better understand the basis for these mitotic defects, DNA content and mitotic index were determined by using flow cytometry. After 48 hr, 14% of control siRNA-transfected (negative control) cells had a 4C or G2/M DNA content, while haspin depletion resulted in an accumulation of more than 30% of cells in this state, indicating an accumulation of G2 and metaphase cells. Hence, haspin depletion arrests mitotic cells (Dai et al

2006). Further experiments revealed that depletion of haspin leads to a loss of sister chromatid cohesion, premature chromatid separation, activation of the spindle assembly checkpoint and finally blocks mitosis at a prometaphase-like state (Dai et al., 2006).
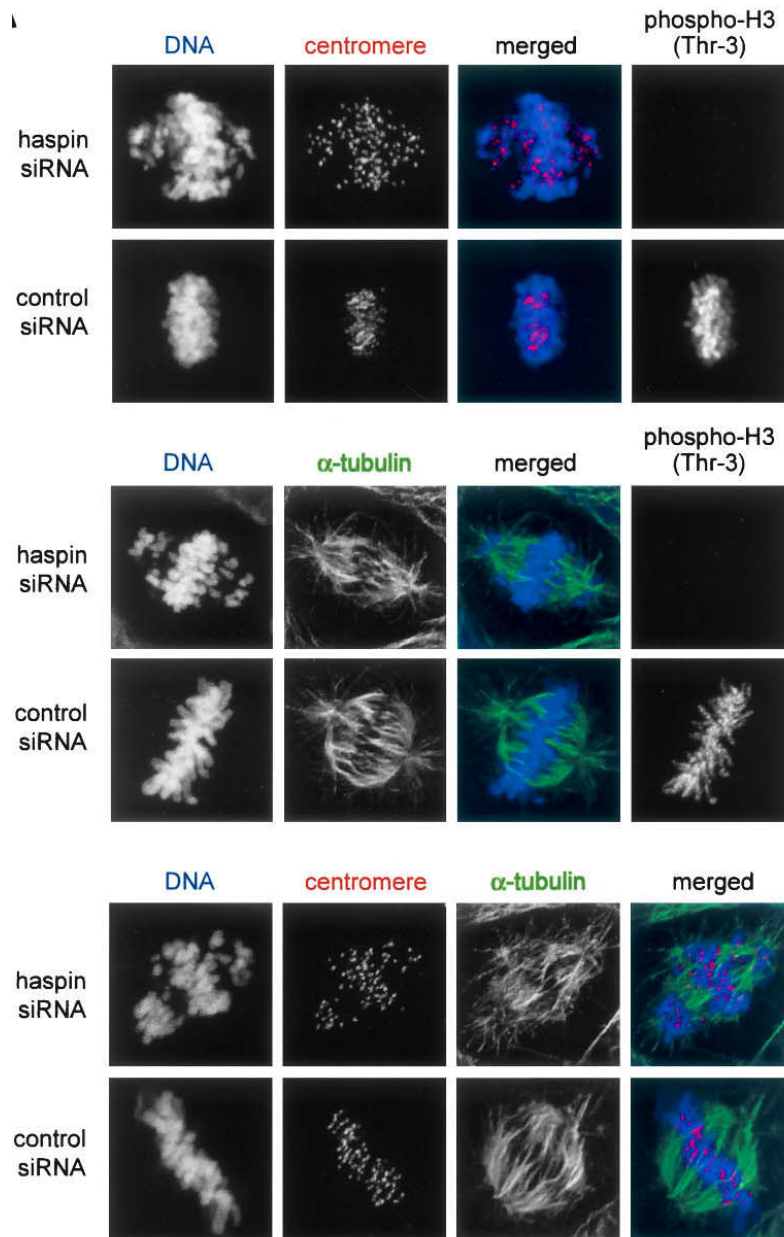
Fig. 5. Mammalian haspin depletion causes a failure of chromosome alignment and congression (Dai et al., 2005). Human cells transfected with haspin siRNA or control siRNA (vector alone) were immunostained with antibodies recognizing human centromeres, α-tubulin and phosphorylated H3Thr3. DNA visualized in blue, centromeres in red, α-tubulin in green.

In contrast to haspin RNAi, EFGP-haspin overexpressing cells revealed opposite effects on cohesion complex and increased cohesion retention (Fig. 6). Synchronized EFGP-haspin overexpressed cells with nocodazole, showed a decreased number of cells with open arms of sister chromatids (34% of the mitotic cells). In contrast, 86% of mitotic control cells had chromosomes with open arms (Dai et al., 2006), indicating that haspin overexpressed cells increase chromosome cohesion and prevent chromosome arm opening .
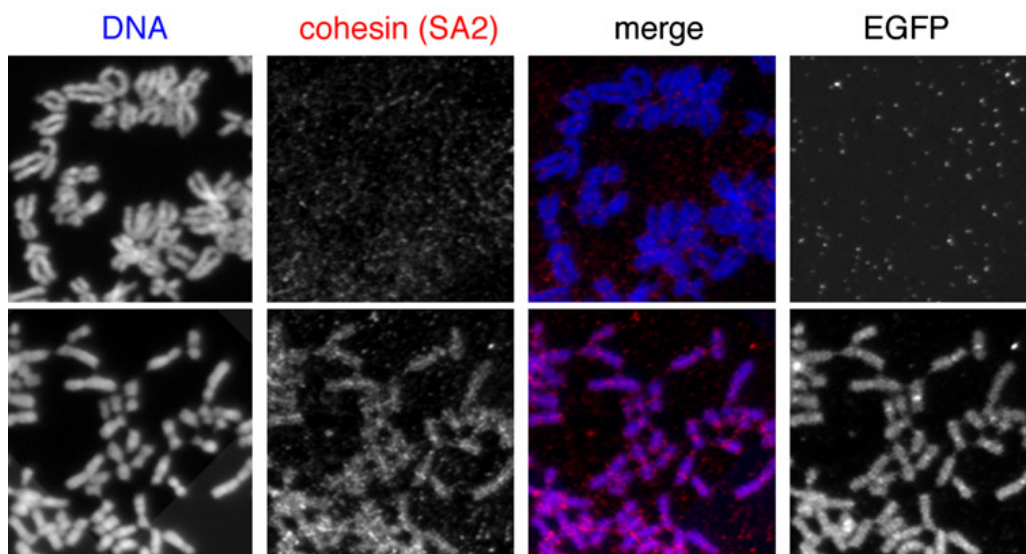
Fig. 6. Haspin overexpression increases cohesin on chromosomes and prevents chromosome arm opening (Dai et al., 2006). Stable HeLa cells transfectants containing vectors encoding EGFP alone or EGFP-haspin were incubated with nocodazole for 3 h, and mitotic chromosome spreads were prepared. Anti-SA2 antibodies to reveal cohesion (in red) and DNA shown in blue.

In general, based on previous studies Dai and his colleagues concluded that haspin is required to maintain centromeric cohesion and regulates chromosome cohesion during mitosis with contribution of other proteins required for maintenance or removal of chromosomal cohesion, such as Sgo1, Bub1, CENP-F, Soronin, Aurora B, and Plk1(Dai et al., 2006; Rosasco-Nitcher et al., 2008).

In addition to mammals, genes encoding hypothetical haspin-like proteins are present in all major eukaryotic phyla, including various vertebrates, invertebrates, plants, fungi, and the microsporidia *Encephalitozoon cuniculi,* but not in one of the sequenced prokaryotic or archaea genomes (Higgins, 2001a; Yoshimura et al., 2001). Interestingly, a haspin-like gene is also present in the genome of the microsporidia *Encephalitozoon cuniculi.* This organism, infecting various mammals, including humans, has a genome which contains only 1997 potential protein-encoding genes and is only 2.9 megabases in size, smaller than that found in many bacteria (Katinka et al., 2001; Higgins, 2003). The existence of a haspin–like gene in such a minimal eukaryotic genome may suggest an important and conserved function in the biology of eukaryotic organisms (Higgins, 2003; Nespoli et al., 2006). Most of eukaryotic species have a single haspin homologue. However, *Saccharomyces cerevisiae* has two such genes, while *C. elegans* possess up to five haspin homologues and approximately 16 haspin-related genes (Higgins, 2003).

S. cerevisiae encodes two haspin-like proteins namely *ALK1 (YGL021W)* and *ALK2 (YBL009W).* Genome-wide transcription analysis indicates that level of *ALK1* mRNA is periodically transcribed during the mitotic cell cycle, with a peak of expression in early M phase. In contrast to *ALK1*, the level of *ALK2* transcripts moderately oscillates during the cell cycle, peaking in G1 (Cho et al., 1998; Spellman et al., 1998). Moreover, the levels of Alk1 and Alk2 proteins were fluctuated during cell cycle and phosphorylation of both proteins is maximal in mitosis (Nespoli et al., 2006). Overexpression of ALK2, but not ALK1 causes a cell cycle arrest in mitosis as in mammals. Kinase assay experiments revealed that Alk1 and Alk2 proteins are capable to undergo *in vitro* autophosphorylation. Mutagenesis within one of the conserved kinase motifs led to a strong reduction in the activity of both proteins. However, histone proteins were not identified as substrates of either Alk1 or Alk2 which suggest that the mitotic role of these proteins may be independent of H3Thr3 phosphorylation (Nespoli et al., 2006). Together, all previous studies in both mammals and yeast suggest that haspin acts during the mitotic cell cycle.

Haspin-like genes are found in *Arabidopsis thaliana, Oryza sativa, Medicago truncatula, Saccharum officinarum*, moss and green alga. But, there is nothing known about the function of haspin-like proteins in plants.

2. Aims of the thesis

In this study I aimed to identify and to characterize the function of a plant haspin-like kinase, particularly in *A. thaliana.* To reach this goal following approaches were employed:

2.1. Isolation and cloning of a haspin-like gene in *A. thaliana*

BLAST search analysis using the deduced amino acid sequence of the catalytic domain of the human haspin gene was performed to identify a haspin-like serine/threonine kinase in *A. thaliana,* called AtHaspin. AtHaspin cDNA were isolated and cloned for further characterization experiments.

2.2. Manipulation of AtHaspin activity via depletion (T-DNA, RNAi) and overexpression

Functional analysis of AtHaspin was performed by manipulation of haspin activity via producing gain or loss of AtHaspin function mutants. To generate a reduced activity of AtHaspin following approaches were employed:

2.2.1. Analysis of available T-DNA insertion lines for AtHaspin to identify homozygous knockout mutants

To identify functional homozygous knockout T-DNA mutants 4 different lines obtained from GABI-Kat (Rosso et al., 2003) and SALK (Alonso et al., 2003; Yamada et al., 2003) consortiums were analysed by PCR and RT-PCR.

2.2.2. Investigation of AtHaspin-RNAi knockdown mutants

The RNAi approach was used to reduce the activity of AtHaspin. The transcription activity of AtHaspin was analysed by RT-PCR. To quantify the copy number of T-DNA insertions and to select single copy insertion lines Southern hybridisation experiments were conducted. RNAi plants with single copy insertions were analysed for three generations to identify homozygous

lines based on the Mendelian segregation behaviour. The phenotypic analysis was performed on all RNAi plants in different generations.

2.2.3. Investigation of AtHaspin overexpression mutants

The gain of function analysis was performed by producing stable overexpressed *A. thaliana* and *Nicotiana tabacum* plants. The transcription activity of AtHaspin was analysed by RT-PCR. Phenotypical analysis was performed in all AtHaspin-overexpressed plants.

2.3. Investigation of AtHaspin localisation

To investigate the localisation of AtHaspin at macroscopical and at microscopical level, a AtHaspin cDNA::YFP fusion construct under the control of strong 35S promoter was generated. YFP signals were analysed by confocal microscopy.

2.4. Promoter analysis of AtHaspin

For promoter analysis, a 1500 bp- and a 705 bp-long genomic fragment upstream of the AtHaspin gene were isolated to generate GUS and GFP expression vectors. The localisation of GUS signals was tested in different tissues.

2.5. Does AtHaspin phosphorylate Thr3 of histone H3?

To test whether AtHaspin phosphorylates H3 on threonine 3 position as in mammals, we performed immunostaining experiments on AtHaspin mutant plants (RNAi and overexpressed) using an antibody recognizing phosphorylated H3Thr3. Intensity and distribution of H3Thr3 phosphorylation sites were investigated in mitotic and meiotic cells.

3. Material and methods

3.1. Plant material and growth conditions

Arabidopsis thaliana, ecotype 'Columbia-0' (Col-0) wild-type plants were used in most studies. In addition, four different *Arabidopsis* lines (SALK_019798, GABI435H08, GABI082D07, and GABI858F01) with T-DNA insertions in the AtHaspin gene available from ABRC (http://www.Arabidopsis.org/abrc) were used.

For cultivation, seeds were surface sterilised (10 minutes in 70% ethanol, 20 minutes in 30% Domestos (a detergent) followed by 4 washes with sterile water) and plated on 1/2 MS medium solidified by 1.5% plant agar (selective markers were used for transgenic plant selection as listed in Table 2). To ensure uniform germination, agar plated seeds were vernalized at 4°C for 2 days before transfer to the growth room or chamber. Seedlings were incubated at 21°C and 16 hours photoperiod. Three weeks after germination, plants were transferred to soil. Plants were grown under 8 hours photoperiod (light intensity 250 µmol $m_{-2} s_{-1}$), 22°C/18°C day/night temperature in controlled environment growth chambers. After 4 weeks plants were cultivated under long day conditions (16 hours photoperiod per day).

3.2. Extraction of genomic plant DNA

Genomic DNA was extracted from 100 mg grinded leaves in 1.5 ml prewarmed at 65ºC extraction buffer (0.1 M Tris, 0.7 M NaCl, 0.05 M EDTA, pH 8.0) for 15 minutes. After adding 0.65 ml isoamylalcohol:chloroform (1:24) the mix was centrifuged at 14,000 rpm, at room temperature. The supernatant was transferred into a new tube, the DNA precipitated with 700 µl isopropanol, the pellet washed with 1 ml 70% ethanol, then dried and resuspended in 100 µl double distilled H_2O (Souza, 2006). For Southern blotting experiments gDNA was extracted by the DNeasy extraction mini kit (QIAGEN).

3.3. Extraction of plant RNA and reverse transcription-PCR (RT-PCR)

Total RNA was isolated from *A. thaliana* tissues by using the Trizol method (Chomczynski and Mackey, 1995). The RNA quality was monitored by denaturing MOPS-formaldehyde gel electrophoresis (Sambrook J, 2001). The RNA concentration was determined spectrophotometrically. Contaminating genomic DNA was digested with TURBO DNase

(Ambion) for 1 hour, followed by inactivation using an inactivation reagent (kit included) for 2 minutes. The cDNA was synthesized using RevertAid H Minus first strand cDNA synthesis kit (Fermentas). 1 µg of the reverse transcription reaction were used as template for subsequent amplification by PCR using a specific primer pair (listed in Table 1).

3.4. Determination of DNA and RNA concentration

DNA and RNA concentration in solutions was determined by measuring the optical absorption of the diluted samples after calibration of the photometer with a buffer control. Absorption (A260) of 1.0 corresponds to 50 µg/ml of DNA and 40 µg/ml of RNA (Sambrook et al., 2001). DNA concentration in ethidium-bromide-stained agarose gels was estimated by comparing band intensities with a defined molecular weight marker.

3.5. DNA cleavage with restriction enzymes

Restriction digests were performed using the buffer system and temperature recommended by the manufacturer (e.g. Fermentas). Completion of digestion was analysed via agarose gel electrophoreses.

3.6. Full-length cDNA and promoter isolation of AtHaspin

Arabidopsis cDNA was used for a PCR reaction to amplify the 1800 bp long coding region of AtHaspin (primers AtHaspin -Gate F and AtHaspin -Gate F, listed in Table 1). To isolate the putative promoter region, genomic DNA was used to amplify 1567 bp (primers AtHaspin -1567 pro F and AtHaspin -pro R, listed in Table 1) and 705 bp (primers AtHaspin -pro R and AtHaspin -705 pro F, listed in Table 1) upstream of the start codon of AtHaspin using the proofreading Expand Long Template PCR enzyme kit (Roche).

3.6.1. DNA extraction from agarose gels

Ethidium-bromide stained DNA bands were excised, transferred to sterile Eppendorf vials and purified with a QIAquick Gel Extraction kit (Qiagen) following the instructions of the manufacturer.

Table 1. List of used primers

Nr.	Name of primers	Sequences 5'—3'
1	AtHaspin-295F	TCGGATACTCTGCCTTTTATTCTTG
2	AtHaspin-295R	CGTTCAAATGACTTCTTGGTAAG
3	AtHaspin-825F	GATGCCTTTGATTCATTGTCTC
4	AtHaspin-825R	GAGTATCCGAGTTATTACGAC
5	AtHaspin-Gate F	CACCATGGGGCAGAGAGTTGATC
6	AtHaspin-Gate R	TCATGATATTTGGTCCATCAAC
7	EF1β-F (α subunit)	AAACCTACATCTCCGGGATCAATT
8	EF1β-R (α subunit)	ACAGAAGACTTTCCACTCTCTTTAG
9	Agri 51	CAACCACGTCTTCAAAGCAA
10	Agri 56	CTGGGGTACCGAATTCCTC
11	Agri 64	CTTGCGCTGCAGTTATCATC
12	Agri 69	AGGCGTCTCGCATATCTCAT
13	AtHaspin-571 F	TTCCAAAGGGAAAAGTTGTTG
14	AtHaspin-571 R	CAGGTTCACAGAATTTAGAG
15	AtHaspin-pro R	TTTAGGTTAGAGGGAACACAAATCAGTACTGC
16	AtHaspin-705 pro F	CACCGTTGACGTAACATTTTTTTGGCTTTAGC
17	AtHaspin-1567 pro F	CACCGCTACATGAAAAATGCTGTGGGAGAG
18	BAR- F	ATGCCAGTTCCCGTGCTTGAAG
19	BAR- R	CATCGTCAACCACTACATCGAGAC
20	LB primer	TTGGGTGATGGTTCACGTAGTGGGCCATCG
21	RP primer	TCGGTGACTGTTGCAGTACTG
22	LP primer	TCTCTTTCTGGAAGTCTGGAGC
23	GABI-TDNA	CCCATTTGGACGTGAATGTAGACAC
24	082D07-F	ATTGAAAAGCCTTGCACATCGC
25	082D07-R	AGGAGAACAAATTAGGGTTAAGCTC
26	435H08-F	CATTTGTTGTTTTGGAATGTTGAC
27	435H08-R	AGAGAGAGAGAGAAAGAG
28	858F01-F	GAGCTGACGAACTACTTGAG
29	858F01-R	AAGGTCTTTGCCACCATG

3.7. Cloning procedures

The cloning and molecular biology procedures were performed as described by (Curtis and Grossniklaus, 2003; Earley et al., 2006).

3.7.1. Vectors and bacteria strains

E. coli strain DH5α (Stratagene) was used for the cloning procedure of most vectors. For plant transformation the *Agrobacterium* binary vector GV3101::pSOUP (Hellens et al., 2000) was used. The different vectors used in these experiments are described in Table 2, which were obtained from ABRC or Invitrogene.

Table 2. List of the different vectors used for cloning

Vector names	Selectable cloning cassettes	Selective marker and concentrations		References
		In plant	In bacteria	
pEarleyGate100	35S-Gateway-OCS -3'	PPT (20 g/ml)	Kan (50 µg/ml)	Earley, et al., 2006
pEarleyGate104	35S- YFP- Gateway-OCS 3' (N-terminal fusion)	PPT (20 g/ml)	Kan (50 µg/ml)	Earley, et al., 2006
pMDC107	Gateway-GFP-6xhis-nosT-3'	Hyg (25µg/ml)	Kan (50 µg/ml)	Curtis and Grossniklaus, 2003
pMDC162	Gateway-GUS-nos T-3'	Hyg (25µg/ml)	Kan (50 µg/ml)	Curtis and Grossniklaus, 2003
PAGRIKOLA,1	35S- Gateway-intron PDK-intron CAT1-Gateway-OCS-3'	PPT (20 g/ml)	Kan (50 µg/ml)	Hilson, et al., 2004

3.7.2. AtHaspin-pENTR vector construction

The Gateway pENTR Directional TOPO cloning Kit (Invitrogene) was used to clone the blunt-ended PCR product into a pENTR/D-TOPO vector. The different pENTR vectors used in the cloning experiments are described in Fig. 7. After TOPO cloning reaction, the pENTR TOPO construct was transformed to *E. coli* (DH5α strain) by electroporation.
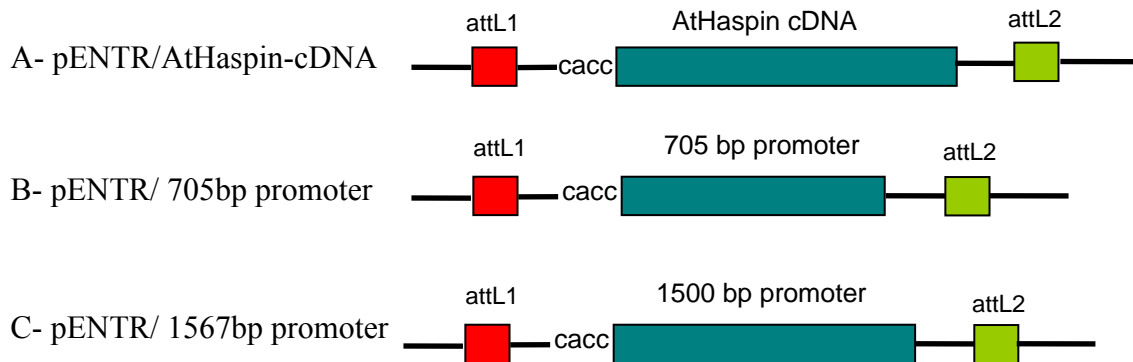
Fig. 7. Diagrams illustrate Gateway-Entry vectors. **(A)** Constitutive pENTR/D-TOPO vector contains 1800 bp of AtHaspin coding cDNA;(B) pENTR/D-TOPO vector contains 1500 bp genomic DNA upstream of the AtHaspin start codon as a promoter region. (C) pENTR/D-TOPO vector contains 705 bp genomic DNA upstream of the AtHaspin starts codon as a promoter region.

3.7.3. Electrotransformation and verification of *E. coli* cells

The DH5α *E. coli* electrocompetent cells were thawed on ice, mixed with 1-2 μl of DNA (e.g. pENTR TOPO construct) and transferred to a precooled sterile electroporation cuvette. After one pulse (2.5 kV) transformed cells were resuspended in 1 ml SOC medium, gently agitated for 1 hour at 37°C plated on LB-agar plates containing 50mg/l kanamycin and cultivated overnight. Transformation of *E. coli* was validated by either PCR reaction using appropriate primer pairs or restriction enzyme digestion.

3.7.4. Plasmid DNA extraction and sequencing

Plasmid DNA was prepared from overnight bacterial cultures using the QIAGEN plasmid mini/midi kit (Qiagen, Hilden, Germany). DNA sequencing was performed using facilities at IPK (Gatersleben) or at MWG Biotech AG (Ebersberg).

3.7.5. Recombination of pENTR TOPO and destination vectors to construct expression vectors

Both pENTR vectors and pEarleyGate vectors contain the same bacterial selection marker, namely kanamycin resistance. Therefore, to increase the efficiency of recombination the entry vectors were linearized by *MluI* digestion. The LR Gateway recombination reaction was performed between entry and destination vector to recombine the sequence of interest into the destination vector (e.g. pEarleyGate vectors) using the LR clonase II reaction (Invitrogene) according to the manufacture instruction. The schemata of all different constitutive expression vectors which were used are illustrated in Fig. 8. The product of the LR reaction was transformed into *E. coli* (DH5α strain) and plated on selective LB media containing 50 mg/l kanamycin.

3.7.6. Transformation of *Agrobacterium tumefaciens* and validation of transformants

50 μl competent *A. tumefaciens* cells (GV3101::pSOUP-positive) were thawed on ice, mixed with 1-2 μl of plasmid DNA, and transferred to a precooled sterile electroporation cuvette. After electroporation (2.5 kV) 50 μl of cells were resuspended in 1 ml LB medium, gently agitated for 2 hour at 28°C and overnight plated on LB-agar plates containing 50mg/l kanamycin, 5mg/l tetracycline and 50mg/l rifampicin. After cultivation of individual colonies in LB selection medium for 2 days at 28°C, plasmid DNA was isolated and PCR reaction were performed using appropriate primer pairs to validate the successful transformation. Alternatively, plasmid DNA was digested with appropriate restriction enzymes.
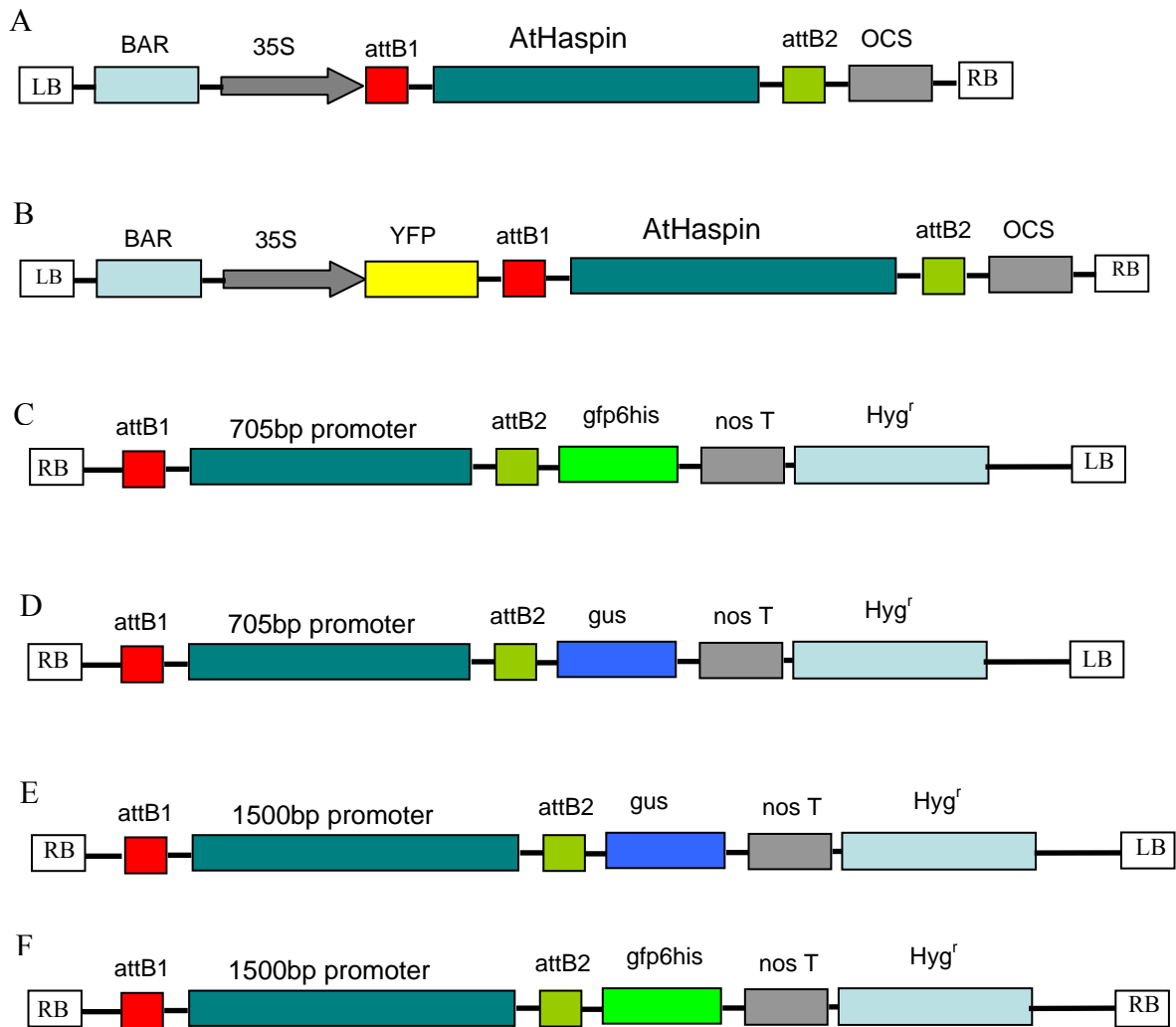
Fig. 8. A schematic illustration of expression vectors used. (A) Constitutive expression vector, resulting from recombination of pEarleyGate100 with pENTR vector, harbouring a 35S promoter and AtHaspin coding sequence for AtHaspin gain of function study; (B) expression vector resulted from recombination of pEarleyGate104 and pENTR vector, harbouring a 35S promoter, C-terminal fusion of YFP and AtHaspin coding sequence, for AtHaspin localisation study; (C, E) promoter test vectors, derived from recombination of pENTR/705bp promoter construct with pMDC107 and pMDC162, respectively; (D, F) promoter test vectors, derived from recombination of pENTR/1567bp promoter construct with pMDC107 and pMDC162, respectively.

3.8. Transformation of plants and selection and transformants

For plant transformation the first inflorescences of *Arabidopsis* plants grown under short day condition (8 hours light per day) were removed as soon as they emerged (to encourage the growth of more inflorescences) and plants were cultivated under long day conditions (16 hours of light per day). After one week, when the secondary inflorescence shoots were around 8 cm tall, the inflorescences are inverted and submerged for 30 second in a solution of *Agrobacterium* cells containing the desired T-DNA plasmid. *Agrobacterium* cells (containing pSOUP and Ti plasmids) were grown to mid-log phase, pelleted by centrifugation at 8,000 g, and resuspended in a 5% sucrose solution that includes 0.05% Silwet L-77 detergent (Clough and Bent, 1998). Transformed plants were selected on appropriate selective media based on resistance gene located in the vector (Table 2).

3.9. Procedure for the generation of RNAi *Arabidopsis* lines

To reduce AtHaspin gene activity via RNAi, a hairpin RNA construct containing a 400 bp AtHaspin specific sequence tag (GST, the GST position is shown in figure 14), which has no significant similarity with any other region in the *A. thaliana* genome, and a spacer containing two head-to-head introns constructed into the pAGRIKOLA vector (Fig. 9) obtained from NASC (The European *Arabidopsis* Stock Centre) was transformed into *Agrobacterium* cells containing the binary vector (GV3101::pSOUP) as described by Hilson et al (2004). To identify homozygous AtHaspin-RNAi-lines, 16 T2 plants of different T1 origin with a single T-DNA insertion were plated on selective MS medium (containing 20 mg/l PPT). Theoretically, 25% of these T2 plants should be homozygous for the T-DNA. To identify these homozygous lines, T3 seeds were collected from each T2 plant and seeds were tested for BASTA resistance. If 100% of the T3 progeny of a single T2 plant are BASTA resistant, it indicates that the T2 parent was homozygous for the T-DNA insertion.

Hairpin cassette with spacer
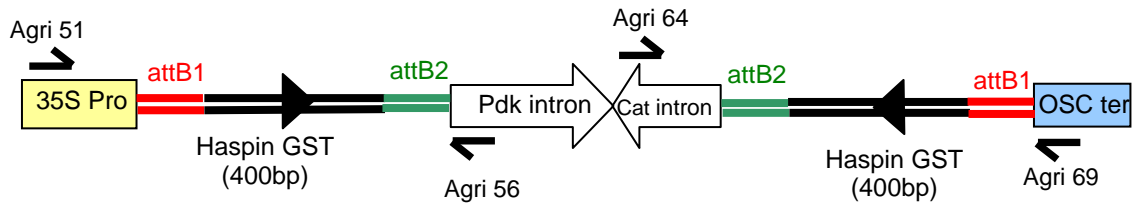
Hairpin cassette with flipped spacer
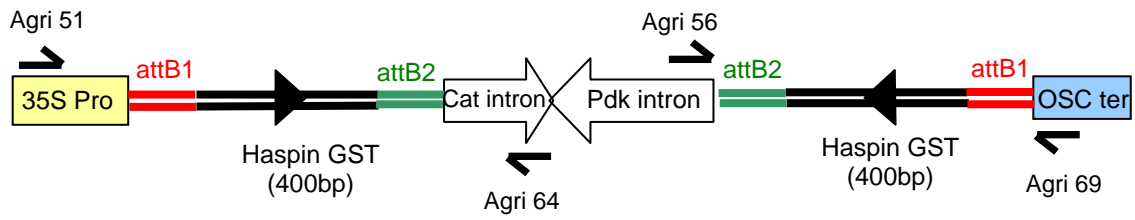
Fig. 9. Structure of recombined hairpin cassettes with inverted 400 bp AtHaspin-GST fragments. Arrows indicate the position of primers used for PCR validation of the clones.

3.10. Restriction enzyme digestion, gel electrophoreses of genomic DNA and Southern hybridization

Southern hybridization was performed according to (Sambrook J, 2001). 10 μg of genomic plant DNA was cleaved overnight with the restriction enzyme *EcoR*I (Fermentas). The digested DNA was size-fractionated by gel electrophoresis (0.8% agarose in TAE buffer, 18-20 hours at 25 V). The gel was denatured in denaturation buffer (1.5 M NaCl, 0.5 M NaOH) for 30 minutes, neutralized in neutralization buffer (1.5 M NaCl, 1 M Tris HCl (pH 7.2), 0.001 M EDTA) 15 minutes twice then, blotted onto Hybond-N$^+$ membrane (GE Healthcare) by in 20x SSC overnight. The DNA was fixed to the membranes by incubating for 5 minutes in 0.4% NaOH.

3.10.1. Radioactive labeling of DNA probes, hybridization and detection
A BAR gene-specific probe (a region adjacent to the T-DNA left border) was PCR amplified using the primer pair BAR-F and BAR-R (Table 1) and purified using a QIAquick gel extraction kit (Qiagen).

To suppress non-specific hybridization, single-stranded salmon sperm DNA was used as blocking reagent. Therefore, salmon sperm DNA was denatured for 5 min at 100°C and mixed with 100 ml prewarmed Church buffer (7% SDS, 10 mM EDTA, 0.5 M phosphate buffer (pH 7.2) prior to use. 100 ng probe was labeled with α-^{32}P CTP 125 μCi P^{32} (GE Healthcare) using the HexaLabel^{TM} DNA Labeling Kit (Fermentas). Nylon membrane was pre-hybridized with Church buffer for 3 h at 65°C before adding the DNA probe. Hybridization was performed at 65°C over night and the membrane washed 2-3 times (20 minutes each time) in buffer containing 2xSSC/0.5% SDS, 0.5xSSC/0.5% SDS and 0.1xSSC/0.5% SDS respectively at 65°C. The membrane was wrapped in plastic wrap and exposed on an X-ray film for 10-15 days at -80°C.

3.11. Histological detection of GUS and YFP expression

For localisation of GUS activity, tissues were fixed for 30 minutes in 90% acetone at room temperature. Tissues were then washed three time for 5 minutes in washing buffer (0.1 M sodium phosphate buffer, pH 7.0, 0.1% Triton X-100, 1mM $K_3Fe(CN)_6$, 1mM $K_4Fe(CN)_6$) on ice. Subsequently, staining buffer (0.1 M sodium phosphate buffer, pH 7.0, 0.1% Triton X-100, 1mM $K_3Fe(CN)_6$, 1mM $K_4Fe(CN)_6$, 1mM X-GLUC) was infiltrated by a brief vacuum (15-20 minutes) and the samples were incubated at 37° C, overnight. GUS stained tissues were washed three time with 70% ethanol to remove soluble (e.g. chlorophyll) until the samples are essentially colourless or very faintly coloured.

YFP fluorescence signals (emission-peak = 527 nm) were studied with a Zeiss LSM 510 META confocal laser scanning microscope (Carl Zeiss, Jena, Germany) in collaboration with Dr. Twan Rutten (IPK). YFP was excited with a 488-nm line and emission was detected with a 505-550 nm band-pass filter. Photospectrometric analysis of the fluorescence signal with the help of the META-detector confirmed the identity of YFP.

3.12. Indirect immunofluorescence analysis

3.12.1. Chromosome preparation

Tissues of *A. thaliana* (root tips from two-day-old seedlings germinated on moist filter paper or very young flower buds) were fixed for 20 minutes in freshly prepared 4% paraformaldehyde solution containing phosphate-buffered saline (PBS, pH 7.3) on ice, washed two time for 15

minutes in PBS on ice, and digested at 37°C for 25 minutes in a mixture of 2.5% cellulase 'Onozuka R-10' and 2.5% pectolyase Y-23 dissolved in PBS. Tissues were then washed for 15 minutes in PBS and squashed between a glass slide and coverslip in PBS. After freezing in liquid nitrogen, the cover lips were removed and the slides were transferred immediately into 1X PBS for immunostaining. For longer storage the slides were kept in 100% glycerol at 4°C.

3.12.2. Detection of antigens and fluorescence microscopy

The stored slides in glycerol were washed with 1X PBS buffer. To avoid non-specific antibody binding, slides were blocked in 5% bovine serum albumin (BSA), 0.1% Tween-20 in 1X PBS in a moist chamber at room temperature for 45 minutes. After 2 time washes in 1X PBS (5 minutes per each time), 50 µl of primary antibody (diluted 1:100 in PBS with 1% BSA) were applied to each slide and covered with parafilm and incubated in a moist chamber overnight at 4°C. Rabbit polyclonal antibodies against phospho-histone H3Thr3 (Cat. Nr. 07-424, Upstate) and against GFP (Cat. Nr. 632459, Clontech) were used for immunodetection. After washing with 1X PBS buffer for 15 minutes the slides were incubated with secondary antibody, anti-rabit-Cy3, and/or anti-rat-FITC (diluted 1:100 in 1X PBS 1% BSA) was performed at 37°C for 1 hour. Slides were counterstained in 10µg/ml antifade containing 4′, 6-diamidino-2-phenylindole (DAPI), and covered with cover slips and analysed with an Olympus BX61 microscope equipped with an ORCA-ER CCD camera. Deconvolution microscopy was employed for superior optical resolution of globular structures. Thus each photograph was collected as sequential image along the Z-axis with approximately 11 slices per specimen. All images were collected in gray scale and pseudocolored with Adobe Photoshop, and projections (maximum intensity) were done with the program Analysis (Soft Imaging System).

3.13. Alexander staining of pollen

Alexander stain was used to evaluate pollen viability. For this analysis, anthers just beginning to dehisce from the open flowers were dissected under a binocular microscope and pollen was gently squashed in Alexander's staining solution under a coverslip (Alexander, 1969). Pollen grains were observed under a light microscope after staining.

3.14. Protein extraction and Western blot analysis

Total proteins were extracted from leaves, flower buds and C24 suspension cells of *A. thaliana.* 200 to 300 mg of sample was ground under liquid nitrogen and suspended in 1 ml of solubilisation buffer (112 mM Na_2CO_3, 112 mM DTT, 4% SDS, 24% sucrose, and 4 mM EDTA). After 20 minutes of incubation at 65°C, cell debris was removed by centrifugation. The protein samples were quantified by Bradford assays, and 40 µg of protein of each sample were separated on 12% SDS-PAGE polyacrylamide gels on a Miniprotean II (Bio-Rad) according to (Laemmli, 1970). Proteins were blotted on a nitrocellulose membrane by a Trans-Blot semi-dry apparatus according to Bio-Rad manual instruction for 2 hours at 20 V in blotting buffer (48 mM Tris, 39 mM glycine, 20% methanol, 1.3 mM SDS, pH 9.2).

Protein loaded membrane was blocked for 1 hour in blocking milk (5% fat free dry milk in PBS + 0.1% Tween 20), and incubated overnight at 4°C with the primary antibody in blocking milk. The secondary antibody (anti-rabbit IgG: IRDye800 conjugated, LI-COR, diluted 1:5000) was applied for 2 hour at room temperature. After 3 times washing with PBST (PBS buffer + 0.1% Tween 20), 5 minutes each time, the signal was detected with the ODYSSEY imaging system (Li-COR).

4. Results

4.1. *Arabidopsis thaliana* encode a conserved haspin-like gene

By BLASTX analysis of the non-redundant nucleotide sequence database of the *A. thaliana* genome (GENEBANK) using the deduced amino acid sequence of the catalytic domain of the human haspin gene we could identify a haspin-like serine/threonine kinase (called AtHaspin) in the genome of *A. thaliana* which is encoded by the locus At1g09450.

The subdomains I to XI of the ePKs (Higgins, 2001a) were identified by alignment of plant haspin-like proteins with haspins of human and mouse (Fig. 10). Overall, the alignment revealed that many of the residues that are essentially invariant in other ePKs, and known to be critical in forming the Mg^{2+}-ATP-binding and catalytic sites are conserved in the majority of haspin proteins (see Fig. 10). Specially, the G-x-G-x-x-G-x-(V/A) motif in region I, the conserved lysine (K) in region II, glutamate (E) in region III , aspartic acid (D) and asparagine (N) in region VIb, aspartic acid (D) in region VII, and aspartic acid (D) or glutamate (E) in region IX (Higgins, 2001a, 2003) are present. A leucine zipper motif (L-x(6)-L-x(6)-L-x(6)-L-x(6)-L) is present in mammalian haspin proteins within the region of VIa and VIb (Fig. 10). The single deviation from the leucine zipper motif was observed in *Arabidopsis* haspin, and the third periodic leucine is replaced by phenylalanine (F). Leucine zipper and leucine zipper-like domains in eukaryotic proteins have been demonstrated to play essential roles in inter- and intramolecular interactions (Ramadevi et al., 1998).

```
             I                    II                        III
H. sapiene     LQRCEKIGEGVFGEVFQTIADHTPVAIKIIAIBGPDLVNGSHQKTFEEILPBIIISKELSLLSG-----
M. musculus    LERCEKIGEGVFGEVFQIINDQAPVALKIIAIBGLDLVNGSHQKTFEEILPBIIISKELSLLSS-----
A. thaliana    PESIVKIGEGTYGEAFRA----GSSVCKIVPIDGDFRVNGEVQKRADELIBEVILSWTLNQLREC--ET
V. vinifera    PESIVKIGEGTYGEAFRA----GKTVCKIVPIDGDLLVNGEVQKRSGELIBEALLSRTLNHLRED--GG
O. sativa      PGSIVKLGEGTFGEAFRA----GSTVCKVVPFDGTSLVNGETQKKAEEVLBEVLLCLTLNNLRADRGDN
P. patens      LRQIKKLGEGTFGEAFKG----GSSVFKIVPMDGKFQVNGEAQKTSAEMLSBVVLSNALNELRGGP-MR
O. tauri       KRGVKKIGEGTYGEAYRGE---DGVVMKIVPMGGEALVNGEVQMGPNEIRSBTSILKALTKLREHVKDE
O. lucimarinus KHGVKKIGEGTYGEAYRGE---DGVVMKIVPMGGDALVNGEVQMGPGEIRSBTSILKALTALRDHEADE
                  *      *

                    IV                                         V
H. sapiene     EVCNRTEGFIGLNSVHCVQGSYPPLLIKAWDHYNSTKGSANDRPDFFKDDQLFIVLEFEFGGIDLEQMRTK
M. musculus    EAYNRTEGFIGLNSVHCVQGLYPPLLIKAWDHYNTTKRSANDRPDFFQEDQLFIILEFEFGGVDLERMKTK
A. thaliana    TAQNLCPTYIKTQDIKLCQGPYDPILIKAWEEWDAKHGSENDHP-DFPEKQCYVMPVLEHGGKDLESFV--
V. vinifera    RVNNSCTSFIETLDLRVCQGPYDAALIRAWEDWDEQHGSENDHPREFPEKQCYVVPVLEHGGKDLESFV--
O. sativa      VKENSCHGFIETKDFWVCQGPYDPSLICAWEDWDAKCCSENDHPNDFSNEQCYIVPVQADGGRDLEKFA--
P. patens      NEPNICSTFVETKATRICQGCYDPELVRAWEEWDSLNTSENDHPSIFPNQQLYVVPFLTDGGRDLESFS--
O. tauri       IEKNFTDGFIRLIDASVCRGPYSKKLLBAWDKYAVTGETENETPGNLPSNQLYISBACEDGGIDLEHFN--
O. lucimarinus NAKNFTDGFIRLLDASVCRGPYSKKLLBAWDKYASTGASENEKPDDLPSNQLYISBACDDGGTDLEHFE--
                      *                                      *

                         VIa                    VIb
H. sapiene     LSSLATAKSILHQLTASLAVAEASLRFEHRDLHWGNVLLKKTSLK----KLHYTLNGKSSTIPSCGIQVSI
M. musculus    LSSVATAKSILHQITASLAVAEASLHFEHRDLHWGNVLLKKTNLK----ELRYTLNGKTSTIPTHGIQVNI
A. thaliana    LLNFDEARSLLVQATAGLAVAEAAFEFEHRDLHWGNILLSRNNSD----TLPBILEGKQVCIKTFGVQISI
V. vinifera    LLNFDEVRSLLVQVTVALAVAEAAYEFEHRDLHWGNILLSRKDSE----MLQBTLEGKNMFVKTFGISISI
O. sativa      LLDYNEACSLLVQVTAALAVAESACEFEHRDLHWGNILLDRDETQDKNHTMGBTLQGKNMCTRTFGINVSI
P. patens      LENFNEARSLLLQIVLALAVAEEACFEHRDLHWGNIVLSRDQRE----HVVBRLLGQEKQVKTYGISVSL
O. tauri       LRSAKEMVALLFQIVVALSVAEEECQFEHRDLHWGNVLIKRVRTK----EKVARINGVDINIQTSGLDVAI
O. lucimarinus LRSMTETVAMLFQIVVALSVAEEASQFEHRDLHWGNVLIKRTRTK----QKRAKLNGVELNIQTSGLDVTI
                 *    ==     ==      ==      ==     ==  *

               VII              VIII              IX                    X
H. sapiene     IDYTLSRLERDGIVVFCDVSMDEDLFTG-DGDYQFDIYRLMKKENNNRWGEYHPYSNVLWLHYLTDKMLK
M. musculus    IDYTLSRLERDGIVVFCDISAEEDLFTG-EGDYQFEIYRLMRKENKNCWGEYHPYNNVLWLHYLTDKILN
A. thaliana    IDFTLSRINTGEKILFLDLTSDPYLFKGPKGDKQSETYRKMKAVTEDYWEGSFARTNVLWLIYLVDILIT
V. vinifera    IDFTLSRINTGEAILFLDLSSDPELEKGPKGDKQSNTYRKMKEITEDFWEGSFPKTNVLWLQYLVDILIL
O. sativa      IDFTLSRINTGDAILFLDLSTDPALFEGPKRDKQAETYRKMKQITNDYWEGSFPKTNVVWLIYLVDIVLQ
P. patens      IDFTLSRINTGNQVLFCNLAADPALFEGPKNDVQANTYRRMKKVTGGQWEQRFLQTNCLWIHYVADILLT
O. tauri       IDFTLSRLTTGEGDVFCDLNADPBELFTGPKGHCQSETYRRMKRVTKGKWSTYNPKTNALWIHYLTDVILE
O. lucimarinus IDFTLSRLTTEDGDAFCDLNADPBELBAGPKGHCQSETYRRMKRVTKGKWNKYCPKTNALWLHYLADTVLE
                    *           *        **        *         *

                                XI
H. sapiene     QMTEK-TKCNTPAMKQIKRKIQEBHR--TMLNFSSATDLLCQHSLFK----
M. musculus    KMKEK-TKCQSAAMKQIRKNLQHBHR--TVLSFSSATDLLCQHSLFR----
A. thaliana    KKSFERSSKHERELRSLKKRMEKYESAKEAVSDPFFSDMLMDQIS------
V. vinifera    KKSFKRTSKDERELRSLKKRMDNYGSAKEATSDPFFTDMFVDHAI------
O. sativa      KRYSTFTSKDDRELRAFKKRLAKYDSAKDCLTDSFFSDLLLSDEDAQPSTA
P. patens      KKTFSSSPAEKRSLRAFRKRVMLYESSGAAVLDEFFNGMWADV--------
O. tauri       QKDFPISVEEKHELVAFRKRALEYESAGKALFDDLFKGIWTSGKKKQ----
O. lucimarinus QKDFNVTAEDKQRLVAFRKRALDYKSAGEIVFDELFSGIWTSGKKN-----
                                             *    *  *
```

Fig. 10. Multiple amino acid sequence alignment of haspin-like kinase domains of plants, human and mouse. Residues that are completely conserved in all haspin-like proteins are shown in white on a black background. Residues that are ≥80% conserved (white on grey background) or ≥60% identical (black in grey background) are indicated. The gaps are shown as dashes. The double underlines indicate the leucine residues for the leucine zipper domain. The alignment was performed by CLUSTAL W. Subdomains I to XI of the kinase fold are indicated with

horizontal lines, and residues that are essentially invariant in previously identified kinases (Hanks and Quinn 1999) and that are identified in the haspins (Higgins, 2001a) are marked with asterisks. The alignments includes residues 483-798 of human (GenBank AF289865), 440-754 of murine haspin (GenBank BAB00640, NP_034483), 287-599 of *Arabidopsis* (GenBank AAC33205, At1g09450), C-terminal regions of hypotetical proteins from 334-647 of *Vitis vinifera* (GenBank CAN65736), *Physcomitrella patens* (XP_001777245), *Ostreococcus lucimarinus* (XP_001417826) and *Ostreococcus tauri* (CAL54142).

Threonine (T), and alanine (A) in region I, Cycteine (C) in region IV, phenylanalanine (F) in region V, glutamic acid (E) in region VIa, arginine (R) in region VIb, threonine in region VII, proline (P) in region VIII, proline (P), lysine (K), and threonine (T) in region IX, arginine (R) , aspartic acid (D) and phenylalanine (F) in region XI are plant -specific residues (asterisks in Fig. 10).

In addition, there are some conserved residues in N-terminal domain of plant haspins (Fig. 11).

```
A. thaliana   ---------------MGQR------------VDLWSEVIKSEEEDGD-IPKIEA
O. sativa     MAREAAAPGRTAGKASAPSGHHHAGARGGGGDLWSEIMASGGGGGA--ARIGV
V. vinifera   ------MAYFSSYSQGQDS-----------VDLWSEIAATEEGEGNRKQQIAV
O. tauri      --MTSTVIDRRALVDATPWPRRRCATTPTGSSPWSDIDVEGRRGRR---RRSA

A. thaliana   VFQRRK-KPDKSSEAVNFG--WLVKGARTSSVNGPKRDSWARSLSTRGRESIA
O. sativa     VYGRRRAAQEASRPRGAVDVRGVAAGEKRASFEPSKRTSWNRSLSIRGRESIL
V. vinifera   IYRRRR-RTENTLKDVDTNQSSLNNGNRLSLAAPVKRVSWNRSLSIRGRTSIA
O. tauri      RWAQTE--EESTVRGTKTTTTTTTTTTIEATARDGGPVKTNAEGRDGGSAAA

A. thaliana   VRAYVNNQPQKKAAGRK-KPPIPKGKVVK----APDFQKEKEYFRDIDAFELL
O. sativa     FAPGTKIQPQQNPCRAQKRPPKPGNRVKRTFGGPPDLKKEKAYFEEVDAFELM
V. vinifera   VFACVEYQPQQRKPRRKAKPPLPR-VWLF----PQSFEQERAYFQEVDAYELL
O. tauri      ATRAATERARTFVFKSRNKLTRCARAEREHRARLAKLAESRAFFDDVDEVSLA

A. thaliana   EESPSPN---KSSTWTMGEQVVP-EMPHLSTRLEKWLISKKLNHTCGPSSTLS
O. sativa     EESPSPK---NFGTWARGMEQN-YIVHDLSAILERWKISKLAKFAA--SRPLF
V. vinifera   EESPSPK---RFGTWAMGVQSDDIVLPHLSSVLNKWLIAKKLNYSYGPSGSLS
O. tauri      EESEGSTPNGRGGALGNRLELSPSGLIEALQGLGLVNDASGLRAKMAATTRRD

A. thaliana   KILENSAIHQESVCDNDAFDSLSLKTPDKSSAGNTSVFRLIPSCDENLAAEDV
O. sativa     DIMETPVVP--SVRS-DCSLHDSCRTPEKDRGSRTNPMRRTIPSGLS--DKTS
V. vinifera   KILETPAMPMEPICG-DGFDALTVKTPEKASPQVYVVGRQTGSQKSN----EV
O. tauri      SMIQSPRAQMLPIGRADAFDRTSDWVSSLPAFSPMKERVESTTLSSP--EENE

A. thaliana   PVRKIKMESIDLEDELKRLSLTSDLIPTHQDFDQPILDLLSACGQMRP--SNF
O. sativa     IFTSFS------ELKIKEEPDDSSIPSLSAEAMTAFAQLLLVCNQSAP--ITL
V. vinifera   SLTTGDEGCEDIDVAIKKLSLTSRSASLGGDHWDSFSALLTVCEQSAP--STL
O. tauri      SIIATDDEVDSLQGDFERLVIDDECS-------PLAALLRACGQSEGDVSSM

A. thaliana   IEAFSKFC------E-------
O. sativa     AEAFSTYCLYSSFNEDVHGNST
V. vinifera   LDVFSKYC------D-------
O. tauri      ASLVRTHVK------------
```

Fig. 11. Multiple amino acid sequence alignment of plant haspins N-terminal domains. Residues that are completely conserved in all haspin-like proteins are shown in white on a black background. Residues that are ≥80% conserved (white on gray background) or ≥60% identical (black in gray background) are indicated. The gaps are shown as dashes.

4.2. Phylogenetic analysis of haspin-like proteins

Alignment of the AtHaspin kinase domain with other putative haspin-like proteins revealed that haspin homologues are found in animals (human, mouse, dog, cattle, fish, etc), plants (*A. thaliana*, *Oryza sativa*, *Medicago truncatula*, *Saccharum officinarum*, moss and green alga), and fungi (Fig. 12).

The existence of at least one haspin homologue in all nearly complete sequenced eukaryotic genomes suggests an important function and apparent origin early in eukaryotic evolution for these proteins, particularly since protein kinases are known to be critical regulators of a wide variety of cellular functions.

Arabidopsis encodes a single haspin-like kinase (AtHaspin), which shows highest similarity to the haspin-like kinases of other dicots (*M. truncatula* and *V. vinifera*, see Table 3). Interestingly, haspin genes are also present in unicellular eukaryotes (*M. brevicollis, O. tauri, and O .lucimarinus*), and in species with a very small genome such as microsporida *E. cuniculi*, with 2.9 megabases in genome size and 1,997 potential protein-encoding genes.

99 Homo sapiens (human).pro
99 Pan troglodytes (chimpanzee)
94 Macaca mulatta (rhesus monkey)
100 Bos taurus (cattle)
76 Canis lupus familiaris (dog)
90 Mus musculus (house mouse)
Rattus norvegicus (rat)
Gallus gallus (red jungle fowl)
99 Danio rerio (zebrafish)
Tetraodon nigroviridis
Xenopus laevis (African clawed frog)
96 Trichoplax adhaerens
100 Drosophila grimshawi
Drosophila mojavensis
Drosophila virilis
Drosophila persimilis
93 Drosophila willistoni
64 Drosophila melanogaster (fruit fly)
Drosophila ananassae
56 Acyrthosiphon pisum (pea aphid)
98 Apis mellifera (honey bee)
91 Nasonia vitripennis (jewel wasp)
Tribolium castaneum (red flour beetle)
92 AT1G09450 A.thaliana   ⎫
Medicago truncatula   ⎬ dicots
100 Vitis vinifera   ⎭
97 100 Oryza sativa Japonica Group ⎫
Saccharum officinarum   ⎬ monocots
93 Triticum aestivum   ⎭
Physcomitrella patens   ⎫
100 Ostreococcus lucimarinus   ⎬ lower plants
Ostreococcus tauri   ⎭
99 Caenorhabditis elegans-AAO27842
100 Caenorhabditis elegans-NP_492043
98 Caenorhabditis elegans-NP_490768
Caenorhabditis briggsae-XP_001671091
Monosiga brevicollis MX1.
Aspergillus clavatus NRRL 1
60 Aspergillus nidulans FGSC A4.
100 Aspergillus niger CBS 513.88
100 Aspergillus terreus
Coccidioides immitis RS
95 100 Magnaporthe grisea 70-15
93 Neurospora crassa OR74A
Botryotinia fuckeliana B05.10
56 Malassezia globosa CBS 7966
Ustilago maydis 521
64 Cryptococcus neoformans
99 Coprinopsis cinerea okayama7
Laccaria bicolor S238N-H82
51 Schizosaccharomyces pombe (fission yeas
Yarrowia lipolytica
96 Brugia malayi-XP_001893934
Brugia malayi-XP_001902094
Encephalitozoon cuniculi GB-M1
Caenorhabditis elegans -NP_001024960
Ashbya gossypii ATCC 10895
Caenorhabditis elegans- NP_001033406
Caenorhabditis elegans-NP_501839
Entamoeba dispar SAW760
Caenorhabditis elegans- NP_496965
Caenorhabditis elegans -NP_741498
Caenorhabditis elegans-NP_501030
94 Caenorhabditis elegans (nematode) ZK177
Caenorhabditis elegans-NP_495212
Dictyostelium discoideum AX4
94 Saccharomyces cerevisiae (baker yeast)1
Saccharomyces cerevisiae (baker yeast)2

51

Fig. 12. The phylogenetic relationships between the kinase domains of haspin kinases revealed by Maximum parsimony consensus analysis calculated from 18 equally parsimonious trees. Numbers depict bootstrap values (above 50%) derived from 200 bootstrap resamples. The GenBank accession numbers of the proteins in the tree are as follows: *H. sapiens* (AF289865), *A. thaliana* (AAC33205), *V. vinifera* (CAN65736), *P. patens* (XP_001777245), *O. lucimarinus* (XP_001417826), *O. tauri* (CAL54142), *A. mellifera* (XP_624666), *A. pisum* (XP_001943663), *A. gossypii* (NP_986039), *A. clavatus* (XP_001271873), *A. nidulans* (XP_659658), *A. niger* (XP_001402071), *A. terreus* (XP_001210832), *B. taurus* (NP_001070012), *B. fuckeliana* (XP_001552115), *B. malayi* (XP_001893934), *B. malayi* (XP_001902094), *C. briggsae* (XP_001671091), *C. elegans* (ZK177.2), *C. elegans* (NP_496965), *C. elegans* (NP_001033406), *C. elegans* (NP_741498), *C. elegans* (NP_001024960), *C. elegans* (AAO27842), *C. elegans* (NP_490768), *C. elegans* (NP_492043), *C. elegans* (NP_495212), *C. elegans* (NP_501030), *C. elegans* (NP_501839), *C. familiaris* (XP_854539), *C. immitis* (XP_001248658), *C. cinerea* (XP_001837441), *C. neoformans* (XP_570611), *D. rerio* (XP_686125), *D. discoideum* (XP_637732), *D. ananassae* (XP_001965899), *D. grimshawi* (XP_001992963), *D. melanogaster* (NP_001015349), *D. mojavensis* (XP_002004084), *D. persimilis* (XP_002023078), *D. virilise* (XP_002052375), *D. willistoni* (XP_002075104), *E. cuniculi* (NP_597598), *E. dispar* (XP_001741183), *G. gallus* (XP_425408), *L. bicolor* (XP_001877035), *M. mulatta* (XP_001090778), *M. grisea* (XP_369926), *M. globosa* (XP_001731553), *M. truncatula* (CA921439), *M. brevicollis* (XP_001749720), *M. musculus* (BAB00640), *N. vitripennis* (XP_001605930), *N. crassa* (XP_957293), *O. sativa* (NP_001060403), *P. troglodytes* (XP_001159222), *R. norvegicus* (XP_001080273), *S. cerevisiae* (CAA96721), *S. cerevisiae* (NP_009544), *S. officinarum* (CA122471), *S. pombe* (NP_593176), *T nigroviridis* (CAF92724), *T. castaneum* (XP_971131), *T. adhaerens* (XP_002110314), *T. aestivum* (TC348601), *U. maydis* (XP_756957), *X. laevis* (TC388096), and *Y. lipolytica* (XP_499618).

Table 3. Percent identity of AtHaspin with other haspin-like proteins. For comparison the conserved kinase domains were selected.

	Mammals		Monocots		Dicots	
	H. sapience	*M. musculus*	*S. officinarum*	*O. sativa*	*M. truncatula*	*V. vinifera*
Arabidopsis	37.6 %	38.6 %	65.2 %	63.6 %	76.3 %	76.7 %

4.3. AtHaspin is highly expressed in tissues with high level of cell proliferation and differentiation

Tissue type-specific expression pattern of AtHaspin was determined by semi-quantitative RT-PCR using the primers AtHaspin -295F and AtHaspin -295R (Table 1 and Fig. 14). To demonstrate equal amounts of cDNA, a primer pair specific for the nearly constitutively expressed elongation factor 1B (primers EF1β-F and EF1β-R) (Becher et al., 2004) was used for RT-PCR control experiments. High abundance of AtHaspin transcripts was detected in highly proliferating and differentiated tissues, like budding flowers and flowers in addition to the stem with shoot meristems (Fig. 13A). Figure 13B shows the expression data obtained from publicly available microarray expression data (Genevestigator, https://www.genevestigator. ethz.ch). The highest expression of AtHaspin was observed in the shoot apex and root tips. Together these data indicate that the expression of AtHaspin is consistent with the level of cell proliferation.

Based on publicly available microarray data (Menges et al., 2003) it is possible to conclude that the transcription profile of AtHaspin during the mitotic cell cycle is rather uniform (Fig. 13C). In contrast, cyclin B is highly active 8 h after the release from the aphidicolin block (blocks the cell cycle at early S-phase). The increase of cyclin B transcription coincides with entry into mitosis, when expression of B-type cyclins is unregulated (Shaul et al., 1996). Thus, these data demonstrate that AtHaspin transcription does not change during the mitotic cell-cycle.

A

Leaf | Cauline leaf | Stem & shoot meristem | Silique | Flower | Budding flower | H2O

AtHaspin

EF-1B

B

C

AtHaspin
Cycb1

absolute signal

Time after aphidicolin removal (h)
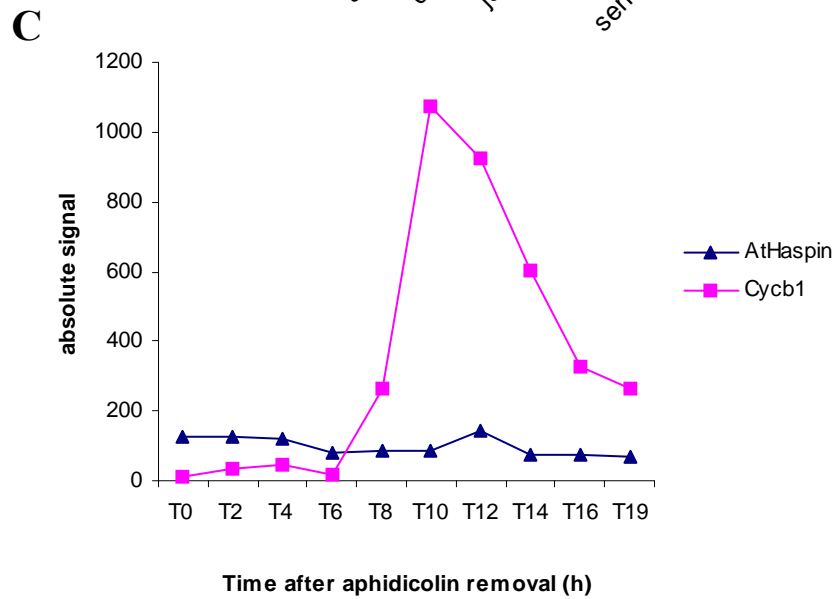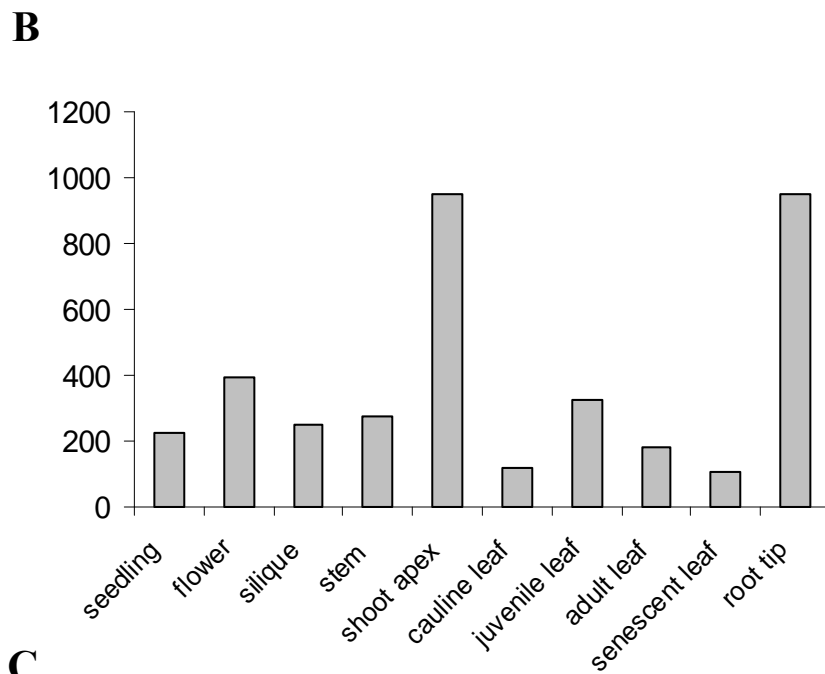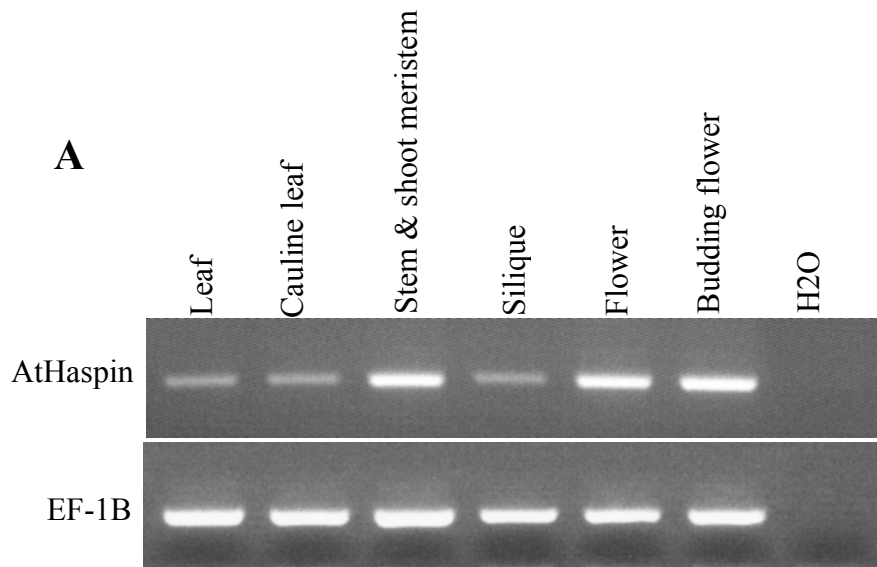
Fig. 13. Transcription analysis of AtHaspin.

(A) Semi-quantitative RT-PCR analysis of AtHaspin expression in different *Arabidopsis* tissues. Elongation factor 1B (EF-1B) was used as a control.

(B) AtHaspin expression behaviour deduced from microarray data (http://www.GeneVestigator.ethz.ch).

(C) mRNA profiles of AtHaspin during the mitotic cell cycle deduced from publicly available microarray data of synchronized *Arabidopsis* suspension cells (Menges et al., 2003). While cyclin Cycb1 is activated at the onset of mitosis, 8 h after release from the aphidicolin block, AtHaspin transcription does not show any changes during mitotic cell cycle.

4.4. Functional analysis of AtHaspin

To identify the function of AtHaspin, *Arabidopsis* mutant plants with altered activity of the AtHaspin gene were either selected (T-DNA insertion lines) or generated (overexpression and RNAi lines) and analysed.

4.4.1. Complete inactivation of AtHaspin by T-DNA insertion is lethal for plants

Four different *Arabidopsis* lines, Columbia ecotype (SALK_019798, GABI435H08, GABI 082D07, and GABI858F01) with T-DNA insertions in the promoter region or introns of the AtHaspin gene (available in SALK http://signal.salk.edu/cgi-bin/tdnaexpress and GABI-Kat, http://www.gabi-kat.de/db/) were identified and analysed. The relative positions of T-DNA insertions are indicated in figure 14. To identify homozygous T-DNA mutant plants, gDNA from about 20 plants per T-DNA line was isolated and PCR was performed using two combinations of different primer pairs illustrated in Table 4.
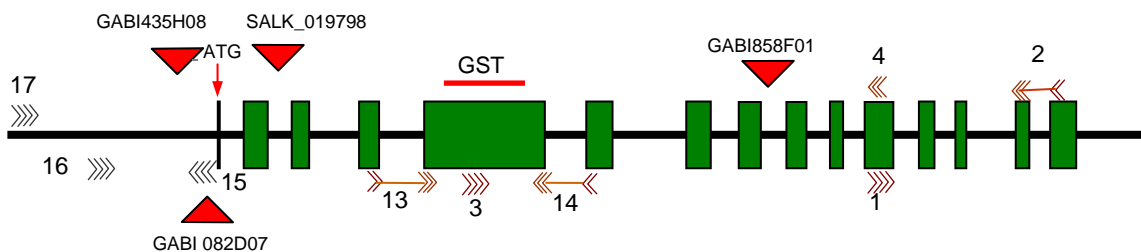
Fig. 14. Intron/exon gene structure of AtHaspin gene and the position of T-DNA insertions. Arrows indicate the position of primers (primer sequences are shown in Table 1). Red triangular showing the position of different T-DNA inserted in the haspin gene. The red line

(GST) is the position of the 400 bp AtHaspin-specific sequence tag to produce a hairpin RNAi construct.

Table 4. Primer combination used to confirm T-DNA insertion.

T-DNA lines	Gene -specific fragment	Gene/T-DNA insertion fragment
SALK_019798	(RP, LP)	(LB, RP)
GABI435H08	(435H08-F, 435H08-R)	(435H08-F, GABI-TDNA)
GABI 082D07	(082D07-F, 082D07-R)	(082D07-R ,GABI-TDNA)
GABI858F01	(858F01-F, 858F01-R)	(858F01-F, GABI-TDNA)

PCR on wild-type and homozygous T-DNA plants amplified only a gene-specific fragment or a gene/T-DNA insertion fragment, respectively. While PCR on heterozygous plants resulted in the amplification of both fragments (Fig. 15).
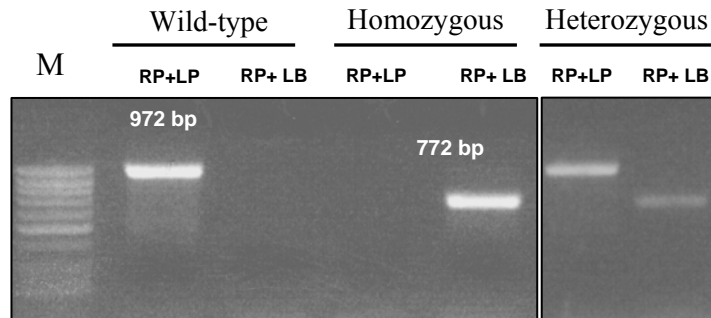
Fig. 15. PCR to select homozygous T-DNA plants. Figure shows an example of genomic PCR on SALK_019798 using two primer combinations (RP+LP and RP+LB). Wild-type plants revealed PCR products only using primers RP and LP, homozygous plants resulted in PCR products only using primers RP and LB, and PCR on heterozygous plants resulted in PCR products using both primer combinations.

Selected homozygous T-DNA plants (lines SALK_019798, GABI435H08, and GABI858F01) were analysed by semi-quantitative RT-PCR using the primers AtHaspin-295F and AtHaspin-

295R (intron-jumping primers to avoid amplification of genomic DNA) (arrows 1 and 2 in fig. 14). The RT-PCR experiments indicate that the level of AtHaspin expression does not notably differ between homozygous T-DNA mutants, and wild-type plants (Fig. 16). Likely, because the T-DNA insertions were located either in the 5'region upstream of the start codon in GABI435H08 line or in intron regions (GABI858F01 and SALK_019798) the transcription behaviour of AtHaspin was unaffected. Also phenotypically, no obvious differences were found between wild-type and T-DNA plants.
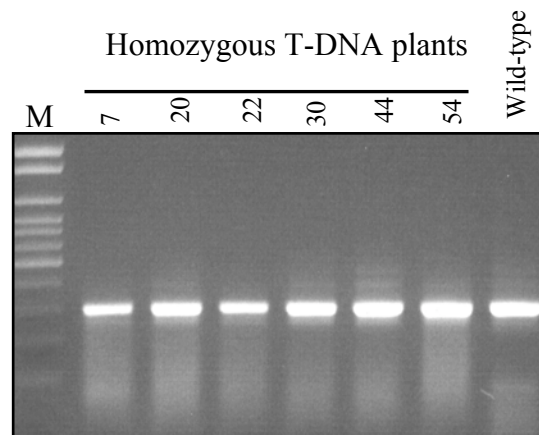
Fig. 16. Semi-quantitative RT-PCR of different homozygous T-DNA plants (SALK-01978) and a wild-type plant using an AtHaspin-specific primer pair.

In line GABI 082D07, the T-DNA insertion was located in 5'untranslated region (UTR) close to the start codon. Notably, no homozygous T-DNA plant for the haspin gene (*has/has*) was found for this T-DNA insertion line. To demonstrate the non-existence of homozygous T-DNA plants (*has/has*), the progeny of heterozygous plants (GABI 082D07-7 and GABI 082D07-14) was analysed by PCR (Table 5). However, no homozygous T-DNA plant (*has/has*) was found in the progeny of heterozygous plants. The PCR product was cloned and the correct position of inserted T-DNA was confirmed by sequencing. This finding suggests that a knockout of AtHaspin is lethal for plants, indicating an essential and important roll for AtHaspin.

Table 5. Genotyping of progenies of the T-DNA heterozygous plants (*Has/has*) line GABI 082D07.

	Heterozygous (*HAS/has*)	Wild-type (*HAS/HAS*)	Homozygous (*has/has*)	Total analysed plants
Number of plants	33	18	0	51
Percentage of plants	64%	32%	0%	100%

4.4.2. Reduction of AtHaspin transcription activity by RNA interference (RNAi)

As the analysis of T-DNA *Arabidopsis* insertion lines did not result in the identification of viable knockout T-DNA plants with reduced AtHaspin transcription activity, we intended to reduce the AtHaspin activity via RNA interference (RNAi). We used the pAgrikola vector (Hilson et al., 2004), containing a 400 bp long AtHaspin-specific gene fragment (GST), which shared no significant similarity with any other region in the *Arabidopsis* genome, provided by the Nottingham *Arabidopsis* Stock Center (NASC: http://arabidopsis.info/). After transformation of *A. tumefaciens* competent cells containing the binary vector GV3101::pSOUP with the pAgrikola-AtHaspin construct PCR reactions were performed to validate the pAgrikola-AtHaspin construct (Fig. 17) using different primer pair combinations (listed in Table 6, the primer positions are shown in Fig. 14). Existence of four different amplified DNA fragments in each colony indicates the presence of both hpRNA expression constructs containing an intron spacer with original or flipped orientation (Fig. 17).

Table 6. Primer combinations used for validation of the AtHaspin-RNAi construct and size of PCR fragments

Mix	Primer combination		Size of amplicons (bp)
1	Agri 51	Agri 56	645
2	Agri 51	Agri 64	842
3	Agri 56	Agri 69	545
4	Agri 64	Agri 69	742
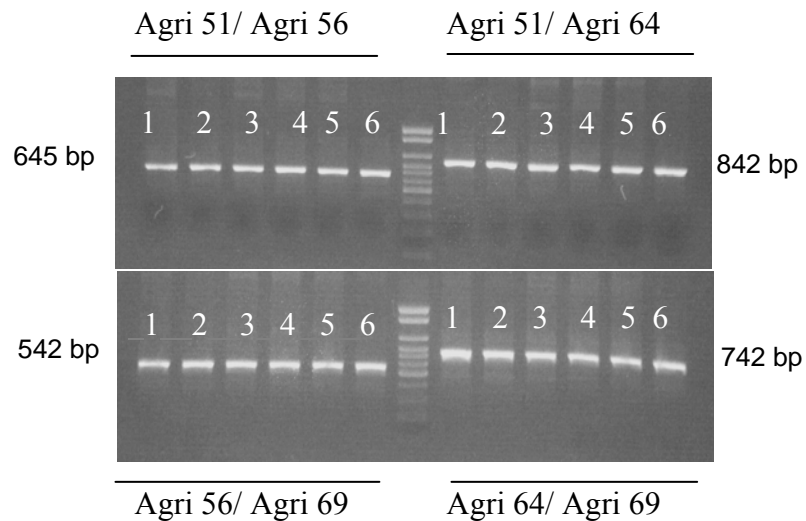
Fig. 17. PCR verification of individual *A. tumefaciens* colonies containing the pAgrikola-AtHaspin construct. Primer combinations used as shown in Table 6.

After *Arabidopsis* plants were transformed with the pAgrikola-AtHaspin-RNAi construct, the preselected plant progeny was PCR genotyped using the same PCR selection strategy (primer combination listed in Table 6). Semi-quantitative RT-PCR was performed on 25 AtHaspin-RNAi T1 plants using the primers AtHaspin-571 F and AtHaspin-571 R (arrows 13 and 14 in figure 14) to select plants with a reduced activity of AtHaspin (Fig. 18). RT-PCR resulted in the identification of RNAi plants (plant 4, 7, 8, 22, 32, 35, 39, 46, 53, 62, 64, 67, 82, 96, 101,) with a reduced transcription activity of AtHaspin.
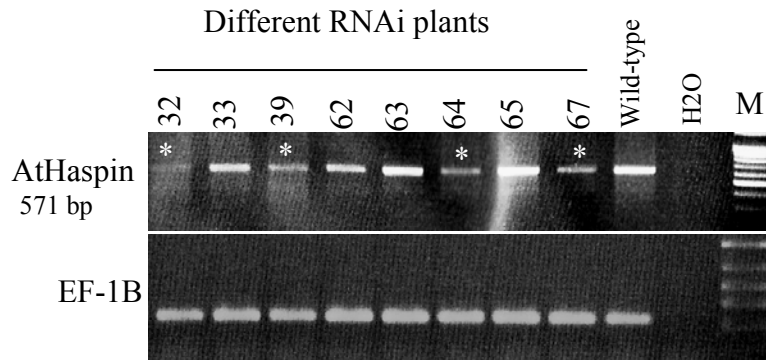
Fig. 18. Semi-quantitative RT-PCR analysis of AtHaspin-RNAi plants. Plants with a reduced expression activity of AtHaspin are marked with asterisks. Elongation factor 1B-specific primers were used as control.

4.4.3. Down regulation of AtHaspin results in the formation of plants with adventitious shoots and shoot meristems, abnormal flowers and reduced fertility

RNAi plants with reduced AtHaspin transcription activity showed pleiotropic developmental defects, including multi-rosettes, secondary shoot formation, defection in vascular formation, abnormal inflorescences and flower morphology as well as reduced fertility (Fig. 19). Because we used the RNAi approach we obtained a series of strong, intermediate and weak phenotypes. One RNAi plant formed a pin-like primary inflorescence without flowers or flower related structures (Fig. 19F- I). Secondary shoots of the same plant formed deformed floral organs (Fig. 19D). Rosette and cauline leaves were strongly curled and crinkled (Fig. 19 F). However, among 110 T1 RNAi plants only plant number 101 displayed such a strong pin-like phenotype (Table 7). Out of 110 RNAi plants, 37 plants (in 34%) revealed the simultaneous formation of additional rosettes and shoots. The obtained bushy phenotype could be the consequence of a loss of apical dominance (Reintanz et al., 2001) (Fig. 19D, E, J; Table 7). Juvenile rosette leaves were strongly crinkled and curled, and the two halves of the blade had the appearance of being hinged (Fig. 19B). In this group of plants fertility was often reduced (Fig. 19K, L).

Table 7. Phenotypical analysis of T1 RNAi plants and percentage of plants with reduction of AtHaspin expression in each phenotypic group.

Number of T1 RNAi plants	Phenotypes	% of plants with reduced AtHaspin transcription activity (based on semi-quantitative RT-PCR)
1	pin-formed inflorescence	100%
37	bushy*	86%
72	non-bushy**	42%

* bushy: a plant with ≥4 branches.
** non-bushy: a plant with <4 branches

RNAi lines were selected for single T-DNA insertions by Southern hybridization to identify plants with a stable reduction of AtHaspin activity (Fig. 20). Therefore, genomic DNA of 53 RNAi T1 plants were hybridized with a T-DNA specific probe. 35% of samples did not reveal any hybridization band because of technical limitations. 21% of plants had only one T-DNA insertion (plant 29, 35, 42, 49, 68, 70, 75, 81, 82, 89, 93) and the remaining plants possessed more than one T-DNA insertion.
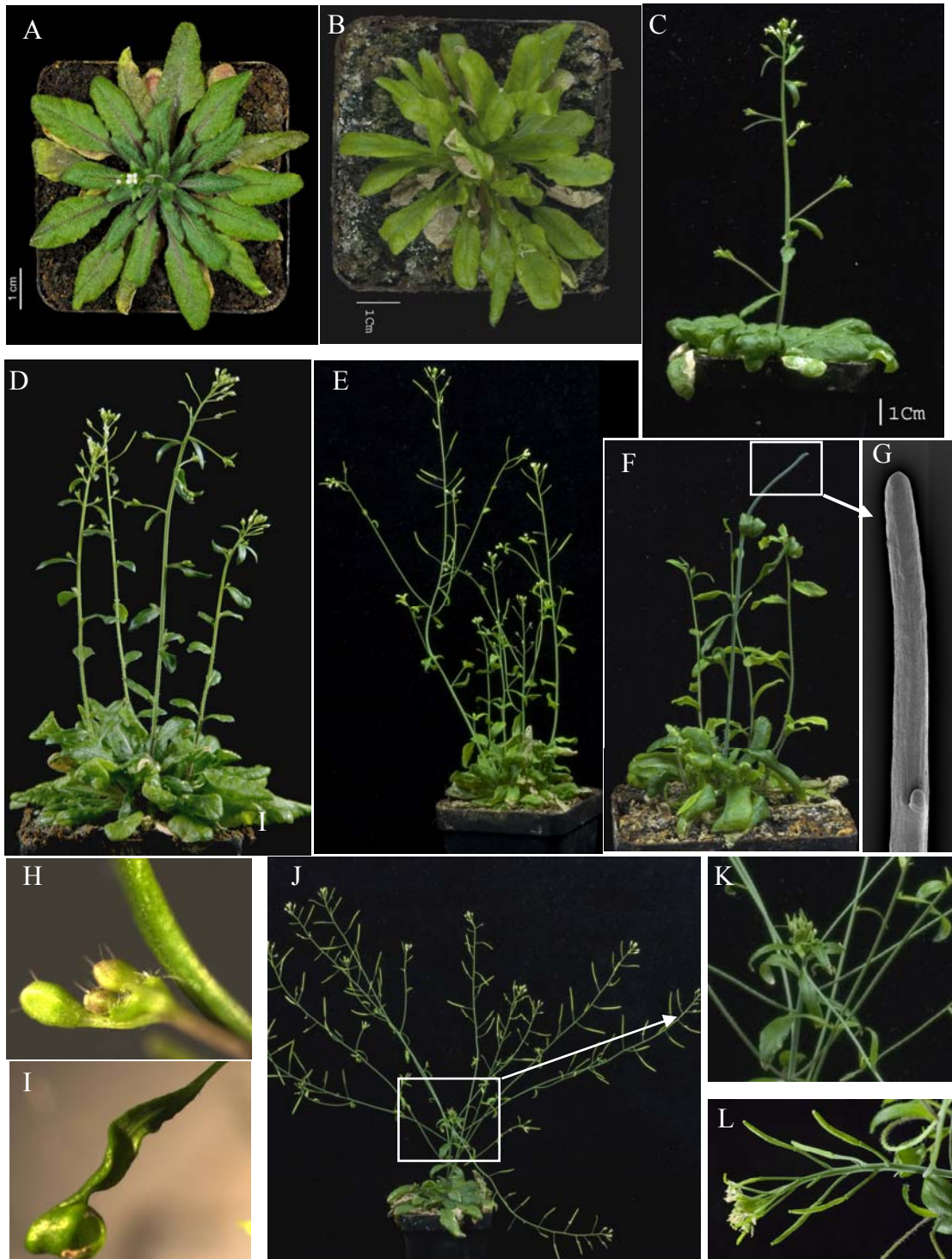
Fig. 19. Phenotype of AtHaspin knockdown RNAi T1 plants. (A, C) wild-type; (B) Developed rosette leaves are crinkled. (F) pin-like primary inflorescence without flowers or flower related structures (RNAi plant 101). (G) Scanning electron micrograph of the pin-like inflorescence. (H, I) abnormal flower and crinkled cauline leaf (RNAi plant 101). AtHaspin-RNAi plants (D, E , J) showing multi-shoots and bushy phenotype, semi fertile and undeveloped siliques, and abnormal flowers (K) and (L).
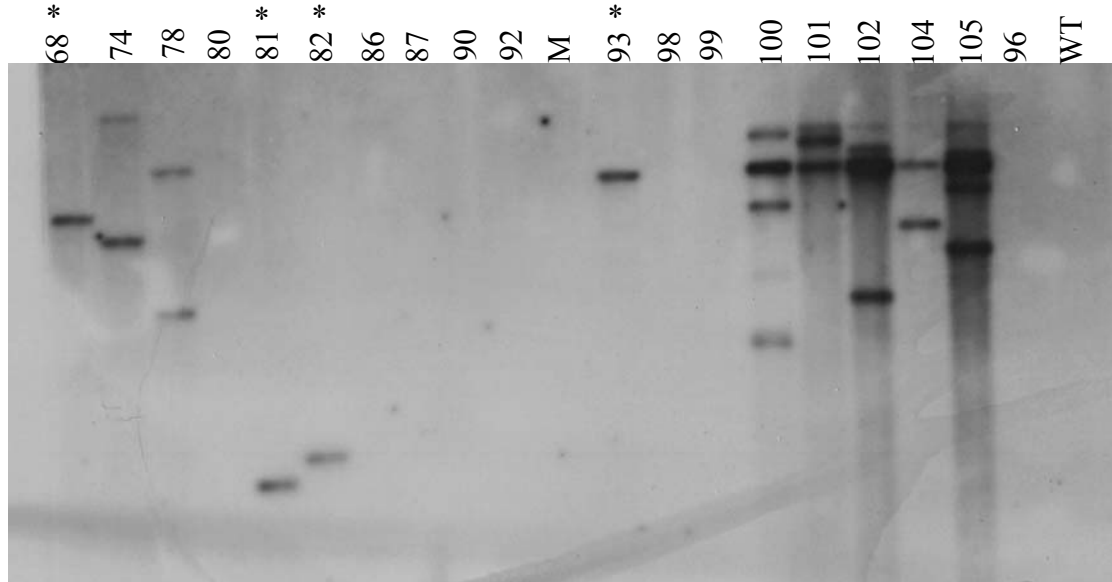
Fig. 20. Southern hybridization of different AtHaspin-RNAi plants and a wild-type plant (WT). Genomic DNA was digested with *Eco*RI and hybridized with a labelled BAR gene specific probe. Plants with a single copy T-DNA insertion are marked with asterisks.

Based on the comparison of the T-DNA insertion copy numbers and the observed phenotypes we could not find any correlation between T-DNA copy number and phenotype (number of branches, Table 8). The RNAi-plant 101 possessed 3 copies of the T-DNA. However, most of the plants with a bushy phenotype showed a lower expression of AtHaspin compared to wild-type plants (Table 7).

Table 8. Percentage of bushy and non-bushy plants and number of RNAi-T-DNA copies

	Bushy plants (in %)	Non-bushy plants (in %)
Single copy insertion	91%	10%
2 copy insertion	70%	30%
Multi copy insertion	54%	46%

To identify homozygous lines at the T3 generation BASTA selection was performed on the progeny of the RNAi-T1 plants 29, 35, 67, 68, 70, 75, 78, 81, 82, 93, 96, 101. Based on this selection we indentified the homozygous RNAi lines (68-1, 78-8, 78-7 and 68). These lines

showed a similar bushy phenotype with crinkled leaves and shoots (Fig. 21B, C), semifertility (Fig. 21C, F), and a prevalently enhanced number of secondary shoots and multi-rosettes formation (Fig 21A, D, E). Shoot meristems also emerged from the axils of leaves (Fig. 21D).

Taken together, RNAi-based down regulation of AtHaspin seems to result in plant phenotypes that are comparable with phenotypes of plants treated with auxin efflux inhibitors (Okada et al., 1991) or plants with a modified auxin transport (e.g. mutant 'pin formed 1' (pin1) (Okada et al., 1991) or '*PINOID*'(Bennett et al., 1995) or modified shoot meristem formation (e. g. mutant '*SCHIZOID*'(Parsons et al., 2000) or '*WUSCHEL*'(Laux et al., 1996).
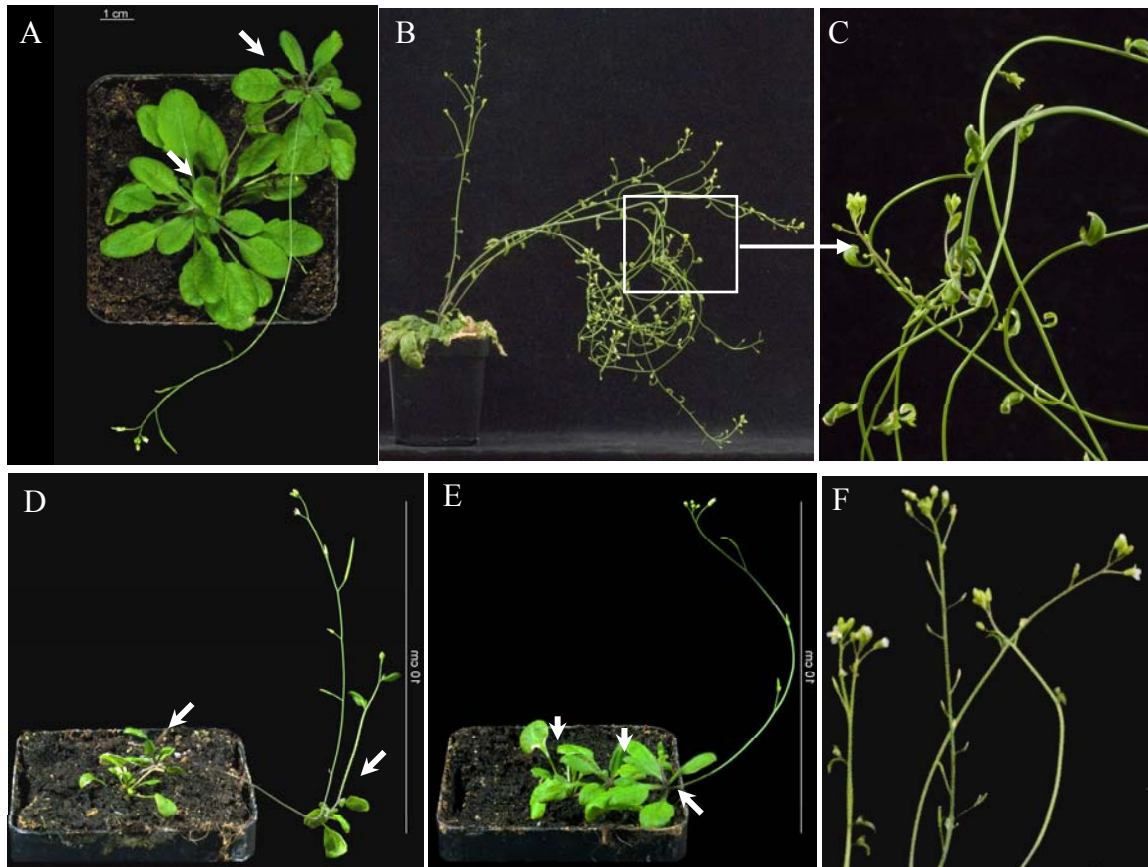
Fig. 21. Homozygous AtHaspin-RNAi lines illustrating multi-rosettes and multi-shoots formation. RNAi homozygous lines 68-1 (A), 78-7 (D) and 78-8 (E) with adventitious shoot meristem and rosette formation. Bushy phenotype with formation of secondary shoot with curly leaves and shoot (B, C) and semi fertile siliques (F) was observed in homozygous lines. Arrows indicate the position of adventitious shoot meristems and lateral rosettes.

4.4.3.1. Pollen viability analysis of AtHaspin-RNAi plants

To determine whether the semi-fertility of AtHaspin-RNAi plants is the consequence of an abnormal male gametogenesis, we investigated the pollen viability using the Alexander staining method (Alexander, 1969). Based on the counting of viable pollen in different RNAi lines we found a significant reduction in the number of viable pollen concluding that the down-regulation of AtHaspin transcription activity affects the male gametogenesis and hence efficiency of fertilization (Fig. 22).
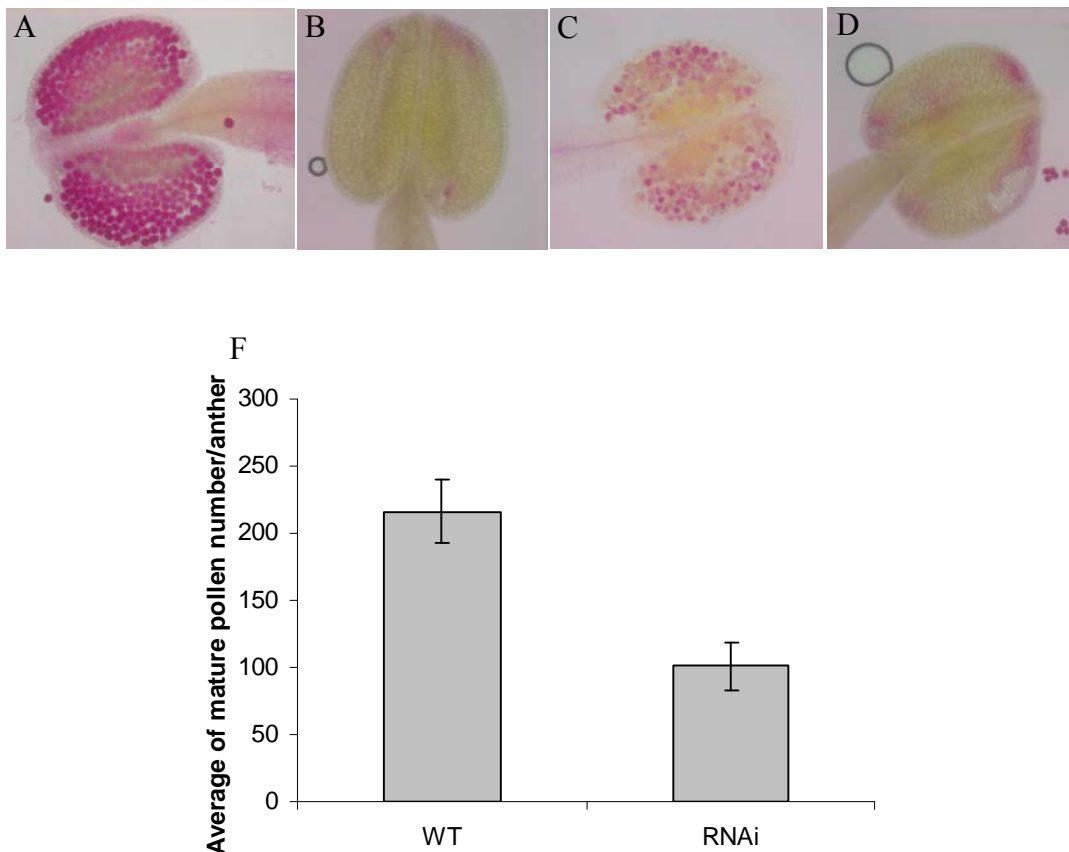
Fig. 22. Alexander staining of pollen from wild-type (A) and RNAi AtHaspin anthers (B–D). (A) Mature pollen from a wild-type plant shows a strong Alexander staining in all anthers. (B-D) AtHaspin-RNAi plants revealed a reduced staining of pollen.
(F) Histogram showing the average number of viable pollen per anther of 4 different RNAi plants and of wild-type plants. About 18 anthers were analysed per plant. RNAi plants showed a significant reduction in average number of viable pollen compared to wild-type plants with the p-value of 0.012 according to t-test. The mill bars indicate the standard error of the samples.

4.4.3.2. AtHaspin-RNAi plants show defects in vascular formation and maturation

Based on the similar phenotype of AtHaspin-RNAi plants with the auxin transporter mutants (pin1, pid), we analysed the vascular patterning of RNAi plants to characterize better the function of AtHaspin. One characteristic of auxin transporter mutant plants, like pin1 and pid mutants is the defection in vascular formation of inflorescence stems and nonfloral tissues including cotyledons and rosette leaves (Okada et al., 1991; Bennett et al., 1995; Christensen et al., 2000).

In order to investigate the venation pattern of AtHaspin-RNAi plants, cross sections were performed on stems of few selected RNAi and wild-type plants. Subsequently undeveloped and defected vascular bundles were detected in AtHaspin-RNAi plants (Fig. 23B).
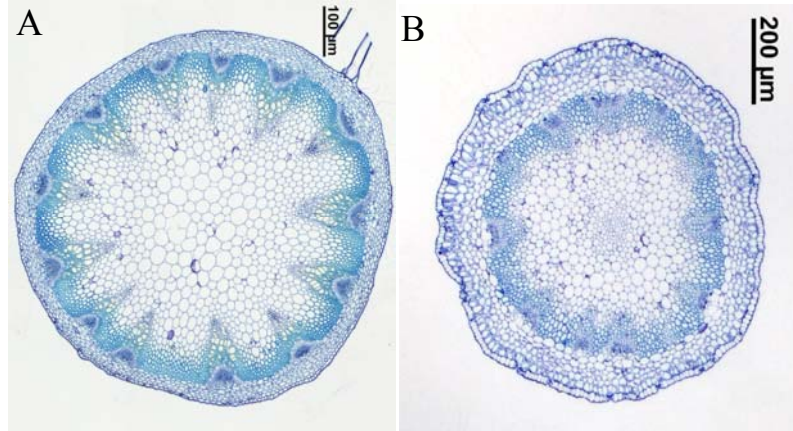
Fig. 23. Analysis of vascular patterning in the stem cross sections of AtHaspin mutants. (A) Stem of a wild-type *Arabidopsis* plant, (B) an of a AtHaspin-RNAi mutant (plant 101).

Next, we compared the vascular patterns of wild-type and of AtHaspin-RNAi cotyledons. The vascular patterning in wild-type cotyledons is highly reproducible, with a recognizable pattern of one primary vein that is continuous with the hypocotyle vasculature, and typically four secondary veins that branch from primary vein (Fig. 24A). Nonetheless, slight differences in developmental stages of individual wild-type seedlings caused small variation of the vascular pattern (Fig. 24F). In contrast, in AtHaspin-RNAi seedlings, the vascular strands of cotyledons were often poorly interconnected (Fig. 24B-E) and we observed frequently an aberrant and undeveloped pattern of the vascular system (Fig. 24 F). Thus, down regulation of AtHaspin seems to interfere with the development of the vascular system in stems and in cotyledons.
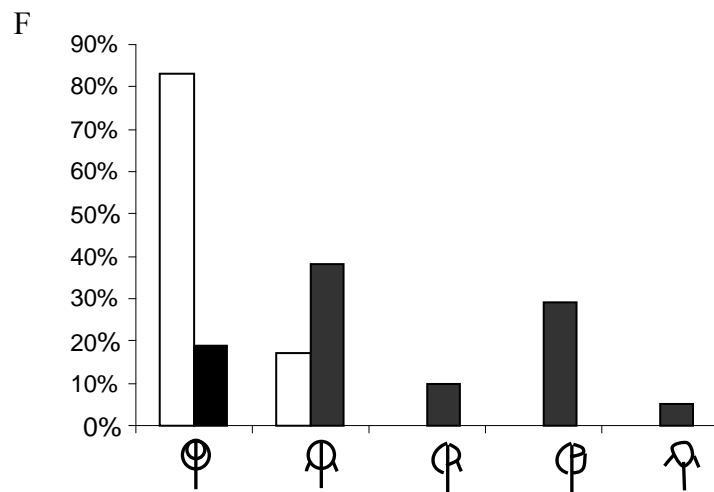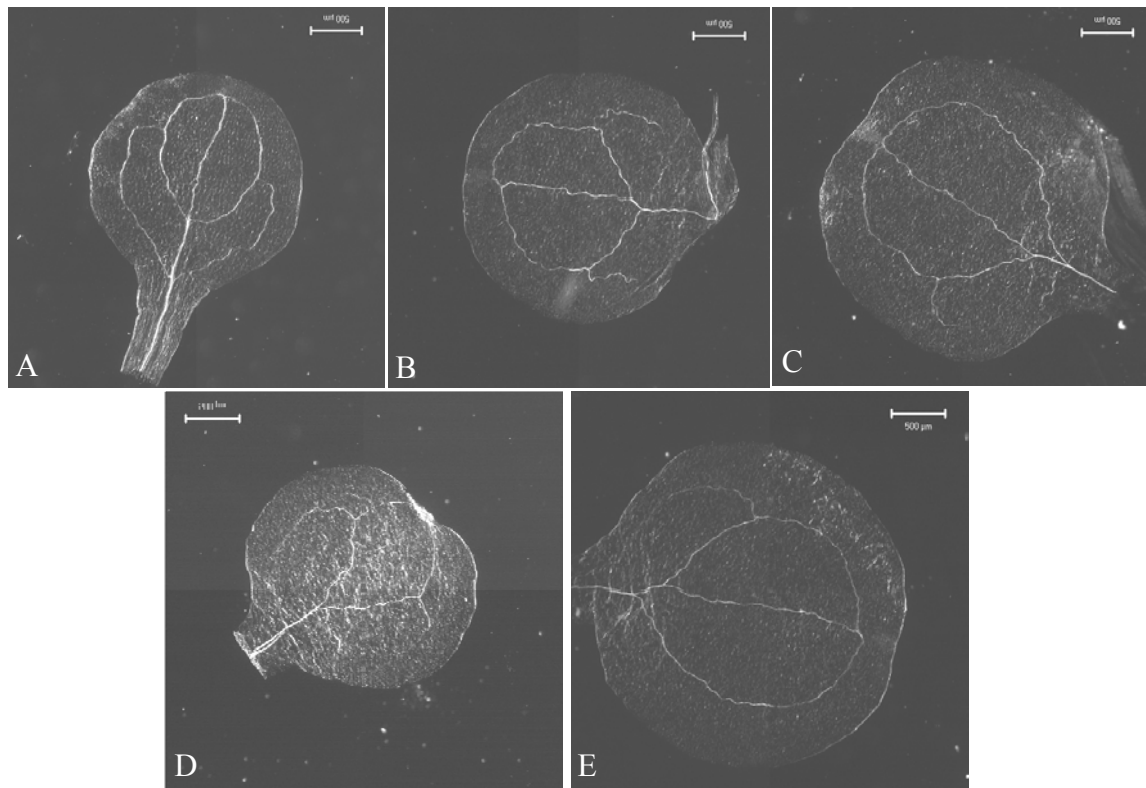
Fig. 24. Vascular defects in AtHaspin-RNAi plants.
Vascular patterning in cotyledons of (A) wild-type and (B-E) different RNAi plants. Scale bars indicate 0.5 mm. (F) Diagram illustrates percentage of vascular pattern complexity in wild-type (white bars) and RNAi plants (black bars) in 80 cotyledons analysed.

4.4.4. AtHaspin promoter is active in young vascular tissue of flower organs, shoot apexes and embryos

To obtain a reliable impression about the distribution and cellular localisation of AtHaspin transcripts, we fused 1500 bp and 705 bp long genomic fragments upstream of the start codon of the AtHaspin gene to the GUS reporter gene using the vector pMDC162 (Fig. 8D-E). We tested two promoter fragments of different length (1500 bp and 705 bp) for the AtHaspin gene. The application of two different sized fragments allowed to discriminate possible effects of the 5'neighbor gene. Because, AtHaspin has a 1600 bp long common intergenic region with the gene At1g09440 which is in reverse orientation with the AtHaspin, and predicted to be the promoter region of both genes (Shahmuradov et al., 2005) (http://mendel.cs.rhul.ac.uk/mendel.php?topic=fgen). As negative control, we used an empty pMDC162 vector.

Transformation of plants with the empty vector did not result in a detectable GUS signal (Fig. 25I). GUS expression in seedlings was mainly detected in the vascular tissue of young leaves, but not in the vascular system of the roots. The strongest signal was observed in the shoot apex (Fig. 25H, K). In inflorescences, expression was detected in vascular system of the pedicles (Fig. 25A), of developing sepals (Fig. 25J), and in the vascular part of stamens (Fig. 25B, D). Pistils revealed a strong expression in the bases part of the pistil (Fig. 25F). AtHaspin is also expressed in funiculus of developing ovules (Fig. 25G) and cotyledon primordia of mature embryos (Fig. 25C). No differences were observed between plants with 1500 bp or 705 bp long promoter GUS fusion constructs regarding the distribution and intensity of promoter$_{AtHaspin}$::GUS signals.
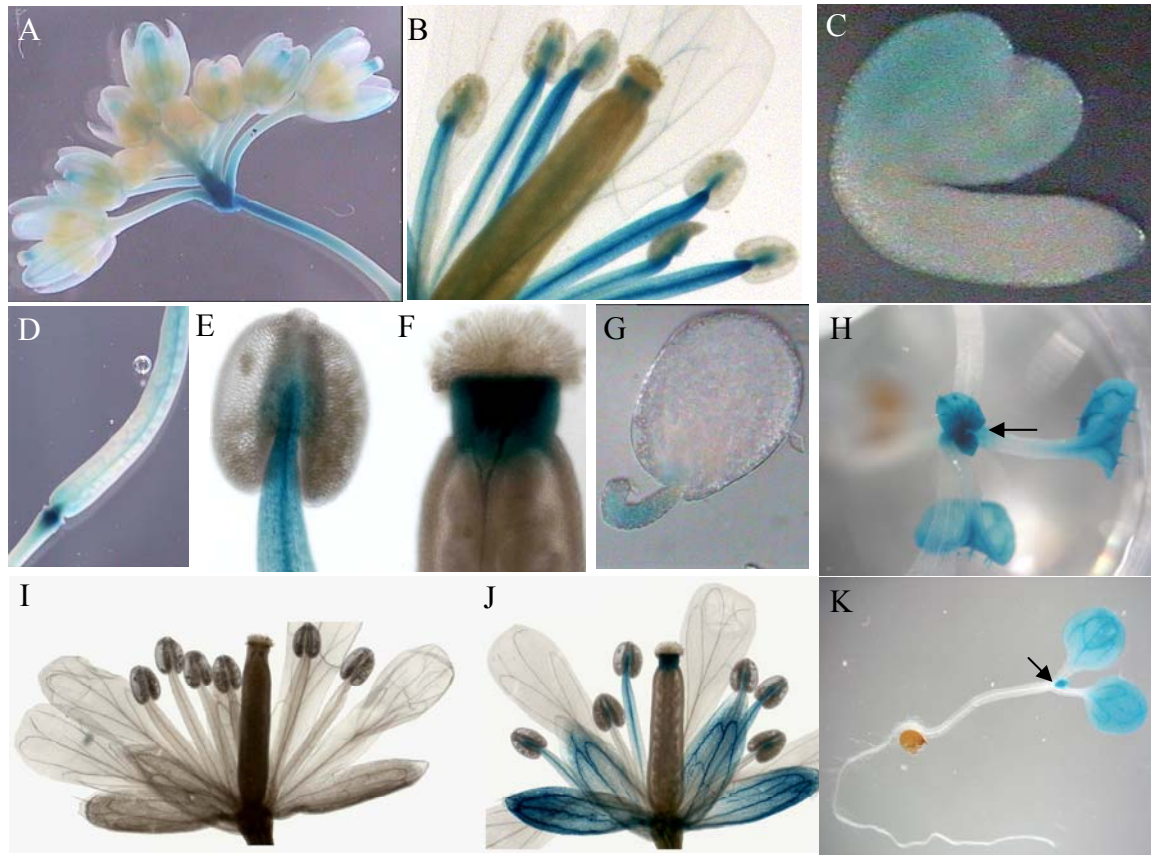
Fig. 25. Promoter$_{AtHaspin}$::GUS activity in different tissues of *A. thaliana* plants. Promoter$_{AtHaspin}$::GUS signals were observed in inflorescences and pedicles (A), vascular system of developing sepals (J) and stamens (B, E, J). In the pistil, expression was detected in the vascular system and strongly in the bases of the style (D, F) and in the funiculus of the fertilized ovules (G). In young seedlings (H, K) promoter$_{AtHaspin}$::GUS was mainly localised in the vascular system of the cotyledons, young leaves and the shoot apical meristem and leaf primordia (arrows). During the embryogenesis promoter$_{AtHaspin}$::GUS is localised to the cotyledon primordia (C). (I) The empty GUS vector as negative did not show any GUS activity.

A similar promoter analysis was conducted with GFP reporter constructs using the vector pMDC107 (Fig. 8F). However, no reliable GFP signals were detected neither by confocal or fluorescence microscopy. Suggesting that the strength of the AtHaspin promoter fragments tested is too weak for the detection of GFP signals.

The AtHaspin promoter GUS localisation pattern correlates with the phenotype found for knockdown RNAi plants, i.e. defection in floral organs and vascular formation, and suggests the importance of AtHaspin function in the development of these organs. GUS localisation

study also confirmed the RT-PCR results (Fig. 13A), and was comparable with the AtHaspin expression-microarray data (Fig. 13B), except for root tips. In roots there were no GUS signals detected.

4.4.5. Cellular and subcellular localisation of AtHaspin proteins

To determine the cellular and subcellular localisation of AtHaspin the following experiments were performed.

4.4.5.1. Analysis of 35S::YFP-AtHaspin signals confirms AtHaspin promoter expression data

Complete cDNA of AtHaspin was fused to the YFP reporter gene under the control of the constitutive cauliflower mosaic virus (CaMV) 35S promoter to investigate the subcellular localisation of AtHaspin (Fig. 8B). Strong 35S::YFP-AtHaspin signals were detected in vascular bundles of the leaf, stem, mature embryo (Fig. 26 A,D,I), in different parts of flower including sepal, petal, stamen, and pistil (Fig. 26E-H), in funiculus of the developing ovules (Fig. 26K) and in the seed endosperm (Fig. 26J). In primary and lateral roots, strong YFP signals were detected in the vascular system (Fig. 26B, C). As negative control the empty vector pEarleyGate104 (35S::YFP) was used, and fluorescence signals were found in peripheral regions of leaves but not in their vascular tissue (Fig. 26M). Notably, YFP signals of the negative control (empty vector) were observed in the vascular system of roots (Fig. 26L).

To test whether YFP-AtHaspin signals are cytosolic or cell wall localised plant tissue was treated with a sugar solution to stimulate plasmolysis. After induction of plasmolysis we detected cytosolic derived YFP-AtHaspin signals (Fig. 26J). Surprisingly, no YFP signals were detected in nuclei of transformed plants (Fig. 26P). In difference, YFP signals derived from the empty reporter vector localised in both, the cytosolic cytoplasm and the nucleus (Fig. 26O).
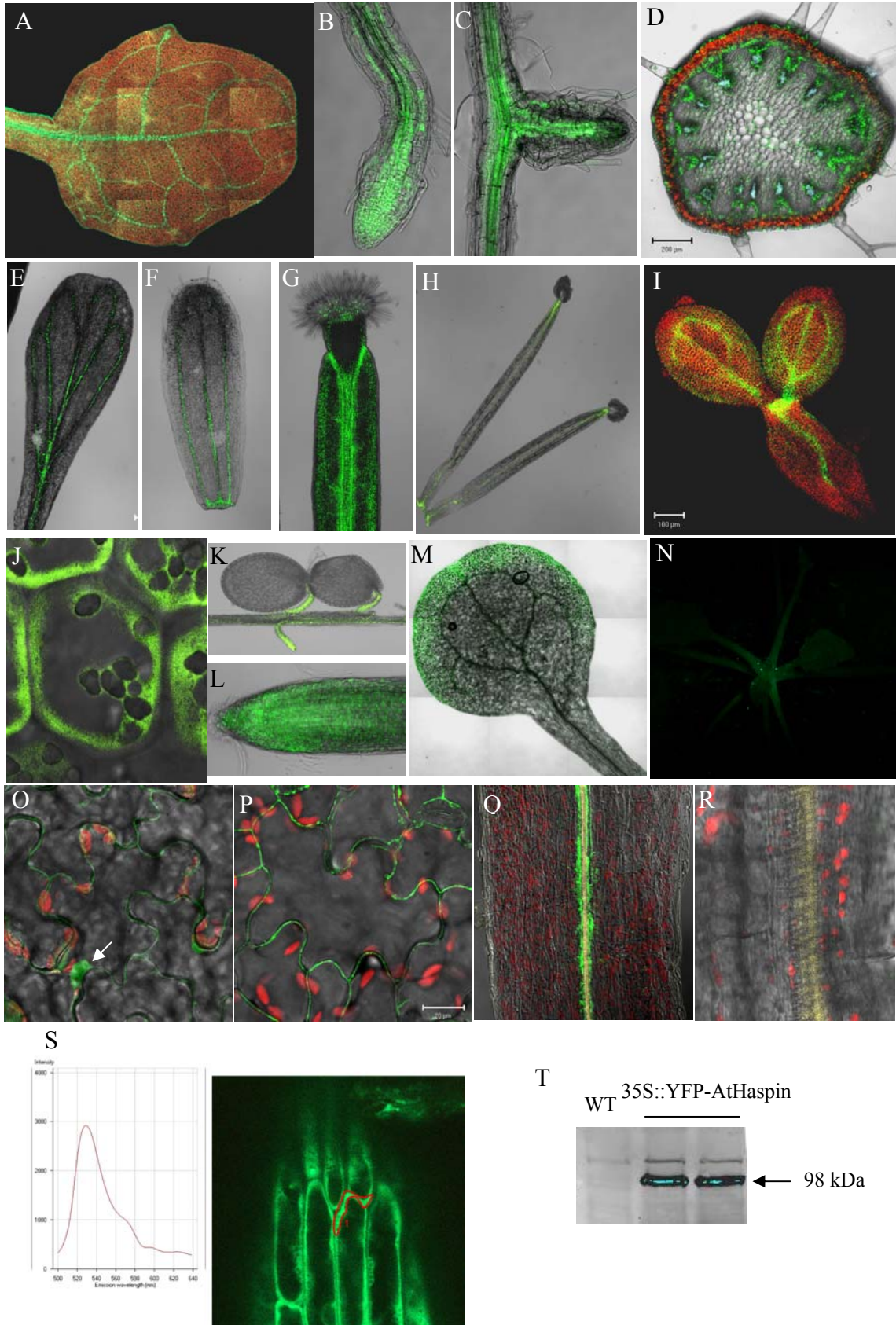
Fig. 26. YFP expression signals of plants transformed with 35S::YFP-AtHaspin or empty 35S::YFP as negative control (A-R).

YFP signals are mainly localised in the vascular tissue of leaf (A), root (B, C), flower component (E-H) and developed embryo (I). A transverse section (D) and longitudinal section (Q) through the stem shows that YFP-AtHaspin signals are highly expressed in vascular phloem and cambium, while the empty control vector did not result in YFP signals in the vascular system of the stem (R). In pistils, expression is detected in the vascular tissue of style and septum (G) and in the funiculus of fertilized ovules (K). YFP localisation in seed endosperm (J) and leaf epidermal cells (P) revealed that AtHaspin is a cytosolic protein. In contrast, YFP signals of empty 35S::YFP mutant plants were observed in the nucleus (arrow) of epidermal cells (O) and of root tips (L). (N) Strong signals were observed in the shoot apex region of the analysed 35S::YFP-AtHaspin seedlings. (S) Wavelength of YFP signals was validated by confocal microscopy around 527nm. (T) Western blot analysis on 35S:YFP-AtHaspin plants revealed corresponding YFP-AtHaspin protein bands (arrow).

To validate the YFP signal, the wavelength of the fluorescence signal was measured for all confocal microscopy images (Fig. 26S). In addition, we performed Western blotting using an anti-GFP antibody to validate the existence of YFP-AtHaspin fusion protein in the transformed plants (Fig. 26T). Proteins of expected size (98 kDa) were revealed. Hence, the localisation of the YFP-AtHaspin fusion protein in the vascular system of different tissues and meristematic cells is comparable with the promoter$_{AtHaspin}$::GUS signals (Fig. 25) and AtHaspin transcription results (Fig. 13A, B).

4.4.5.2. 35S::YFP-AtHaspin signals are not cell cycle-dependent in mitotic cells

To analyse the distribution of the AtHaspin protein during the mitotic cell division, squashed flower buds of a 35S::YFP-AtHaspin plant were simultaneously labeled with a mouse anti-GFP antibody and an antibody recognizing histone H3 phosphorylated at threonine 3 (H3Thr3ph). Unlike the distribution of phosphorylated histone H3Thr3, no cell cycle-dependent distribution of anti-AtHaspin signals was found in dividing cells (Fig. 27). Thus, our experiment failed to detect any cell-cycle dependent distribution of YFP-AtHaspin signals. However, this experiment should be repeated using other tissue and GFP-antibody sources.

| DNA | YFP-AtHaspin | Histone H3Thr3ph | Merged |
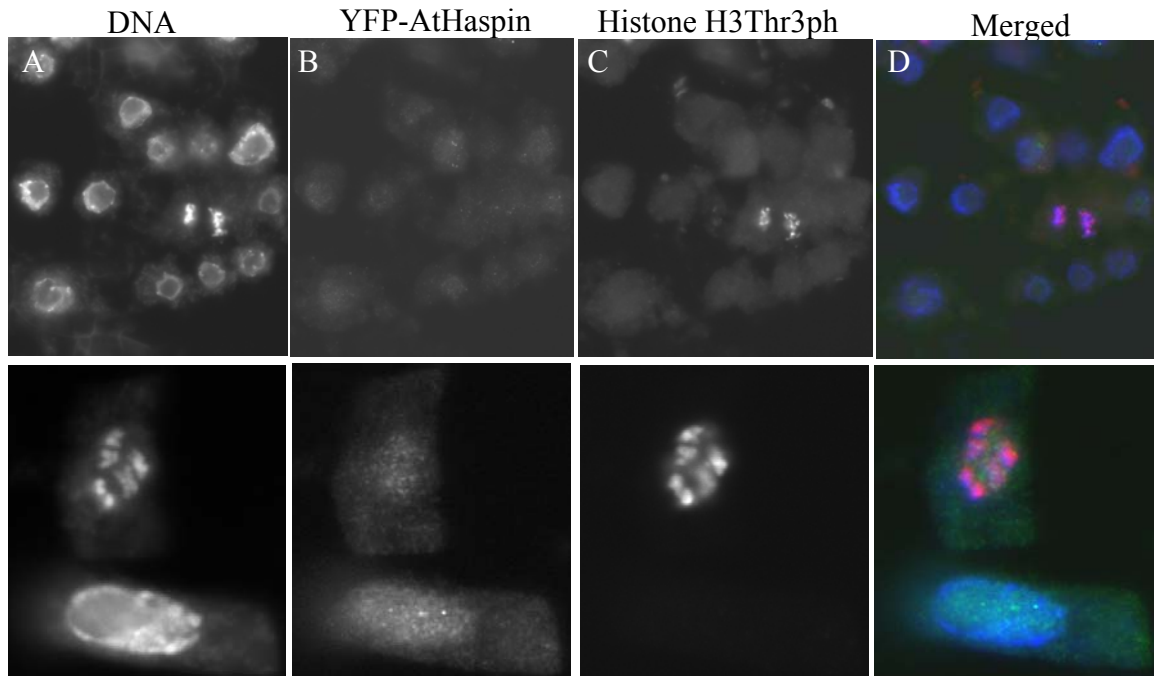
Fig. 27. Double immunostaining of *A. thaliana* cells prepared from flower buds of a 35S::YFP-AtHaspin plant with antibodies specific for anti-GFP (B) and for phosphorylated histone H3 at threonine 3 (C). No cell cycle-dependent signals were found for AtHaspin. (A) DNA was counterstained with DAPI. The merged pictures show DAPI in blue, anti-YFP in green and anti-H3Thr3ph in red.

4.4.5.3. Characterisation of putative AtHaspin-specific antibodies

Rabbit polyclonal anti-serum against two KLH-conjugated peptides corresponding to the amino acid residues 57-71 and 506-520 of AtHaspin was generated (double peptide antibody generated by Eurogentec) to obtain an AtHaspin-specific antibody. To determine whether AtHaspin associates with condensed chromosomes during cell division as mammalian haspin does (Dai et al., 2005), we performed immunostaining experiments on root tips from two-day-old seedlings of wild-type *A. thaliana* plants. Three different immune sera (38, 66 and 90 days after immunization) of two different rabbits were used for immunostaining experiments. Pre-immune sera were used as negative control. Squashed wild-type root tips were immunostained with three different concentrations of the putative anti-AtHaspin antibodies (1:500, 1:300, 1:100 in PBS with 1% BSA). Microscopical analysis did not reveal specific immunosignals regarding AtHaspin, neither in dividing cells nor in interphase cells (Fig. 28A-C). In addition, the distribution pattern of immunofluorescence signals derived from pre-immune serum was

similar to other immune sera (Fig. 28D). Hence, the generated antibodies are not AtHaspin-specific and therefore are not suitable for *in situ* detection of the AtHaspin protein.
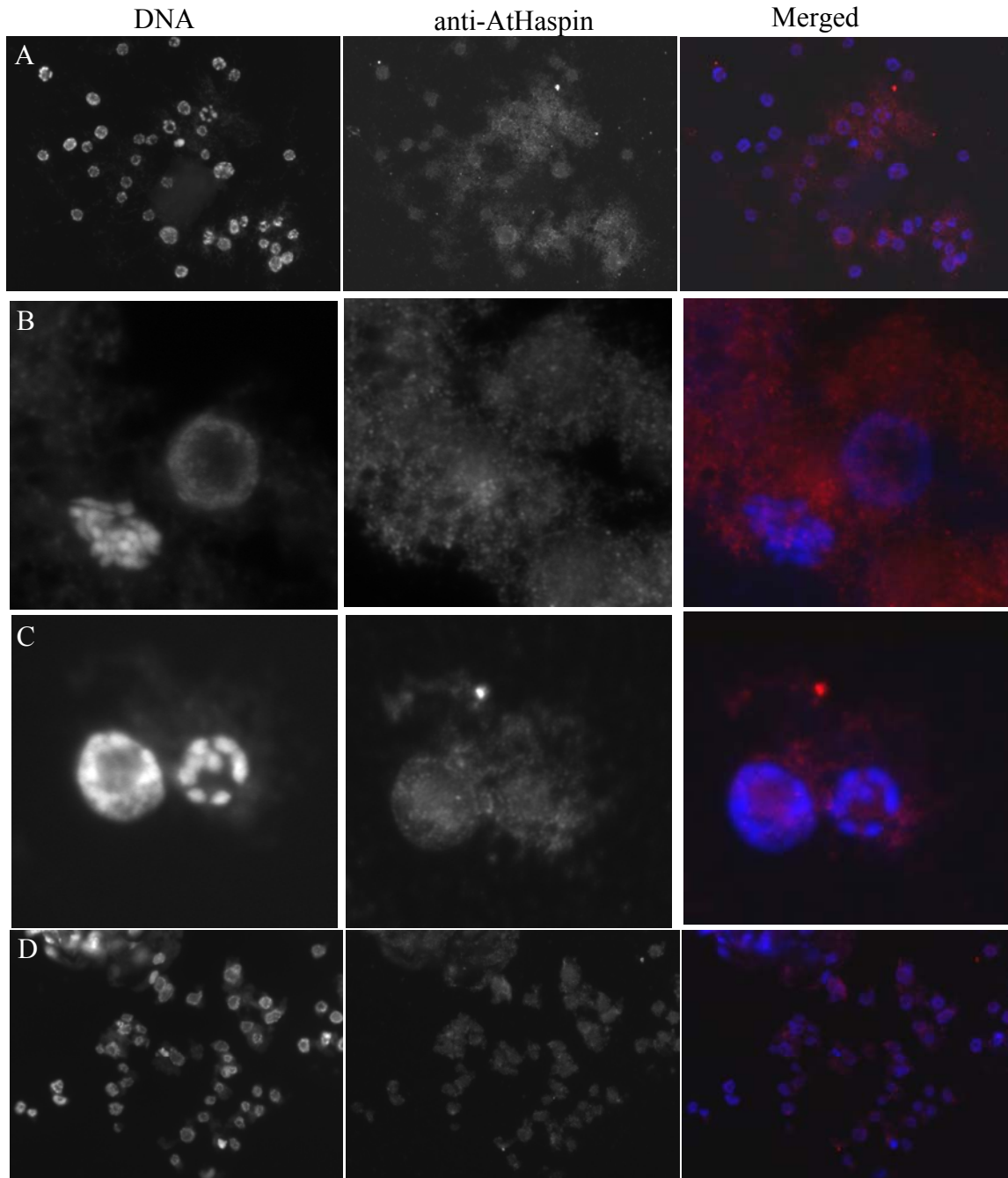
Fig. 28. Immunostaining experiment using a putative rabbit anti-AtHaspin peptide antibody (A-C) and rabbit pre-immune serum as control (D). DNA was counterstained with DAPI. The merged pictures show DAPI in blue and rabbit antibody signals in red.

In addition, we decided to test the specificity of the AtHaspin peptide antibody by Western blot analysis on total protein extracts isolated from cultured suspension cells and from different parts of wild-type *A. thaliana* plants. However, our immunoblotting experiments on *A. thaliana* total proteins (Fig. 29) using anti-AtHaspin antibodies did not show a specific immunoreaction. Therefore, the generated peptide AtHaspin antibody is not suitable for distribution analysis of AtHaspin protein.
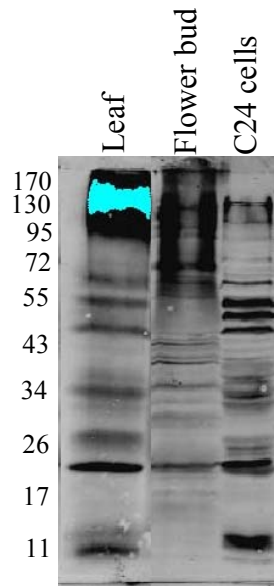
Fig. 29. Western blot experiment using an anti-AtHaspin antibody. Total protein was extracted from leaves, flower buds of wild-type *A. thaliana* plants and from C24 cell suspension cells. Appropriate AtHaspin protein band should be located at 68 kDa.

4.4.6. Ectopic expression of AtHaspin has pleiotropic effects

To further define the function of AtHaspin, 35S::AtHaspin overexpression plants were generated. Therefore, AtHaspin cDNA was cloned in sense orientation, under the control of the strong constitutive 35S promoter and transformed into *Agrobacterium* cells containing the binary vector GV3101::pSOUP. After transformation of *A. thaliana* plants with the 35S::AtHaspin construct, the progeny was selected for transgenic plants on MS medium containing PPT. To select plants with increased activity of AtHaspin semi-quantitative RT-PCR was performed on 20 preselected T1 plants (on PPT) using the primers AtHaspin-295F and

AtHaspin-295 R (arrows 1 and 2 in Fig. 14). All analysed transgenic plants showed an elevated level of AtHaspin transcription activity in comparison to the wild-type plants (Fig. 30).

35S::AtHaspin overexpression plants
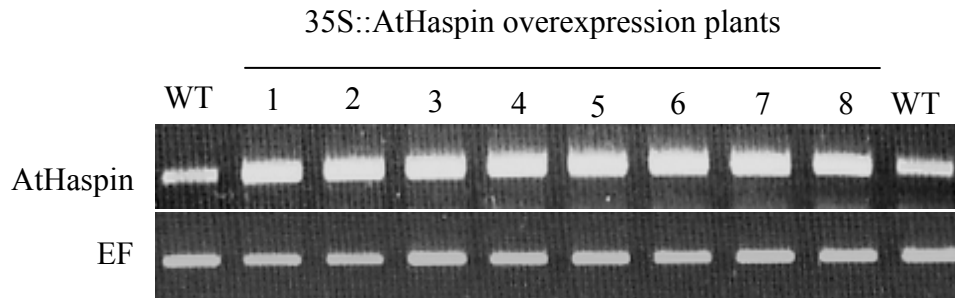
Fig. 30. Semi-quantitative RT-PCR analysis of 35S::AtHaspin overexpression plants (1-8) in comparison to wild-type (WT) plants. Elongation factor 1B-specific primers were used as a control (EF).

35S::AtHaspin overexpression plants showed multiple vegetative shoot apices (Fig. 31C). Most of the vegetative meristems produced inflorescence stems and consequently a multi-shoots phenotype was observed in AtHaspin overexpression mutants (Fig. 31A,B, D). Thirty-one plants displayed a multi-shoots phenotype (more than 4 branches) among 90 T1 AtHaspin overexpression plants.
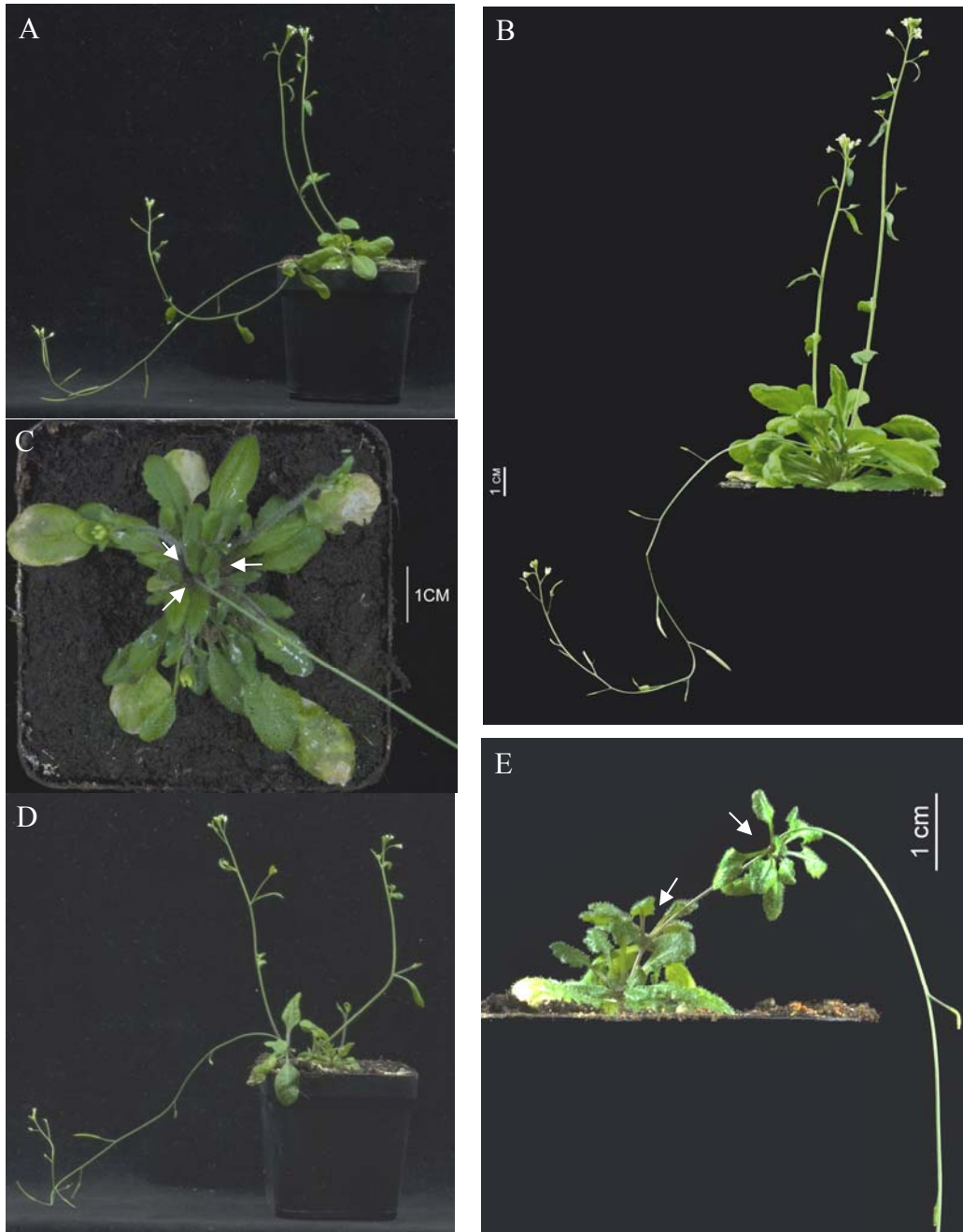
Fig. 31. Phenotype of 35S::AtHaspin overexpression mutants. A multi-shoot phenotype was observed (A, B, D) and (C) vegetative shoot meristems are indicated with arrows. Adventitious meristems are formed on the primary inflorescence of AtHaspin overexpression mutants (E).

AtHaspin overexpressing plants also produced thin and hanging stems (Fig. 31A,B,D,E) with a reduced number of vascular bundles compared to the wild-type plants (Fig. 32). Figure 31E shows that, adventitious meristems are formed on the primary stem. The adventitious meristem

produced axillary shoots. AtHaspin-overexpressed plants did not show differences in flower morphology.
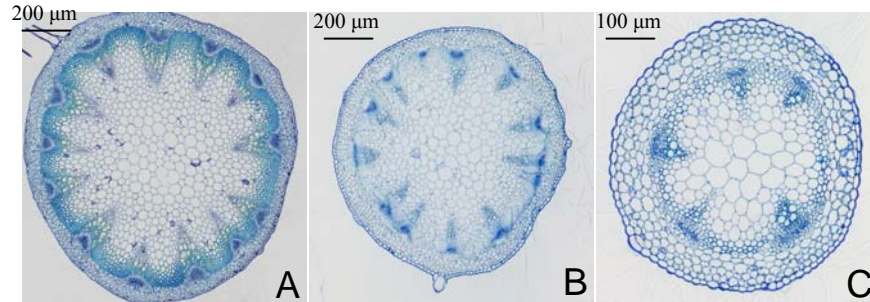
Fig. 32. Cross sections of a wild-type plant (A), of the lateral shoot (B) and of a thin primary stem (C) of 35S::AtHaspin overexpression plants. Based on few analysed plants the number of vascular bundles of 35S::AtHaspin overexpression plants was lower than in wild-type inflorescence.

In order to test the role of AtHaspin in a heterologous system, stable transformation of tobacco (*N. tabacum*) plants was performed with the 35S::AtHapin construct. Interestingly, out of 25 tobacco plants analysed, 20% displayed a multi-shoots structure (Fig. 33A). Small axillary leaves initiated from the angle of petioles and stems (Fig. 33C). On the basis of the observed similar multi-shoots phenotype in AtHaspin-overexpressed *A. thaliana* and tobacco plants, we propose that the AtHaspin gene may causes loss of apical dominance and might play directly or indirectly a role in auxin signalling pathway.

Fig. 33. Phenotype of tobacco plants overexpressing AtHaspin. Overexpressed plants are showing a multi-shoots structure (A) and axillary leafs and organ initiations (arrowed in C), while most wild-type tobacco plants have one stem only (B) without adventitious tissue (D).

4.4.7. Down regulation of AtHaspin results in a redistribution of phosphorylated threonine 3 of histone H3 in meiotic and mitotic chromosomes

To understand whether an altered activity of AtHaspin influences the dynamics of the cell cycle-dependent phosphorylation of histone H3, we performed immunostaining experiments on mitotic and meiotic cells obtained from flower bud tissue of AtHaspin down regulation (AtHaspin-RNAi) and gain of function (35S::AtHaspin) mutants using an antibody recognizing histone H3 phosphorylated at threonine 3 (H3Thr3ph). In dividing cells of analysed wild-type

plants H3Thr3 phosphorylation occurred along the entire length of chromosomes and co-localised with the position of condensed meiotic (Fig. 34A) chromosomes (metaphase I) and mitotic (Fig. 34B) as previously reported (Caperta et al., 2008).
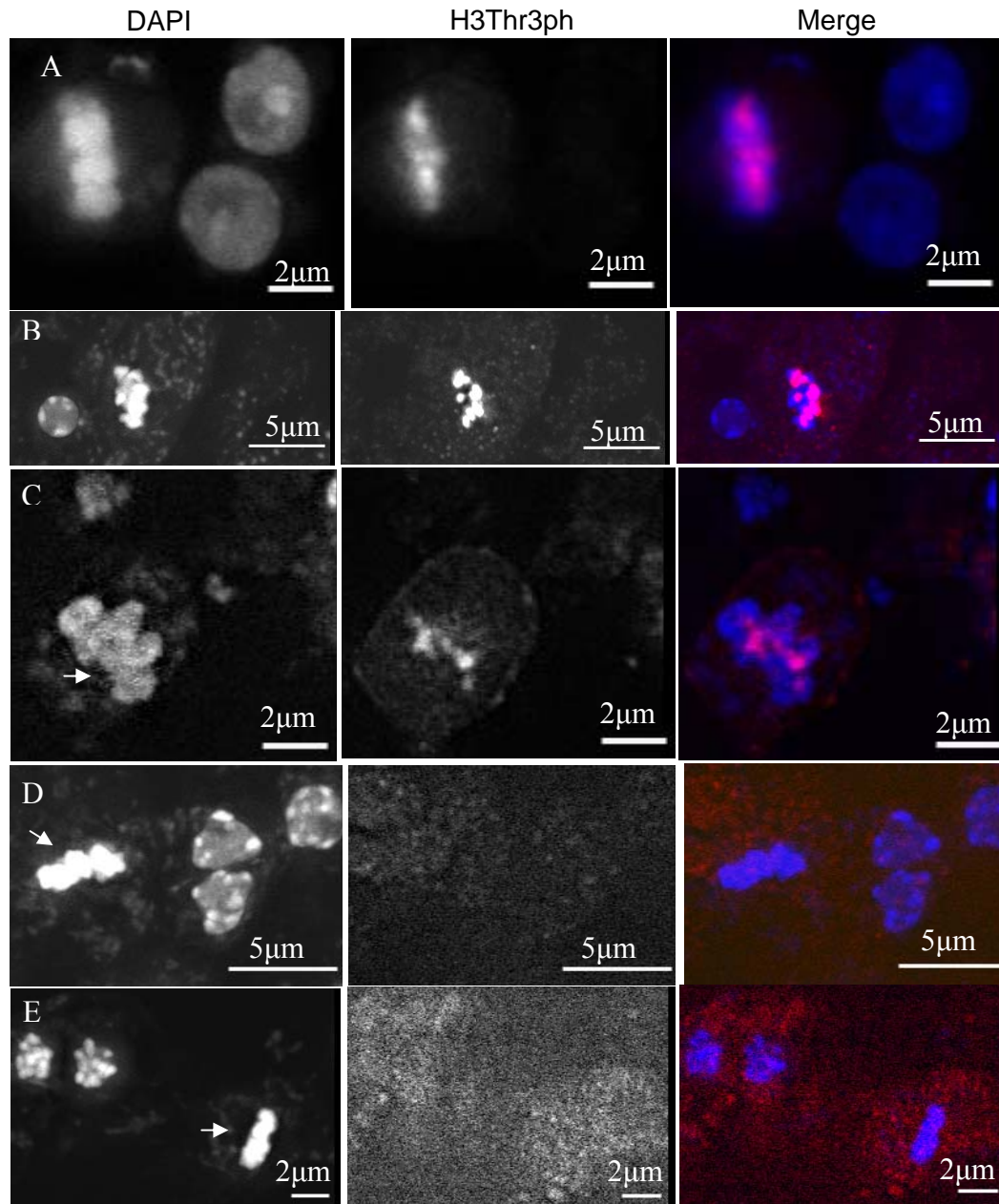
Fig. 34. Immunolabelling of histone H3 phosphorylated at threonine 3 in meiotic and mitotic cells. Wild-type meiotic metaphase I (A) and mitotic metaphase (B) cells of *A. thaliana*, and AtHaspin-RNAi knockdown mutants (C-E) .The level of histone H3Thr3 phosphorylation is reduced in RNAi meiotic (C, D) and mitotic (E) cells of RNAi plants compared to wild-type

(A, B) cells. Arrows indicate metaphase cells. DNA was counterstained with DAPI. The merged picture shows DAPI in blue and phosphorylated H3Thr3 in red.

In difference, in meiotic and mitotic cells of AtHaspin-RNAi homozygous lines first evidence exists that a reduction in the level of histone H3Thr3 phosphorylation occurred (Fig. 34). In AtHaspin down regulated plants phosphorylation of H3Thr3 were reduced and more restricted to pericentromeric regions of condensed chromosomes in both mitotic (Fig. 34E) and meiotic cells (Fig. 34C, D). No immunofluorescence signals were detectable in interphase cells.

In difference to AtHaspin down regulated plants, mitotic cells of AtHaspin overexpression plants did not reveal obvious alterations in the distribution of phosphorylated histone H3Thr3 (Fig. 35).

Thus, indirect evidence exists, that AtHaspin is involved in the cell cycle-dependent phosphorylation of histone H3Thr3 in plants.
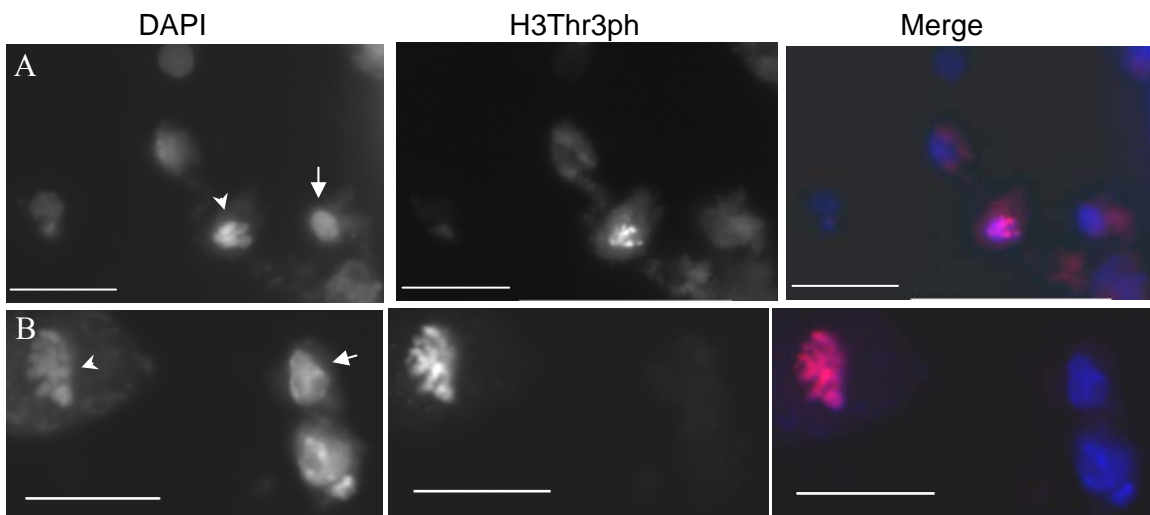
Fig. 35. Immunodetection of phosphorylated histone H3 at threonine 3 in mitotic cells of *A. thaliana* wild-type (A) and 35S::AtHaspin overexpression plants (B). The merged figure show DNA counterstained with DAPI in blue and phosphorylated H3Thr3 in red. Arrows indicate interphase nuclei which do not undergo phosphorylation of histone H3Thr3 in contrast to the dividing chromosomes (arrow heads). Scale bar indicate 10 μm.

5. Discussion

5.1. *A. thaliana* encodes a conserved haspin-like kinase

The data presented here indicate that *A. thaliana* encodes only one haspin-like kinase, analogous to haspin of non-plant organisms. The existence of only one haspin-like kinase is surprising as plant genomes contain a high proportion of duplicated genes. The majority of the *Arabidopsis* genome is represented in large segmental duplications, most likely because of whole genome duplication events (The *Arabidopsis* Genome Initiative, 2000; Blanc et al., 2000). This genome duplication resulted in a high number (65% of total genes) of duplicated genes and gene families (Zhang, 2003). Duplication events might play a major role in the evolution of new biological functions. Nevertheless, unique proteins (only 9.7% of the whole proteome) which are products of single-copy genes are encoded by a small part of the *Arabidopsis* genome (Armisen et al., 2008). The question on the origin of unique genes could be answered by either purifying selection against duplicates or rapid divergence and gene evolution (Kondrashov et al., 2002; Armisen et al., 2008).

A rapid divergence of haspin is less likely because of following reasons. First, the existence of a high number of introns in the body of the AtHaspin gene of *Arabidopsis* (14 introns) and of other plant haspin-like genes (13 and 16 introns in *O. sativa* and *V. vinifera*, respectively) is in agreement with the fact that, in general, evolutionarily conserved genes preferentially accumulate more introns than fast evolving genes (Carmel et al., 2007). Hence, the high number of introns in haspin-like genes suggests that these genes are slowly evolving genes. At second, the positions of some of the introns are precisely conserved in the kinase encoding regions of haspin genes from animal and plants (Higgins, 2001b, 2003). Overall, intron position conservation is the best proof that the members of genes have evolved from a common ancestor, and are not consequence of convergence (Armisen et al., 2008). In addition, the products of haspin-like genes are highly conserved and identical with a low percentage of amino-acid divergence between species (Table 3 and (Higgins, 2001a)). Based on these facts, we could suggest that, haspin orthologous are highly conserved and slowly evolving genes which could not be controlled by the rapid divergence.

Interestingly, haspin is a unique and single-copy gene in most of the eukaryotic species. The reason of multiple haspin-like proteins existence in *C. elegans* is not clear yet. In general, observation probably suggests that, the members of haspin–like genes are panorthologs (conserved single copy genes in two or more species) under negative selection pressure to keep them in a low divergence rate. This situation reinforces the idea of a probable crucial conserved function of haspin genes in eukaryotes.

All plant and non-plant haspin-like kinases share similar structures as other members of the eukaryotic protein kinase superfamily (ePKs) (Higgins, 2001a, 2003), with the conserved catalytic domains (Fig. 10 regions I-XI) flanked by N-terminal domains of variable lengths. Alignment of haspin-like proteins showed that most of the residues that are essentially invariant in other ePKs are known to be critical in forming catalytic sites and kinase activity (Hanks and Quinn, 1991; Higgins, 2001a, 2003), are conserved in the majority of haspin proteins including *Arabidopsis* haspin. These conserved sequence motifs are known to be critical in forming the Mg^{+2}-ATP-biding and catalytic site including, the potential ATP-binding site G-x-G-x-x-G-x-(V/A) in region I, lysine (K) in region II, glutamate (E) in region III, aspartic acid (D) and asparagine (N) in region VIb, aspartic acid (D) in region VII, as well as aspartic acid (D) or glutamate (E) in region IX (Fig. 10).

In addition, AtHaspin has some features which are highly conserved in most of haspin-like proteins which are not found in other members of the ePKs superfamily (Higgins, 2001a, 2003). Haspin-specific features are the L-A-V-A-E motif in region VIa, the catalytic loop of region VIb with the conserved sequence of (F/L)-E-H-R-(D/N)-L-(H/T/N), (I/L)-I-D-(Y/F)-(S/T)-(L/C)-S-R motif in region VII with the invariant isoleucine-aspartate and arginine residues, a D-x-x-L-F motif in region VIII with invariant phenylalanine residue, a (E/D)-(I/V/T)-Y-R-x-M-(R/K) motif in region IX with the conserved tyrosine and methionine, as well as a W-x6-(T/S)-N-(V/I/L)-hydrophobic-WL-x-Y-L motif in which the second tryptophan residue is invariant in region X (Fig. 10). However, there are also some plant-specific features in the catalytic site (marked by asterisks in Fig. 10) and N-terminal domain of AtHaspin (Fig. 11) which could distinguish plant haspins from other haspin-like proteins.

Phylogenetic analysis of haspin-like kinases based on conserved catalytic domains demonstrated that haspin-like kinases undergo lineage-specific expansion throughout eukaryotic evolution, while they are consistent in amino acid sequences. Haspins of plants are clearly separated from animal and fungi haspin, and are divided into three categories of lower plants and monocots and dicots (Fig. 12). In general, existence of highly conserved haspin homologs in all different eukaryotic genomes including the *E. cuniculi* with very small genome size (only 2.9 million base pairs) suggests important and perhaps fundamental function of haspin genes in eukaryotic life.

5.2. Inactivation of AtHaspin is lethal for plants

The analysis of the T-DNA *Arabidopsis* insertion line (082D07 with the T-DNA insertion in the 5' UTR region) did not give rise to any homozygous (*has/has*) mutant plant. Therefore, complete inactivation of AtHaspin must be lethal for plants, which suggests an essential function for AtHaspin in plant development. The lethality of homozygous T-DNA plants could be explained either by the inability of homozygous plants to produce viable gametes (pollen and/or egg cells) or by crucial defective effects of missing AtHaspin in embryogenesis.

Considering the observed segregation ratio of the progeny of self-pollinated heterozygous plants of T-DNA line 082D07 (Table. 5), with the percentage of 32% wild-type, 64% heterozygous and 0% homozygous plants, which coupled with the 1:2:0 ratio, we could suggest that the mutation of AtHaspin most likely results in embryo lethality. In the case of gamete lethality the segregation ratio should be 1:1:0, which is not in agreement with our observation.

5.3. AtHaspin plays a role in cell proliferation, differentiation and organ development

5.3.1. RNAi and overexpression of AtHaspin generate more axillary shoots and adventitious meristems

The shoot meristem is established during plant embryogenesis. During postembryonic development of *Arabidopsis*, the shoot meristem give rise to the shoot axis (stem), leaves and axillary meristems in a repetitive indeterminate fashion while being maintained by self-renewal

(Jurgens et al., 1991; Kerstetter and Hake, 1997). Over the past several years a number of studies have led to the identification of some important genes which have a major regulatory role in shoot branching and shoot meristem development (Fletcher, 2002; Bennett et al., 2006; Ongaro and Leyser, 2007; Shimizu-Sato et al., 2009). These genes appear to regulate cell division, cell differentiation and control a variety of important developmental events by interacting hormonal signals that move through the plant.

Many mutants in the transcription-regulating auxin signalling pathway (AxRs) (Lincoln et al., 1990; Stirnberg et al., 1999) and in regulating of polar auxin transport (PINs) (Galweiler et al., 1998; Christensen et al., 2000; Benjamins et al., 2001) have shoot branching defects and auxin-response defects in their floral organs and inflorescences. Hence, the auxin signalling pathway regulates floral bud and lateral organ outgrowth and apical dominance. Similarly, mutation of genes involved in the *MAX* (more axillary growth) pathway results in increased branching of rosettes which is caused by increased auxin transport capacity in the main stem (Stirnberg et al., 2002; Sorefan et al., 2003). An increased branching correlates with increased PIN1 activity and the accumulation of other PINs in plant stems (Bennett et al., 2006).

The *SHOOT MERISTEMLESS* (SML) gene encodes a protein that maintains undifferentiated cells in the apical meristem and is required for the initiation of shoot meristems in *Arabidopsis* (Clark et al., 1996; Endrizzi et al., 1996). Ectopic expression of *KNOTTED1* or related genes produced multiple shoots, adventitious meristems, and stunted leaves (Sinha et al., 1993; Lincoln et al., 1994; Chuck et al., 1996). A large number of undifferentiated cells accumulate in the meristems of the *CLAVATA (CLV)* mutant plants (Leyser and Furner, 1992; Clark et al., 1996).

Shoot meristem structures are disturbed by mutations in *SCHIZOID* genes. The mutant of SCHIZOID gene shz-2 forms adventitious meristems, and shows an abnormal cell division in the apical meristem (Medford et al., 1992; Parsons et al., 2000). The *WUSCHEL* (*WUS*) gene probably functions in the same pathway as *SHOOT MERISTEMLESS (STM)* and the *CLAVATA (CLV)* genes. *WUSCHEL* appears to be negatively regulated by *CLV* genes (Laux et al., 1996) and positively regulated by STM (Endrizzi et al., 1996). *WUSCHEL* mutants have a negative effect on floral and shoot meristem differentiation, and therefore initiate numerous secondary

shoot meristems that give rise to several rosettes and shoots and floral organs (Laux et al., 1996). Together, studies on shoot and shoot meristems mutants indicate that most of the genes which regulate shoot development, directly or indirectly, affect cell differentiation.

Recent studies on *Arabidopsis* mutants indicate that intercellular signaling molecules such as auxin, cytokinin, brassinosteroids and xylogen regulate the maintenance or differentiation of shoot meristematic procambial cells into vascular tissues through distinct intracellular-signal transduction and gene-expression machineries. This intercellular- and intracellular-signalling system might be involved in determining the continuity and pattern formation of vascular tissues (Fukuda, 2004).

RNAi-AtHaspin mutants exhibit abnormalities in inflorescence and floral organ development (Fig. 19, 20). Repetitively we observed the formation of adventitious shoot meristems and lateral shoots (Fig. 20). Overexpression of AtHaspin generates a similar phenotype which is characterized by the formation of axillary shoot meristems and shoots (Fig. 31). Based on the similar phenotype between AtHaspin mutants and gene mutants involved in adventitious shoot and shoot meristem development it is probable, that AtHaspin regulates cell differentiation through hormone mediated signalling pathway and hormone interactions during plant development.

The reason why the observed phenotype both in AtHaspin-RNAi and AtHaspin overexpression mutants is similar as reported for the auxin response factor 2 (ARF2) (Okushima et al., 2005), could be explained by two facts. The first explanation might be that translational repression of AtHaspin protein occurs in AtHaspin-overexpressed plants by a mechanism like miRNA repression. MiRNAs are essential regulators of various processes such as proliferation, differentiation, development, cell death and interaction between virus and host cell (Kusenda et al., 2006). Few studies have documented the important contribution of plant miRNA in translational regulation, which is less understood than RNA cleavage in plants (Mallory et al., 2008). One way to test this possibility would be to quantify AtHaspin overexpression plants by Western blot experiments using an AtHaspin-specific antibody. However, because the generation of an AtHaspin-specific antibody was unsuccessful the suggested experiment could not be performed. The second possibility is the function of AtHaspin as a part of one or more

protein complexes and imbalance in AtHaspin stoichiometry by gain or loss of function alters the function of the entire protein complex. Responsible regulatory genes exhibiting a stoichiometric balance have been found to be members of signal transduction factors or transcription factors of various types (Birchler et al., 2001; Birchler and Veitia, 2007). Dosage-sensitivity and stoichiometric balance of AtHaspin could explain the single copy retention of the AtHaspin gene by purifying selection following diploidization of ancient polyplodization events during evolution.

Based on the studies on AtHaspin mutant plants, we could speculate that, AtHaspin acts upstream of the shoot apical meristem related genes (e.g. *CLVs, WUS*) and hormone signal transduction pathway and its mutation showing similar effect as mutation of other genes which function at downstream of AtHaspin to regulate cell division and differentiation.

5.3.2. AtHaspin is expressed in shoot meristem, young vascular tissue and aerial organ primordial

The promoter$_{AtHaspin}$::GUS results suggest that AtHaspin is highly expressed in shoot apical meristems, very young rosette leaves, and cotyledons as well as in young floral organs. Based on published microarray data (https://www.genevestigator .com/gv/index.jsp) highest activity of AtHaspin exists in the shoot apex and root tips. Our RT-PCR results showed highest transcription of AtHaspin in flower and flower buds. All tissue types characterised by a strong activity of AtHaspin are enriched in cell proliferation and differentiation. In difference to published microarray data, no promoter$_{AtHaspin}$::GUS activity was found in roots. The difference in the expression pattern of AtHaspin in microarray data and promoter$_{AtHaspin}$::GUS could be explained by the absence of putative root-specific regulatory elements, which were not included in promoter$_{AtHaspin}$::GUS construct. However, AtHaspin mutants also do not display an obvious root phenotype.

Lower expression of promoter$_{AtHaspin}$::GUS was detected in the vascular tissue of all major aerial plant organs including stems, rosettes, flowers, siliques and in cotyledon primordias of embryos which was consistence with the transcription profile of RT-PCR experiment.

AtHaspin expression in vascular tissues suggests that AtHaspin might play a role in vascular development and function. However, cotyledons of AtHaspin-RNAi plants revealed only mild vascular defects. Only few RNAi plants revealed defects in the vascular development of the stem. No defection was observed in vascular bundle formation of AtHaspin overexpression plants, while the number of vascular bundles was decreased in few AtHaspin overexpression plants only. All the observation indicating that the regulation of vascular development is not the primary function of AtHaspin. More likely, based on the AtHaspin gene expression pattern and interpretation of the AtHaspin mutant phenotypes, we could suggest that AtHaspin functions in a tissue-specific manner to regulate the development of aerial organs and outgrowth by influencing cell proliferation and differentiation.

Notably, analysis of coexpression data of AtHaspin and of different auxin transporter genes, like AtPIN1, AtPIN6 and *PINOID*, which function in organ development and plant growth by regulation of auxin signalling (Christensen et al., 2000; Benjamins et al., 2001) revealed a similar expression dynamic of the genes analysed (Fig. 36). It was already published that a close correlation exists between the expression patterns of AtPIN1, AtPIN6 and *PINOID* (Benjamins et al., 2001; Paponov et al., 2005). Transcripts encoding all three proteins are always strongly up-regulated at the shoot apex and at the base of the inflorescence stem. Similarity in the expression patterns of these genes could either suggest high conservation motif between their respective promoter regions or most probably interdependent and complementary function of their respective proteins (Paponov et al., 2005).
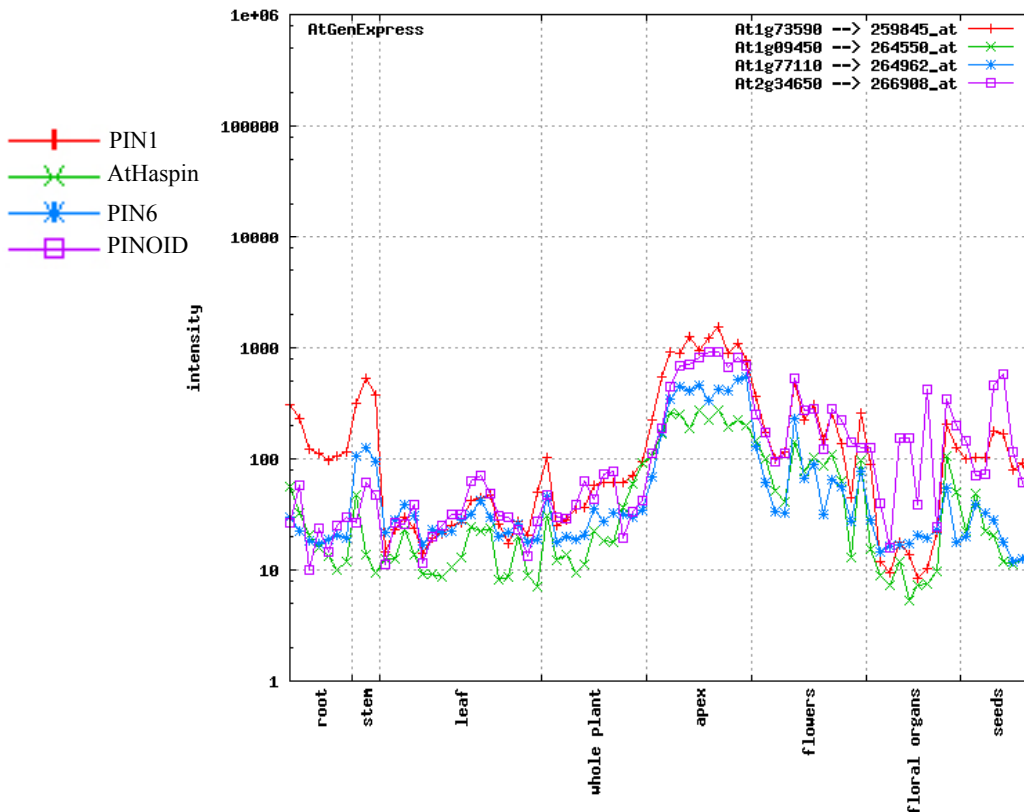
Fig. 36 The expression pattern of AtHaspin of polar auxin transport genes (PIN1, PIN6 and *PINOID*) is similar in different tissues and organs of *Arabidopsis*. Analysis was conducted using the AtGenExpress Visualization Tool (http://jsp.weigelworld. org/expviz/expviz.jsp).

5.4. Does AtHaspin regulate cell division and differentiation via phosphorylation of histone H3Thr3?

The eukaryotic cells react to a large number of extracellular stimuli to ensure the correct proliferation and differentiation. This stimulus are registered at the cell surface and transferred via signalling pathways to the nucleus where they induce appropriate responses, by the activation or repression of specific processes (Hagen and Guilfoyle, 2002). In addition, some of the studies showed that, many of these signal transduction pathways converge towards a common, very complex and dynamic substrate, in the chromatin fiber (Turner, 1999; Thomson et al., 1999b; Cheung et al., 2000a; Strahl and Allis, 2000).

Protein phosphorylation is the major posttranslational modification involved in the signalling pathway (Hans and Dimitrov, 2001). Histone H3 is specifically phosphorylated during both mitosis and meiosis, but also plays a role in gene activation and stress regulation (reviewed in (Hans and Dimitrov, 2001). Phosphorylation at histone H3 threonine 3 is accompanied by the condensation of chromosome during mitosis and meiosis in plant species (Polioudaki et al., 2004; Dai et al., 2005; Caperta et al., 2008) suggesting a functional role for this post translational modification in chromosome formation. In addition, a mutant of human haspin kinase (the responsible kinase for phosphorylation of histone H3 at threonine 3), exhibited perturbed chromosome alignment at metaphase, abnormal segregation and cell arrest in mitosis (Dai and Higgins, 2005; Dai et al., 2005; Dai et al., 2006), further confirming the important role of phosphorylation of histone H3 at threonine 3 in dividing cells.

Our investigation of *Arabidopsis* haspin loss and gain of function mutants led us to propose a function of this kinase in cell proliferation and cell differentiation. Concordantly with the probable function of AtHaspin in cell differentiation and cell proliferation in meristematic tissues (such as shoot apical meristem) and embryos (AtHaspin knockout T-DNA plants are nonviable) immunostaining of AtHaspin-RNAi down regulated plants revealed a reduction of the histone H3Thr3 phosphorylation level.

These data suggest that a functional interplay might exist between a signalling pathway involved in the regulation of cell division and shoot meristem formation and the cell cycle-dependent histone H3Thr3 phosphorylation.

5.5. *In silico* analysis of AtHaspin promoter emphasize the proposed function of AtHaspin in shoot apical meristem regulation

In silico search using the MEME motif discovery tool (http://meme.sdsc.edu/meme4_1/intro.html, (Bailey et al., 2006) revealed several conserved motifs in the 1000 bp-long 5' region immediately upstream of AtHaspin start codon.

The (GA)$_7$/(CT)$_7$ dinucleotide repeat, which is located 57 bp upstream of AtHaspin start codon might represent a so-called GAGA element (Fig. 37). GAGA elements are recognized by specific GAGA-box-binding factors (Sangwan and O'Brian, 2002; Santi et al., 2003). In *A. thaliana*, (GA/TC)n repeats occur particularly in some homeodomain genes of different classes (Santi et al., 2003) . In *Drosophila* GAGA elements may play a role in chromatin remodelling by recruiting specific non-histone protein complexes (Lehmann, 2004).

Several ACGT motifs are present in the promoter of AtHaspin (Fig. 37). ACGT core *cis*-elements can be recognized by different basic/leucine zipper (bZIP) proteins (the largest known family of plant DNA-binding transcriptional factors), which function in mediating signals from diverse environmental, developmental, and physiological stimuli (Foster et al., 1994; Liu et al., 1994).

Several (A/T)AAAG motifs were observed 1 kb upstream of the AtHaspin start codon (Fig. 37). (A/T)AAAG motifs are recognized by DNA-binding with one finger (Dof) transcription factors (Yanagisawa, 2001; Umemura et al., 2004). Dof proteins are plant-specific single-zinc finger DNA-binding proteins that enhance transcription from the promoters of various genes (Yanagisawa, 2001; Umemura et al., 2004). The tobacco Dof protein (NtBBF1) is binding to the CTTTA domain of the promoter of the rolB oncogene (Baumann et al., 1999). The strongest expression of rolB was observed in root and shoot apical meristems and has lower activity in the vascular system (Altamura et al., 1991; Capone et al., 1991). The stimulation of meristem formation is the primary effect of rolB (Altamura et al., 1994), Moreover, rolB has been found to be induced by auxin (Baumann et al., 1999). Promoter expression analysis of transformed tobacco plants with a mutated region within the CTTTA motif of rolB revealed completely suppressed promoter activity in apical meristems and severe reduction in the vascular system (Baumann et al., 1999).

In addition, several GT elements also were found in the 5' regulatory region of AtHaspin (Fig. 37). GT elements with the common characteristic of four or five nucleotides, T or A, preceded by one or two G nucleotide at the 5', are regulatory sequences usually found in tandem repeats present in the promoter region of numerous plant genes. The GT elements can exhibit promotion or repression depending on the structural context (Zhou, 1999).

A/T-rich sequences were found 623 bp upstream of the start site (Fig. 37). A/T-rich sequences can function as TATA boxes to interact with TATA-binding proteins (TBP) in the process of transcription (Smale and Kadonaga, 2003).

Interestingly, all GAGA elements, GT elements and the consensus binding site of Dof proteins were already identified as common regulatory motifs in the promoter region of genes which are up-regulated in shoot apical meristems of *A. thaliana* (Haerizadeh et al., 2009).

```
-1000   CCTCTACATTTCCGTGAAGAGTATGATGTTTTAACTACCCAAAGTAACTGTCCGATCTTTTAT

 -937   ATTACACGGCTATGAAGAAACCTTTAAATAAGAAAGTATTGTTGATGGCATTGCGTTAAAACA

 -874   TTAAAAGGACTAGTAATTATCAAATTAATAATATTTATGTTAGAGAAATGTTCAAATGAATCA

 -811   TGGAGTAGTGGGGGCTGGCTGACCTCAAAATTTGAAAATTGTTTTTCTTACATTTCAAATTAC

 -748   AATTAAGGTAATTTAATTCCTTTTTCATTTGTTGTTTTGGAATGTTGACGTAACATTTTTTTG

 -685   GCTTTAGCTAAATCCGCACAATCACATGATCACATCGACGTTCTAAATTTTTGTTCGGTATGT

 -622   ATAAATATATAATTAGCATAATATACATATACATACATAATTAGTATGTTGTGTTGTGATAAC

 -559   TTGAATACAGCACACTAATAATGTGTTAATCTTATACAATCGCAGAGTAGTACATCTTTACGT

 -496   AACAGACGTTAATCTACAAGCAGATCAACAAACTGGATCCAAAATATATGTGTGTGTGCGTCA

 -433   ACAATTGTGTTAAGCTTTTTTTCTTTCATTATATATACAATATCCGAAAATAGAGAGAAGTTA

 -370   TAGTCTTCTAGAATAGCTTTTGACTTGTGAAGTAATTAACATTTTACATGTTGTTGCTTAATC

 -307   TTTGTTCATCATCGTTCCTCTCCTTGAAAGAGAAACTCCAACAAATTGAAAAGCCTTGCACAT

 -244   CGCTTGCGATAAAACCAATATTAATAATCGTTTGGTTCGGTTAGAGAAACCCGGTTTAAGAAC

 -181   AGACAAGTCTTGGGCTTGAAATTAGATTCGGAGCCCAATTTTGATTTTGGATTTTAAATTTTA

 -118   GACCCACGAAATTTCTCCCGCCTTCCCGGTCCACAACTTCGATTCAAATCGACTTTTCTCTTT

  -55   CTCTCTCTCTCTCGGTGACTGTTGCAGTACTGATTTGTGTTCCCTCTAACCTAAA
```

Fig. 37. *In silico* analysis of the 1000 bp 5'upstream region of the AtHaspin start codon. Arrow indicates the position of start codon. (GA/TC)7 elements are shown in red, 57 bp upstream of the start site. (A/T)AAAG motifs which are potentially recognized by (Dof) transcription factors are found in both orientations at positions illustrated by blue color. GT elements are found in tandem repeats and shown with underlines. The green rectangular demonstrates the position of A/T-rich sequences. ACGT motifs are illustrating with black rectangular.

5.6. Predicted protein structure of AtHaspin

In silico analysis of the AtHaspin protein structure (http://www.ch.embnet .org/software/COILS_form. html) revealed three coiled-coil motifs in the C-terminus region (Fig. 38). Coiled-coil motifs are a frequent motif in protein structures formed by two to five alpha-helices wound around each other (Burkhard et al., 2001). These motifs are often used to mediate protein–protein interaction or to build filaments and other macroscopic and cellular structures, such as the Golgi, centromers, or the nuclear envelope (Liu and Rost, 2001; Rose et al., 2004). Short coiled-coil domains of six or seven heptad repeats, also called leucine zippers, are frequently found as homo- and hetero dimerization motifs in transcription factors (Rose et al., 2004). It has been estimated that approximately 10% of all proteins of an organisms contain a coiled-coil motif (Liu and Rost, 2001). The involvement of coiled-coil proteins in very different and important biological functions makes predictions highly valuable for biologists, beyond the general interest in tertiary structure.
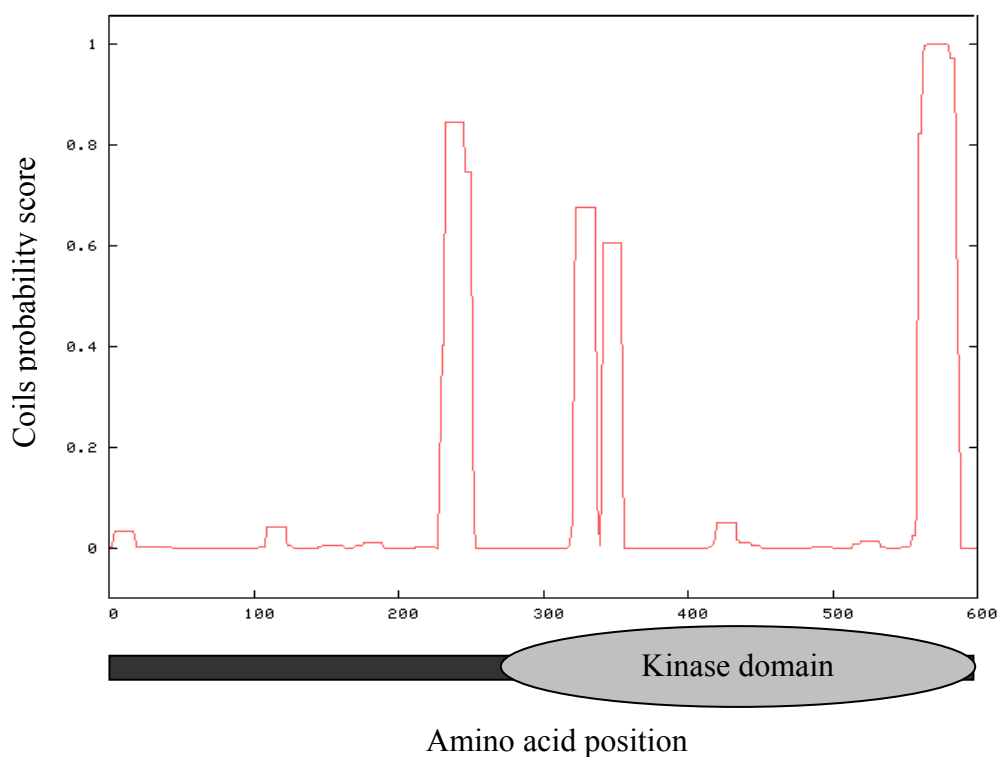
Fig. 38 Schematic representation of the structures of the AtHaspin protein. The serine/threonine kinase domain is shown as grey oval. The diagram shows putative coiled-coil domains in red. Y-axis depicts the predicted probability score. X-axis shows the amino acid position.

94

5.7. Proposed model for the function of haspin in plants

Our studies have demonstrated that AtHaspin is highly expressed in aerial meristematic tissues with high proportion of cell proliferation and differentiation. The similar phenotype of AtHaspin mutants with the mutant genes, function in polar auxin transport and meristem regulation suggests a probable interdependent and complementary function of AtHaspin with those respective genes. In addition, the cell cycle-dependent phosphorylation of histone H3 at Thr3 was altered in AtHaspin-RNAi mutants.

Based on our observations we propose following model for the function of plant haspin (Fig. 39): AtHaspin phosphorylates histone H3 at position threonine 3 and also phosphorylates and interact with proteins involved in meristem function and development. From there AtHaspin could be involved in the hormone signalling pathway directly or by mediating of meristem regulatory genes to promote organ outgrowth and development. The control and regulation of meristem activity by cytokinin/auxin interaction has been already shown (Leibfried et al., 2005; Kurakawa et al., 2007; Veit, 2009). It remains to be demonstrated whether histone H3Thr3 phosphorylation, regulation of hormone transduction pathway and meristem development are part of the same regulatory pathway. Alternatively, AtHapsin phosphorylates substrates which are involved in different processes.
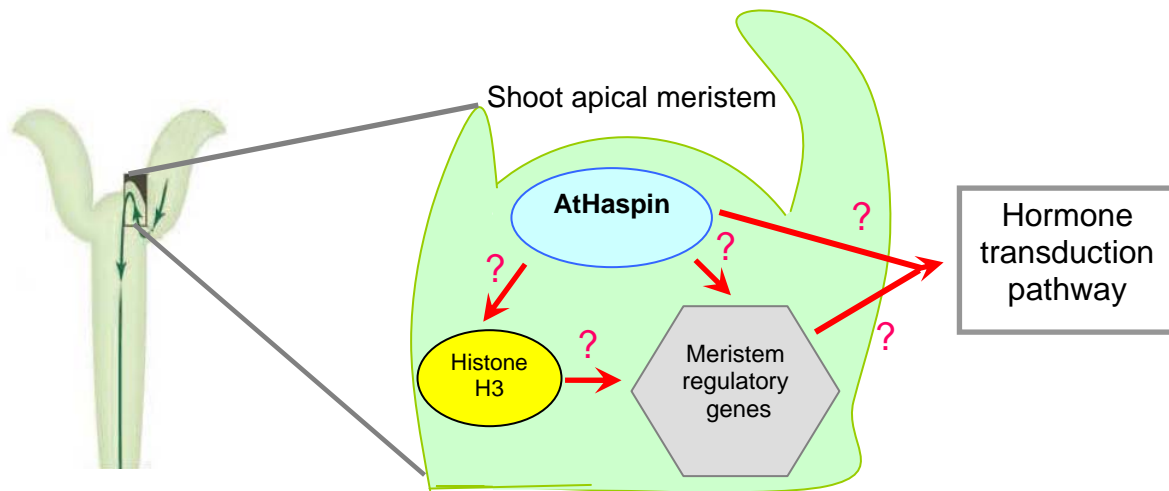
Fig. 39. Proposed functions of the haspin-like kinase in plants. AtHaspin seems to be involved in regulation of meristem proliferation and differentiation by phosphorylation of histone H3Thr3 in dividing cells and interaction with shoot meristem regulatory genes. Moreover, a direct or indirect involvement of the AtHaspin protein kinase exists in the hormone signal transduction pathway to regulate shoot meristem regulatory genes.

6. Outlook

To confirm the proposed function of AtHaspin following experiments should be conducted in future.

6.1. Identification of AtHaspin loss of function mutants using the TILLING approach

To reconfirm the results obtained by the analysis of AtHaspin-RNAi and T-DNA mutants we intend to generate mutand plants with modified AtHaspin activity using the TILLING (Targeting Induced Local Lesions IN Genome) approche (McCallum et al., 2000). TILLING is reported to be a valuable method especially for essential genes which knockout T-DNA mutant is lethal for plants (like AtHaspin) by producing allelic series of point mutations and phenotypical analysis of sublethal alleles (Colbert et al., 2001). These mutations constitute allelic series that potentially confer a range of phenotypes from subtle to strong, and allow structure function studies (Slade and Knauf, 2005).

6.2. Analysis of the cell-cycle dependent distribution of AtHaspin in mitotic and meiotic cells

The subcellular localisation of AtHaspin should be determined in mitotic cells of transformed 'BY2' tobacco and/or *Arabidopsis* suspension cells using 35S::YFP-AtHaspin, 35S::AtHaspin-YFP constructs and reporter constructs containing the endogenous AtHaspin promoter. A potential influence of the 35S-promoter on the cell cycle progression will be determined by flow cytometry. For the analysis of meiotic cells immunostaining experiments will be performed on flower buds of 35S::YFP-AtHaspin plants using an anti-GFP antibody.

6.3. Verification of AtHaspin kinase activity towards histone H3Thr3 using an *in vitro* kinase assay

To demonstrate specificity of AtHaspin kinase activity towards histone H3Thr3 an *in vitro* kinase should be performed using recombinant histone H3 and total core histones as substrates. The specificity of the kinase assay will be tested via Western blotting using antibodies specific for phosphorylated histone H3 at either Thr3, Thr11, S10 or S28. Available GATEWAY

compatible tandem affinity peptide tag-AtHaspin constructs (Earley et al., 2006) will be used to produce recombinant AtHaspin protein *in planta*, which will be affinity purified and used for the kinase assay. As negative control an 'AtHaspin dead mutant' (with a mutated kinase domain) will be used for the production of an inactive kinase. Alternativly, recombinant AtHaspin with kinase activily could be produced recombinantly in *E. coli.*

6.4. Identification of AtHaspin interacting proteins

Affinity purification for AtHaspin complex should be performed in *Arabidopsis* plants transformed with different tandem affinity peptide (TAG) tag-AtHaspin constructs (Earley et al., 2006). After successful isolation of the complex, interacting proteins will identify by mass spectrometry.

6.5. Investigation of the shoot meristem configuration in AtHaspin mutant plants using histological tissue section and RNA *in situ* hybridization

In order to trace the role of AtHaspin in shoot meristem formation longitudinal sections through meristematic region of AtHaspin loss and gain of function mutants should be performed and analysed. The sections should also be used for RNA *in situ* hybridization to localise the regions of highest AtHaspin expression activity.

6.6. Analysis of a potential interplay between AtHaspin function and hormone transport signalling

To proof our assumption that between AtHaspin and the process of hormone signal transduction a functional interrelationsship exists, we intend to treat AtHaspin mutant seedlings (AtHaspin-RNAi, overexpression and promoter::GUS) with different synthetic auxins (IAA, 2-4-D and NAA) and auxin transport inhibitors (e.g. NPA) and synthetic cytikinines. In addition, we wish to investigate the root and hypocotyls growth behaviour, gravity tropisms and lateral root formation. Furthermore, AtHaspin mutant plants will be crossed with DR5-reporter plants and the distribution and intensity of the reporter signals (GFP or GUS) will be analysed in the F1 generation and compared with the distribution of DR5-reporter in wild-type plants. DR5 is a highly active synthetic auxin response element widely used for auxin transport studies (Ulmasov et al., 1997).

7. Summary

Using the deduced amino acid sequence of the catalytic domain of the human haspin gene, BLASTX analysis of the non-redundant nucleotide sequence database of the *Arabidopsis. thaliana* genome (GENEBANK) was done. Subsequently, we identified a haspin-like serine/threonine kinase (called AtHaspin) in the genome of *A. thaliana* that is encoded by the locus At1g09450. Alignment of the AtHaspin kinase domain with other putative haspin-like proteins revealed that haspin homologues are found in all different eukaryotic phyla including animals, higher plants, moss and green alga, and fungi. This suggests an important function and apparent origin early in eukaryotic evolution for these proteins.

Tissue-type specific expression analysis of AtHaspin by semi-quantitative RT-PCR showed a high abundance of AtHaspin transcripts in stem-bearing shoot meristems, buds and flowers, These tissues have a significant level of cellular proliferation and differentiation.

The homozygous *A. thaliana* T-DNA insertion line (GABI 082D07) was lethal and signifies an important and essential role of AtHaspin for plant development. Down regulation (via RNAi) or overexpression (via 35S promoter) of AtHaspin results in pleiotropic phenotypes with defects in floral organs and vascular tissue, reduced fertility and loss of apical dominance. Hence, adventitious shoot apical meristems and multi- rosettes and multi-shoots formation were formed. The characteristic phenotype of AtHaspin mutant plants was similar to plants with mutations in genes involved in shoot meristem function and polar auxin transport pathway.

Promoter$_{AtHaspin}$::GUS signals are mainly localised in the shoot apical meristem, flower buds and in the aerial organ of young embryos with high level of cell proliferation and differentiation. The GUS signal was also detected at lower levels in the vascular tissues of young leaves and flowers. Analysis of 35S::YFP-AtHaspin plants revealed a high level of YFP signal in the cytoplasm of highly proliferating and differentiated cells in shoot apexes and root tips, and in the vascular tissue of young seedlings. Localisation of AtHaspin, using both Promoter$_{AtHaspin}$::GUS and 35S::YFP-AtHaspin constructs was consistent with the expression data obtained from semi-quantitative RT-PCR experiments.

To find a functional link between histone H3 phosphorylation at Thr3 and the action of AtHaspin, dividing cells from *A. thaliana* plants with altered activity of AtHaspin (RNAi and overexpressed) were immunostained using an antibody specific for phosphorylated H3Thr3. AtHaspin-RNAi plants were depleted in histone H3Thr3 phosphorylation in mitotic and meiotic cells. However, there were no obvious changes in the level of H3Thr3ph in dividing cells of overexpressed plants. Thus, there is indirect evidence that AtHaspin is involved in the cell cycle-dependent phosphorylation of histone H3Thr3 in plants.

It has been assumed that AtHaspin phosphorylates histone H3 at position threonine 3 and also phosphorylates and interact with proteins involved in meristem function and development. If this is so, AtHaspin could be involved in the hormone signalling pathway directly or by mediating meristem regulatory genes to promote organ outgrowth and development. It is still unclear whether histone H3Thr3 phosphorylation, regulation of hormone transduction pathway and meristem development are part of the same regulatory pathway.

8. Zusammenfassung

Eine haspin-ähnliche Serin/Threonin Kinase (genannt AtHapin) wurde mit Hilfe der BLASTX Analyse im *A. thaliana* Genom (At1g09450) identifiziert. Die hohe Proteinähnlichkeit der Kinasedomäne haspin-ähnlicher Kinasen aus dem Tier, Pflanzen oder Pilzreich deutet daraufhin, dass es sich hierbei um eine Kinase mit essentieller Funktion handelt, welche sich bereits früh in der Evolution der Eukaryoten ausbildete.

Expressionsanalyse von AtHaspin mittels semi-quantitativer RT-PCR zeigte die höchste Genaktivität dieser Kinase in Sprossmeristemen, Blütenknospen und Blüten. Diese Gewebe sind durch hohe Zellteilung und Zelldifferenzierung gekennzeichnet.

Die homozygote AtHaspin *A. thaliana* T-DNA Mutante (GABI 082D07) ist nicht lebensfähig, was darauf hindeutet, dass AtHaspin essentiell für die Funktion der Pflanze ist. Eine künstlich abgeschwächte (via RNAi) oder erhöhte Aktivität (via 35S Promoter) von AtHaspin resultiert in pleiotrophe Phänotypen, welche durch fehlerhafte Entwicklung der Blüte und des vaskulären Systems gekennzeichnet sind. Weiterhin wurde eine reduzierte Fertilität, der Verlust der apikalen Dominanz, zusätzliche Sprosse und Blattrosetten beobachtet. Dieser Phänotyp zeigt eine gewisse Ähnlichkeit zu Pflanzen mit Defekten in Genen, welche Sprossmeristeme und/oder den Transport von Auxin regulieren.

Promoter$_{AtHaspin}$::GUS-Signale wurden hauptsächliche in teilungsaktiven und sich differenzierenden Geweben wie, Sproßapikalmeristemen, Blütenknospen und jungen Embryonen nachgewiesen. Schwächere GUS-Signale zeigte das vaskuläre System junger Blätter und Blüten. Eine ähnliche Verteilung wurde für 35S::YFP-AtHaspin-Signale nachgewiesen. Auf subzellulärer Ebene zeigte das Cytoplasma YFP-AtHaspin-Signale.

Um eine funktionelle Verbindung zwischen der Phosphorylierung von Histon H3 an der Position Threonin 3 und der Aktivität von AtHaspin zu detektieren, wurden teilungsaktive Zellen von *A. thaliana* Pflanzen mit veränderter AtHaspin-Aktivität (RNAi und Überexpression) mit Hilfe der indirekten Immunofärbung unter Nutzung eines Histon H3Thr3phos-spezifischen Antikörper untersucht.

Überexpression von AtHaspin veränderte nicht die zellteilungs-abhängige Verteilung von Histon H3Thr3ph. Dagegen zeigten AtHaspin-RNAi-Pflanzen eine reduzierte Histonphosphorylierung. Somit gibt es einen indirekten Hinweis, dass AtHaspin an der zellteilungs-abhängigen Histon H3Thr3 Phosphorylierung beteiligt ist.

Basierend auf den Beobachtungen wird postuliert, dass neben der Phosphorylierung von Histon H3Thr3, AtHaspin auch mit Proteinen direkt oder indirekt interagiert, welche für die Meristementwicklung und/oder den Transport von Hormonen wichtig sind. Unbekannt ist, inwieweit die Phosphorylierung von H3Thr3 direkt an der Meristemregulierung beteiligt ist.

9. Literature

Alberts,B., Johnson, A., Lewis, J., Raff, M., Roberts, K., Walter, P. (2002). Molecular Biology of the Cell. Book.

Arabidopsis **Genome Initiative.,** (2000). Analysis of the genome sequence of the flowering plant *Arabidopsis thaliana*. Nature 408, 796-815.

Alexander, M.P. (1969). Differential staining of aborted and nonaborted pollen. Stain technology 44, 117-122.

Alonso, J.M., Stepanova, A.N., Leisse, T.J., Kim, C.J., Chen, H., Shinn, P., Stevenson, D.K., Zimmerman, J., Barajas, P., Cheuk, R., Gadrinab, C., Heller, C., Jeske, A., Koesema, E., Meyers, C.C., Parker, H., Prednis, L., Ansari, Y., Choy, N., Deen, H., Geralt, M., Hazari, N., Hom, E., Karnes, M., Mulholland, C., Ndubaku, R., Schmidt, I., Guzman, P., Aguilar-Henonin, L., Schmid, M., Weigel, D., Carter, D.E., Marchand, T., Risseeuw, E., Brogden, D., Zeko, A., Crosby, W.L., Berry, C.C., and Ecker, J.R. (2003). Genome-wide insertional mutagenesis of *Arabidopsis thaliana*. Science 301, 653-657.

Altamura, M.M., Archilletti, T., Capone, I., and Costantino, P. (1991). Histological Analysis of the Expression of Agrobacterium-Rhizogenes Rolb-Gus Gene Fusions in Transgenic Tobacco. New Phytologist 118, 69-78.

Altamura, M.M., Capitani, F., Gazza, L., Capone, I., and Costantino, P. (1994). The Plant Oncogene Rolb Stimulates the Formation of Flower and Root Meristemoids in Tobacco Thin Cell-Layers. New Phytologist 126, 283-293.

Armisen, D., Lecharny, A., and Aubourg, S. (2008). Unique genes in plants: specificities and conserved features throughout evolution. BMC evolutionary biology 8, 280.

Bailey, T.L., Williams, N., Misleh, C., and Li, W.W. (2006). MEME: discovering and analyzing DNA and protein sequence motifs. Nucleic Acids Res 34, W369-373.

Baumann, K., De Paolis, A., Costantino, P., and Gualberti, G. (1999). The DNA binding site of the Dof protein NtBBF1 is essential for tissue-specific and auxin-regulated expression of the rolB oncogene in plants. Plant Cell 11, 323-334.

Becher, M., Talke, I.N., Krall, L., and Kramer, U. (2004). Cross-species microarray transcript profiling reveals high constitutive expression of metal homeostasis genes in shoots of the zinc hyperaccumulator *Arabidopsis halleri*. Plant J 37, 251-268.

Benjamins, R., Quint, A., Weijers, D., Hooykaas, P., and Offringa, R. (2001). The *PINOID* protein kinase regulates organ development in *Arabidopsis* by enhancing polar auxin transport. Development 128, 4057-4067.

Bennett, S., ALVAREZ, J., BOSSINGER, G., and SMYTH, D. (1995). Morphogenesis in *PINOID* mutants of *Arabidopsis thaliana*. Plant J 8, 505-520.

Bennett, T., Sieberer, T., Willett, B., Booker, J., Luschnig, C., and Leyser, O. (2006). The *Arabidopsis MAX* pathway controls shoot branching by regulating auxin transport. Curr Biol 16, 553-563.

Birchler, J.A., and Veitia, R.A. (2007). The gene balance hypothesis: from classical genetics to modern genomics. The Plant cell 19, 395-402.

Birchler, J.A., Bhadra, U., Bhadra, M.P., and Auger, D.L. (2001). Dosage-dependent gene regulation in multicellular eukaryotes: implications for dosage compensation, aneuploid syndromes, and quantitative traits. Developmental biology 234, 275-288.

Blanc, G., Barakat, A., Guyot, R., Cooke, R., and Delseny, M. (2000). Extensive duplication and reshuffling in the Arabidopsis genome. Plant Cell 12, 1093-1101.

Bottomley, M.J. (2004). Structures of protein domains that create or recognize histone modifications. EMBO Rep 5, 464-469.

Brownell, J.E., Zhou, J., Ranalli, T., Kobayashi, R., Edmondson, D.G., Roth, S.Y., and Allis, C.D. (1996). Tetrahymena histone acetyltransferase A: a homolog to yeast Gcn5p linking histone acetylation to gene activation. Cell 84, 843-851.

Burkhard, P., Stetefeld, J., and Strelkov, S.V. (2001). Coiled coils: a highly versatile protein folding motif. Trends in cell biology 11, 82-88.

Caperta, A.D., Rosa, M., Delgado, M., Karimi, R., Demidov, D., Viegas, W., and Houben, A. (2008). Distribution patterns of phosphorylated Thr 3 and Thr 32 of histone H3 in plant mitosis and meiosis. Cytogenet Genome Res 122, 73-79.

Capone, I., Cardarelli, M., Mariotti, D., Pomponi, M., De Paolis, A., and Costantino, P. (1991). Different promoter regions control level and tissue specificity of expression of Agrobacterium rhizogenes rolB gene in plants. Plant molecular biology 16, 427-436.

Carmel, L., Rogozin, I.B., Wolf, Y.I., and Koonin, E.V. (2007). Evolutionarily conserved genes preferentially accumulate introns. Genome Res 17, 1045-1050.

Carmena, M., and Earnshaw, W.C. (2003). The cellular geography of aurora kinases. Nat Rev Mol Cell Biol 4, 842-854.

Casas-Mollano, J.A., Jeong, B.R., Xu, J., Moriyama, H., and Cerutti, H. (2008). The MUT9p kinase phosphorylates histone H3 threonine 3 and is necessary for heritable epigenetic silencing in Chlamydomonas. Proc Natl Acad Sci U S A 105, 6486-6491.

Cheung, P., Allis, C.D., and Sassone-Corsi, P. (2000). Signaling to chromatin through histone modifications. Cell 103, 263-271.

Cho, R.J., Campbell, M.J., Winzeler, E.A., Steinmetz, L., Conway, A., Wodicka, L., Wolfsberg, T.G., Gabrielian, A.E., Landsman, D., Lockhart, D.J., and Davis, R.W. (1998). A genome-wide transcriptional analysis of the mitotic cell cycle. Mol Cell 2, 65-73.

Chomczynski, P., and Mackey, K. (1995). Short technical reports. Modification of the TRI reagent procedure for isolation of RNA from polysaccharide- and proteoglycan-rich sources. Biotechniques 19, 942-945.

Christensen, S.K., Dagenais, N., Chory, J., and Weigel, D. (2000). Regulation of auxin response by the protein kinase *PINOID*. Cell 100, 469-478.

Chuck, G., Lincoln, C., and Hake, S. (1996). *KNAT1* induces lobed leaves with ectopic meristems when overexpressed in *Arabidopsis*. Plant Cell 8, 1277-1289.

Clark, S.E., Jacobsen, S.E., Levin, J.Z., and Meyerowitz, E.M. (1996). The *CLAVATA* and *SHOOT MERISTEMLESS* loci competitively regulate meristem activity in Arabidopsis. Development 122, 1567-1575.

Clough, S.J., and Bent, A.F. (1998). Floral dip: a simplified method for *Agrobacterium*-mediated transformation of *Arabidopsis thaliana*. Plant J 16, 735-743.

Cloutier, M., Vigneault, F., Lachance, D., and Seguin, A. (2005). Characterization of a poplar NIMA-related kinase PNek1 and its potential role in meristematic activity. FEBS letters 579, 4659-4665.

Colbert, T., Till, B.J., Tompa, R., Reynolds, S., Steine, M.N., Yeung, A.T., McCallum, C.M., Comai, L., and Henikoff, S. (2001). High-throughput screening for induced point mutations. Plant Physiology 126, 480-484.

Crosio, C., Fimia, G.M., Loury, R., Kimura, M., Okano, Y., Zhou, H., Sen, S., Allis, C.D., and Sassone-Corsi, P. (2002). Mitotic phosphorylation of histone H3: spatio-temporal regulation by mammalian Aurora kinases. Mol Cell Biol 22, 874-885.

Curtis, M.D., and Grossniklaus, U. (2003). A gateway cloning vector set for high-throughput functional analysis of genes in planta. Plant Physiol 133, 462-469.

Dai, J., and Higgins, J.M. (2005). Haspin: a mitotic histone kinase required for metaphase chromosome alignment. Cell Cycle 4, 665-668.

Dai, J., Sullivan, B.A., and Higgins, J.M. (2006). Regulation of mitotic chromosome cohesion by Haspin and Aurora B. Dev Cell 11, 741-750.

Dai, J., Sultan, S., Taylor, S.S., and Higgins, J.M. (2005). The kinase haspin is required for mitotic histone H3 Thr 3 phosphorylation and normal metaphase chromosome alignment. Genes Dev 19, 472-488.

De Souza, C.P., Osmani, A.H., Wu, L.P., Spotts, J.L., and Osmani, S.A. (2000). Mitotic histone H3 phosphorylation by the NIMA kinase in *Aspergillus nidulans*. Cell 102, 293-302.

Demidov, D., Van Damme, D., Geelen, D., Blattner, F.R., and Houben, A. (2005). Identification and dynamics of two classes of aurora-like kinases in *Arabidopsis* and other plants. Plant Cell 17, 836-848.

Demidov, D., Hesse, S., Tewes, A., Rutten, T., Fuchs, J., Karimi Ashtiyani, R., Lein, S., Fischer, A., Reuter, G., Houben, A. 2009 (in press). Aurora1 phosphorylation activity on histone H3 and its cross talk with other post-translational histone modifications in *Arabidopsis*

Earley, K.W., Haag, J.R., Pontes, O., Opper, K., Juehne, T., Song, K., and Pikaard, C.S. (2006). Gateway-compatible vectors for plant functional genomics and proteomics. Plant J 45, 616-629.

Elgin, S.C., and Workman, J.L. (2002). Chromosome and expression mechanisms: a year dominated by histone modifications, transitory and remembered. Curr Opin Genet Dev 12, 127-129.

Endrizzi, K., Moussian, B., Haecker, A., Levin, J.Z., and Laux, T. (1996). The *SHOOT MERISTEMLESS* gene is required for maintenance of undifferentiated cells in Arabidopsis shoot and floral meristems and acts at a different regulatory level than the meristem genes *WUSCHEL* and *ZWILLE*. Plant J 10, 967-979.

Felsenfeld, G., and Groudine, M. (2003). Controlling the double helix. Nature 421, 448-453.

Ferrari, S. (2006). Protein kinases controlling the onset of mitosis. Cell Mol Life Sci.

Fischle, W., Wang, Y., and Allis, C.D. (2003). Histone and chromatin cross-talk. Curr Opin Cell Biol 15, 172-183.

Fletcher, J.C. (2002). Shoot and floral meristem maintenance in *Arabidopsis*. Annu Rev Plant Biol 53, 45-66.

Foster, R., Izawa, T., and Chua, N. (1994). Plant bZIP proteins gather at ACGT elements. Faseb J 8, 192-200.

Fry, A.M. (2002). The Nek2 protein kinase: a novel regulator of centrosome structure. Oncogene 21, 6184-6194.

Fuchs, J., Demidov, D., Houben, A., and Schubert, I. (2006). Chromosomal histone modification patterns - from conservation to diversity. Trends Plant Sci.

Fukuda, H. (2004). Signals that control plant vascular cell differentiation. Nat Rev Mol Cell Biol 5, 379-391.

Galweiler, L., Guan, C., Muller, A., Wisman, E., Mendgen, K., Yephremov, A., and Palme, K. (1998). Regulation of polar auxin transport by AtPIN1 in *Arabidopsis* vascular tissue. Science 282, 2226-2230.

Gernand, D., Demidov, D., and Houben, A. (2003). The temporal and spatial pattern of histone H3 phosphorylation at serine 28 and serine 10 is similar in plants but differs between mono- and polycentric chromosomes. Cytogenet Genome Res 101, 172-176.

Giet, R., and Glover, D.M. (2001). Drosophila aurora B kinase is required for histone H3 phosphorylation and condensin recruitment during chromosome condensation and to organize the central spindle during cytokinesis. J Cell Biol 152, 669-682.

Goto, H., Yasui, Y., Nigg, E.A., and Inagaki, M. (2002). Aurora-B phosphorylates Histone H3 at serine28 with regard to the mitotic chromosome condensation. Genes Cells 7, 11-17.

Goto, H., Tomono, Y., Ajiro, K., Kosako, H., Fujita, M., Sakurai, M., Okawa, K., Iwamatsu, A., Okigaki, T., Takahashi, T., and Inagaki, M. (1999). Identification of a novel phosphorylation site on histone H3 coupled with mitotic chromosome condensation. J Biol Chem 274, 25543-25549.

Grant, P.A. (2001). A tale of histone modifications. Genome Biol 2, REVIEWS0003.

Grunstein, M. (1997). Histone acetylation in chromatin structure and transcription. Nature 389, 349-352.

Gurley, L.R., Walters, R.A., and Tobey, R.A. (1975). Sequential phsophorylation of histone subfractions in the Chinese hamster cell cycle. J Biol Chem 250, 3936-3944.

Gurley, L.R., D'Anna, J.A., Barham, S.S., Deaven, L.L., and Tobey, R.A. (1978). Histone phosphorylation and chromatin structure during mitosis in Chinese hamster cells. Eur J Biochem 84, 1-15.

Gurtley, L.R., Walters, R.A., and Tobey, R.A. (1975). Sequential phosphorylation of histone subfractions in the Chinese hamster cell cycle. J Biol Chem 250, 3936-3944.

Haerizadeh, F., Wong, C.E., Singh, M.B., and Bhalla, P.L. (2009). Genome-wide analysis of gene expression in soybean shoot apical meristem. Plant Mol Biol 69, 711-727.

Hagen, G., and Guilfoyle, T. (2002). Auxin-responsive gene expression: genes, promoters and regulatory factors. Plant Mol Biol 49, 373-385.

Hanks, S.K. (2003). Genomic analysis of the eukaryotic protein kinase superfamily: a perspective. Genome Biol 4, 111.

Hanks, S.K., and Quinn, A.M. (1991). Protein kinase catalytic domain sequence database: identification of conserved features of primary structure and classification of family members. Methods in enzymology 200, 38-62.

Hanks, S.K., and Hunter, T. (1995). Protein kinases 6. The eukaryotic protein kinase superfamily: kinase (catalytic) domain structure and classification. Faseb J 9, 576-596.

Hans, F., and Dimitrov, S. (2001). Histone H3 phosphorylation and cell division. Oncogene 20, 3021-3027.

Hauf, S., Cole, R.W., LaTerra, S., Zimmer, C., Schnapp, G., Walter, R., Heckel, A., van Meel, J., Rieder, C.L., and Peters, J.M. (2003). The small molecule Hesperadin reveals a role for Aurora B in correcting kinetochore-microtubule attachment and in maintaining the spindle assembly checkpoint. J Cell Biol 161, 281-294.

Hellens, R., Mullineaux, P., and Klee, H. (2000). Technical Focus:a guide to *Agrobacterium* binary Ti vectors. Trends Plant Sci 5, 446-451.

Hendzel, M.J., Wei, Y., Mancini, M.A., Van Hooser, A., Ranalli, T., Brinkley, B.R., Bazett-Jones, D.P., and Allis, C.D. (1997). Mitosis-specific phosphorylation of histone H3 initiates primarily within pericentromeric heterochromatin during G2 and spreads in an ordered fashion coincident with mitotic chromosome condensation. Chromosoma 106, 348-360.

Higgins, J.M. (2001a). Haspin-like proteins: a new family of evolutionarily conserved putative eukaryotic protein kinases. Protein Sci 10, 1677-1684.

Higgins, J.M. (2001b). The Haspin gene: location in an intron of the integrin alphaE gene, associated transcription of an integrin alphaE-derived RNA and expression in diploid as well as haploid cells. Gene 267, 55-69.

Higgins, J.M. (2003). Structure, function and evolution of haspin and haspin-related proteins, a distinctive group of eukaryotic protein kinases. Cell Mol Life Sci 60, 446-462.

Hilson, P., Allemeersch, J., Altmann, T., Aubourg, S., Avon, A., Beynon, J., Bhalerao, R.P., Bitton, F., Caboche, M., Cannoot, B., Chardakov, V., Cognet-Holliger, C., Colot, V., Crowe, M., Darimont, C., Durinck, S., Eickhoff, H., de Longevialle, A.F., Farmer, E.E., Grant, M., Kuiper, M.T., Lehrach, H., Leon, C., Leyva, A., Lundeberg, J., Lurin, C., Moreau, Y., Nietfeld, W., Paz-Ares, J., Reymond, P., Rouze, P., Sandberg, G., Segura, M.D., Serizet, C., Tabrett, A., Taconnat, L., Thareau, V., Van Hummelen, P., Vercruysse, S., Vuylsteke, M., Weingartner, M., Weisbeek, P.J., Wirta, V., Wittink, F.R., Zabeau, M., and Small, I. (2004). Versatile gene-specific sequence tags for *Arabidopsis* functional genomics: transcript profiling and reverse genetics applications. Genome Res 14, 2176-2189.

Houben, A., Demidov, D., Rutten, T., and Scheidtmann, K.H. (2005). Novel phosphorylation of histone H3 at threonine 11 that temporally correlates with condensation of mitotic and meiotic chromosomes in plant cells. Cytogenet Genome Res 109, 148-155.

Houben, A., Wako, T., Furushima-Shimogawara, R., Presting, G., Kunzel, G., Schubert, I.I., and Fukui, K. (1999). Short communication: the cell cycle dependent phosphorylation of histone H3 is correlated with the condensation of plant mitotic chromosomes. Plant J 18, 675-679.

Hsu, J.Y., Sun, Z.W., Li, X., Reuben, M., Tatchell, K., Bishop, D.K., Grushcow, J.M., Brame, C.J., Caldwell, J.A., Hunt, D.F., Lin, R., Smith, M.M., and Allis, C.D. (2000). Mitotic phosphorylation of histone H3 is governed by Ipl1/aurora kinase and Glc7/PP1 phosphatase in budding yeast and nematodes. Cell 102, 279-291.

Joubes, J., Chevalier, C., Dudits, D., Heberle-Bors, E., Inze, D., Umeda, M., and Renaudin, J.P. (2000). CDK-related protein kinases in plants. Plant Mol Biol 43, 607-620.

Jurgens, G., Mayer, U., Ruiz, R.A.T., Berleth, T., and Misera, S. (1991). Genetic-Analysis of Pattern-Formation in the *Arabidopsis* Embryo. Development, 27-&.

Kaszas, E., and Cande, W. (2000). Phosphorylation of histone H3 is correlated with changes in the maintenance of sister chromatid cohesion during meiosis in maize, rather than the condensation of the chromatin. J Cell Sci 113, 3217-3226.

Katinka, M.D., Duprat, S., Cornillot, E., Metenier, G., Thomarat, F., Prensier, G., Barbe, V., Peyretaillade, E., Brottier, P., Wincker, P., Delbac, F., El Alaoui, H., Peyret, P., Saurin, W., Gouy, M., Weissenbach, J., and Vivares, C.P. (2001). Genome sequence and gene compaction of the eukaryote parasite Encephalitozoon cuniculi. Nature 414, 450-453.

Kawabe, A., Matsunaga, S., Nakagawa, K., Kurihara, D., Yoneda, A., Hasezawa, S., Uchiyama, S., and Fukui, K. (2005). Characterization of plant Aurora kinases during mitosis. Plant Mol Biol 58, 1-13.

Kerstetter, R.A., and Hake, S. (1997). Shoot meristem formation in vegetative development. Plant Cell 9, 1001-1010.

Kondrashov, F.A., Rogozin, I.B., Wolf, Y.I., and Koonin, E.V. (2002). Selection in the evolution of gene duplications. Genome Biol 3, RESEARCH0008.

Kornberg, R.D. (1974). Chromatin structure: a repeating unit of histones and DNA. Science (New York, N.Y 184, 868-871.

Kostich, M., English, J., Madison, V., Gheyas, F., Wang, L., Qiu, P., Greene, J., and Laz, T.M. (2002). Human members of the eukaryotic protein kinase family. Genome Biol 3, RESEARCH0043.

Kurakawa, T., Ueda, N., Maekawa, M., Kobayashi, K., Kojima, M., Nagato, Y., Sakakibara, H., and Kyozuka, J. (2007). Direct control of shoot meristem activity by a cytokinin-activating enzyme. Nature 445, 652-655.

Kurihara, D., Matsunaga, S., Uchiyama, S., and Fukui, K. (2008). Live cell imaging reveals plant aurora kinase has dual roles during mitosis. Plant Cell Physiol 49, 1256-1261.

Kusenda, B., Mraz, M., Mayer, J., and Pospisilova, S. (2006). MicroRNA biogenesis, functionality and cancer relevance. Biomedical papers of the Medical Faculty of the University Palacky, Olomouc, Czechoslovakia 150, 205-215.

Laemmli, U.K. (1970). Cleavage of structural proteins during the assembly of the head of bacteriophage T4. Nature 227, 680-685.

Laux, T., Mayer, K.F., Berger, J., and Jurgens, G. (1996). The *WUSCHEL* gene is required for shoot and floral meristem integrity in Arabidopsis. Development 122, 87-96.

Lehmann, M. (2004). Anything else but GAGA: a nonhistone protein complex reshapes chromatin structure. Trends Genet 20, 15-22.

Leibfried, A., To, J.P., Busch, W., Stehling, S., Kehle, A., Demar, M., Kieber, J.J., and Lohmann, J.U. (2005). *WUSCHEL* controls meristem function by direct regulation of cytokinin-inducible response regulators. Nature 438, 1172-1175.

Leonard, C.J., Aravind, L., and Koonin, E.V. (1998). Novel families of putative protein kinases in bacteria and archaea: evolution of the "eukaryotic" protein kinase superfamily. Genome Res 8, 1038-1047.

Leyser, H.M.O., and Furner, I.J. (1992). Characterization of 3 Shoot Apical Meristem Mutants of *Arabidopsis thaliana*. Development 116, 397-&.

Lincoln, C., Britton, J.H., and Estelle, M. (1990). Growth and development of the axr1 mutants of Arabidopsis. Plant Cell 2, 1071-1080.

Lincoln, C., Long, J., Yamaguchi, J., Serikawa, K., and Hake, S. (1994). A *knotted1*-like homeobox gene in Arabidopsis is expressed in the vegetative meristem and dramatically alters leaf morphology when overexpressed in transgenic plants. Plant Cell 6, 1859-1876.

Liu, J., and Rost, B. (2001). Comparing function and structure between entire proteomes. Protein Sci 10, 1970-1979.

Liu, Z.B., Ulmasov, T., Shi, X.Y., Hagen, G., and Guilfoyle, T.J. (1994). Soybean Gh3 Promoter Contains Multiple Auxin-Inducible Elements. Plant Cell 6, 645-657.

Luger, K., Mader, A.W., Richmond, R.K., Sargent, D.F., and Richmond, T.J. (1997). Crystal structure of the nucleosome core particle at 2.8 A resolution. Nature 389, 251-260.

Mallory, A.C., Elmayan, T., and Vaucheret, H. (2008). MicroRNA maturation and action--the expanding roles of ARGONAUTEs. Curr Opin Plant Biol 11, 560-566.

Manning, G., Plowman, G.D., Hunter, T., and Sudarsanam, S. (2002). Evolution of protein kinase signaling from yeast to man. Trends Biochem Sci 27, 514-520.

Manzanero, S., Arana, P., Puertas, M.J., and Houben, A. (2000). The chromosomal distribution of phosphorylated histone H3 differs between plants and animals at meiosis. Chromosoma 109, 308-317.

Matsui, M., Ichihara, H., Kobayashi, S., Tanaka, H., Tsuchida, J., Nozaki, M., Yoshimura, Y., Nojima, H., Rochelle, J.M., Nishimune, Y., Taketo, M.M., and Seldin, M.F. (1997). Mapping of six germ cell-specific genes to mouse chromosomes. Mammalian Genome 8, 873-874.

McCallum, C.M., Comai, L., Greene, E.A., and Henikoff, S. (2000). Targeting induced local lesions IN genomes (TILLING) for plant functional genomics. Plant physiology 123, 439-442.

Medford, J.I., Behringer, F.J., Callos, J.D., and Feldmann, K.A. (1992). Normal and Abnormal Development in the *Arabidopsis* Vegetative Shoot Apex. Plant Cell 4, 631-643.

Mendenhall, M.D., and Hodge, A.E. (1998). Regulation of Cdc28 cyclin-dependent protein kinase activity during the cell cycle of the yeast Saccharomyces cerevisiae. Microbiol Mol Biol Rev 62, 1191-1243.

Menges, M., Hennig, L., Gruissem, W., and Murray, J.A. (2003). Genome-wide gene expression in an Arabidopsis cell suspension. Plant Mol Biol 53, 423-442.

Mironov, V.V., De Veylder, L., Van Montagu, M., and Inze, D. (1999). Cyclin-dependent kinases and cell division in plants- the nexus. Plant Cell 11, 509-522.

Morgan, D.O. (1997). Cyclin-dependent kinases: engines, clocks, and microprocessors. Annu Rev Cell Dev Biol 13, 261-291.

Motose, H., Tominaga, R., Wada, T., Sugiyama, M., and Watanabe, Y. (2008). A NIMA-related protein kinase suppresses ectopic outgrowth of epidermal cells through its kinase activity and the association with microtubules. Plant J 54, 829-844.

Nespoli, A., Vercillo, R., di Nola, L., Diani, L., Giannattasio, M., Plevani, P., and Muzi-Falconi, M. (2006). Alk1 and Alk2 are two new cell cycle-regulated haspin-like proteins in budding yeast. Cell Cycle 5, 1464-1471.

Nigg, E. (2001). Mitotic kinases as regulators of cell division and its checkpoints. NAT REV MOL CELL BIO 2, 21-32.

Nigg, E.A. (1995). Cyclin-dependent protein kinases: key regulators of the eukaryotic cell cycle. Bioessays 17, 471-480.

O'Connell, M.J., Krien, M.J., and Hunter, T. (2003). Never say never. The NIMA-related protein kinases in mitotic control. Trends Cell Biol 13, 221-228.

Okada, K., Ueda, J., Komaki, M.K., Bell, C.J., and Shimura, Y. (1991). Requirement of the Auxin Polar Transport System in Early Stages of *Arabidopsis* Floral Bud Formation. Plant Cell 3, 677-684.

Okushima, Y., Mitina, I., Quach, H.L., and Theologis, A. (2005). AUXIN RESPONSE FACTOR 2 (ARF2): a pleiotropic developmental regulator. Plant J 43, 29-46.

Ongaro, V., and Leyser, O. (2007). Hormonal control of shoot branching. J Exp Bot.

Osmani, A.H., O'Donnell, K., Pu, R.T., and Osmani, S.A. (1991). Activation of the nimA protein kinase plays a unique role during mitosis that cannot be bypassed by absence of the bimE checkpoint. Embo J 10, 2669-2679.

Osmani, S.A., and Ye, X.S. (1996). Cell cycle regulation in *Aspergillus* by two protein kinases. The Biochemical journal 317 (Pt 3), 633-641.

Paponov, I.A., Teale, W.D., Trebar, M., Blilou, I., and Palme, K. (2005). The PIN auxin efflux facilitators: evolutionary and functional perspectives. Trends Plant Sci 10, 170-177.

Parsons, R.L., Behringer, F.J., and Medford, J.I. (2000). The SCHIZOID gene regulates differentiation and cell division in Arabidopsis thaliana shoots. Planta 211, 34-42.

Peterson, C.L., and Laniel, M.A. (2004). Histones and histone modifications. Curr Biol 14, R546-551.

Polioudaki, H., Markaki, Y., Kourmouli, N., Dialynas, G., Theodoropoulos, P.A., Singh, P.B., and Georgatos, S.D. (2004). Mitotic phosphorylation of histone H3 at threonine 3. FEBS Lett 560, 39-44.

Preuss, U., Landsberg, G., and Scheidtmann, K.H. (2003). Novel mitosis-specific phosphorylation of histone H3 at Thr11 mediated by Dlk/ZIP kinase. Nucleic Acids Res 31, 878-885.

Prigent, C., and Dimitrov, S. (2003). Phosphorylation of serine 10 in histone H3, what for? J Cell Sci 116, 3677-3685.

Ramadevi, N., Rodriguez, J., and Roy, P. (1998). A leucine zipper-like domain is essential for dimerization and encapsidation of bluetongue virus nucleocapsid protein VP4. Journal of Virology 72, 2983-2990.

Reintanz, B., Lehnen, M., Reichelt, M., Gershenzon, J., Kowalczyk, M., Sandberg, G., Godde, M., Uhl, R., and Palme, K. (2001). Bus, a bushy *A*rabidopsis CYP79F1 knockout mutant with abolished synthesis of short-chain aliphatic glucosinolates. Plant Cell 13, 351-367.

Renaudin, J.P., Doonan, J.H., Freeman, D., Hashimoto, J., Hirt, H., Inze, D., Jacobs, T., Kouchi, H., Rouze, P., Sauter, M., Savoure, A., Sorrell, D.A., Sundaresan, V., and Murray, J.A. (1996). Plant cyclins: a unified nomenclature for plant A-, B- and D-type cyclins based on sequence organization. Plant molecular biology 32, 1003-1018.

Richards, E.J., and Elgin, S.C. (2002). Epigenetic codes for heterochromatin formation and silencing: rounding up the usual suspects. Cell 108, 489-500.

Rosasco-Nitcher, S.E., Lan, W., Khorasanizadeh, S., and Stukenberg, P.T. (2008). Centromeric Aurora-B activation requires TD-60, microtubules, and substrate priming phosphorylation. Science 319, 469-472.

Rose, A., Manikantan, S., Schraegle, S.J., Maloy, M.A., Stahlberg, E.A., and Meier, I. (2004). Genome-wide identification of *Arabidopsis* coiled-coil proteins and establishment of the ARABI-COIL database. Plant Physiol 134, 927-939.

Rosso, M.G., Li, Y., Strizhov, N., Reiss, B., Dekker, K., and Weisshaar, B. (2003). An Arabidopsis thaliana T-DNA mutagenized population (GABI-Kat) for flanking sequence tag-based reverse genetics. Plant Mol Biol 53, 247-259.

Sakai, T., Honing, H., Nishioka, M., Uehara, Y., Takahashi, M., Fujisawa, N., Saji, K., Seki, M., Shinozaki, K., Jones, M.A., Smirnoff, N., Okada, K., and Wasteneys, G.O. (2008). Armadillo repeat-containing kinesins and a NIMA-related kinase are required for epidermal-cell morphogenesis in *Arabidopsis*. Plant J 53, 157-171.

Sambrook J., Russell, D.W., (2001). Molecular cloning: a laboratory manual. Cold Spring Harbor Laborator press.

Sangwan, I., and O'Brian, M.R. (2002). Identification of a soybean protein that interacts with GAGA element dinucleotide repeat DNA. Plant Physiol 129, 1788-1794.

Santi, L., Wang, Y., Stile, M.R., Berendzen, K., Wanke, D., Roig, C., Pozzi, C., Muller, K., Muller, J., Rohde, W., and Salamini, F. (2003). The GA octodinucleotide repeat binding factor BBR participates in the transcriptional regulation of the homeobox gene Bkn3. Plant J 34, 813-826.

Shahmuradov, I.A., Solovyev, V.V., and Gammerman, A.J. (2005). Plant promoter prediction with confidence estimation. Nucleic Acids Res 33, 1069-1076.

Shaul, O., Mironov, V., Burssens, S., Van Montagu, M., and Inze, D. (1996). Two Arabidopsis cyclin promoters mediate distinctive transcriptional oscillation in synchronized tobacco BY-2 cells. Proc Natl Acad Sci U S A 93, 4868-4872.

Shimizu-Sato, S., Tanaka, M., and Mori, H. (2009). Auxin-cytokinin interactions in the control of shoot branching. Plant Mol Biol 69, 429-435.

Sinha, N.R., Williams, R.E., and Hake, S. (1993). Overexpression of the maize homeo box gene, *KNOTTED*-1, causes a switch from determinate to indeterminate cell fates. Genes Dev 7, 787-795.

Slade, A.J., and Knauf, V.C. (2005). TILLING moves beyond functional genomics into crop improvement. Transgenic research 14, 109-115.

Smale, S.T., and Kadonaga, J.T. (2003). The RNA polymerase II core promoter. Annual review of biochemistry 72, 449-479.

Sorefan, K., Booker, J., Haurogne, K., Goussot, M., Bainbridge, K., Foo, E., Chatfield, S., Ward, S., Beveridge, C., Rameau, C., and Leyser, O. (2003). MAX4 and RMS1 are orthologous dioxygenase-like genes that regulate shoot branching in *Arabidopsis* and pea. Genes & Development 17, 1469-1474.

Souza, E.D. (2006). Eigenes Protokoll statt DNA-Kit. Protokoll für die Extraktion von DNA aus Blättern. Laborjournal 7, 58.

Spellman, P.T., Sherlock, G., Zhang, M.Q., Iyer, V.R., Anders, K., Eisen, M.B., Brown, P.O., Botstein, D., and Futcher, B. (1998). Comprehensive identification of cell cycle-regulated genes of the yeast Saccharomyces cerevisiae by microarray hybridization. Mol Biol Cell 9, 3273-3297.

Stirnberg, P., Chatfield, S.P., and Leyser, H.M.O. (1999). *AXR1* acts after lateral bud formation to inhibit lateral bud growth in Arabidopsis. Plant Physiology 121, 839-847.

Stirnberg, P., van De Sande, K., and Leyser, H.M. (2002). *MAX1* and *MAX2* control shoot lateral branching in Arabidopsis. Development 129, 1131-1141.

Tanaka, H., Iguchi, N., Nakamura, Y., Kohroki, J., de Carvalho, C.E., and Nishimune, Y. (2001). Cloning and characterization of human haspin gene encoding haploid germ cell-specific nuclear protein kinase. Mol Hum Reprod 7, 211-218.

Tanaka, H., Yoshimura, Y., Nozaki, M., Yomogida, K., Tsuchida, J., Tosaka, Y., Habu, T., Nakanishi, T., Okada, M., Nojima, H., and Nishimune, Y. (1999). Identification and characterization of a haploid germ cell-specific nuclear protein kinase (Haspin) in spermatid nuclei and its effects on somatic cells. The Journal of biological chemistry 274, 17049-17057.

Tanaka, H., Y. Yoshimura, et al. (1999). "Identification and characterization of a haploid germ cell-specific nuclear protein kinase (Haspin) in spermatid nuclei and its effects on somatic cells." J Biol Chem 274(24): 17049-57.

Ulmasov, T., Murfett, J., Hagen, G., and Guilfoyle, T.J. (1997). Aux/IAA proteins repress expression of reporter genes containing natural and highly active synthetic auxin response elements. Plant Cell 9, 1963-1971.

Umemura, Y., Ishiduka, T., Yamamoto, R., and Esaka, M. (2004). The Dof domain, a zinc finger DNA-binding domain conserved only in higher plants, truly functions as a Cys2/Cys2 Zn finger domain. Plant J 37, 741-749.

Van Hooser, A., Goodrich, D.W., Allis, C.D., Brinkley, B.R., and Mancini, M.A. (1998). Histone H3 phosphorylation is required for the initiation, but not maintenance, of mammalian chromosome condensation. J Cell Sci 111 (Pt 23), 3497-3506.

Veit, B. (2009). Hormone mediated regulation of the shoot apical meristem. Plant Mol Biol 69, 397-408.

Vigneault, F., Lachance, D., Cloutier, M., Pelletier, G., Levasseur, C., and Seguin, A. (2007). Members of the plant NIMA-related kinases are involved in organ development and vascularization in poplar, *Arabidopsis* and rice. Plant J 51, 575-588.

Wang, D., Harper, J.F., and Gribskov, M. (2003). Systematic trans-genomic comparison of protein kinases between *Arabidopsis* and *Saccharomyces cerevisiae*. Plant Physiol 132, 2152-2165.

Wu, J., and Grunstein, M. (2000). 25 years after the nucleosome model: chromatin modifications. Trends Biochem Sci 25, 619-623.

Yamada, K., Lim, J., Dale, J.M., Chen, H., Shinn, P., Palm, C.J., Southwick, A.M., Wu, H.C., Kim, C., Nguyen, M., Pham, P., Cheuk, R., Karlin-Newmann, G., Liu, S.X., Lam, B., Sakano, H., Wu, T., Yu, G., Miranda, M., Quach, H.L., Tripp, M., Chang, C.H., Lee, J.M., Toriumi, M., Chan, M.M., Tang, C.C., Onodera, C.S., Deng, J.M., Akiyama, K., Ansari, Y., Arakawa, T., Banh, J., Banno, F., Bowser, L., Brooks, S., Carninci, P., Chao, Q., Choy, N., Enju, A., Goldsmith, A.D., Gurjal, M., Hansen, N.F., Hayashizaki, Y., Johnson-Hopson, C., Hsuan, V.W., Iida, K., Karnes, M., Khan, S., Koesema, E., Ishida, J., Jiang, P.X., Jones, T., Kawai, J., Kamiya, A., Meyers, C., Nakajima, M., Narusaka, M., Seki, M., Sakurai, T., Satou, M., Tamse, R., Vaysberg, M., Wallender, E.K., Wong, C., Yamamura, Y., Yuan, S., Shinozaki, K., Davis, R.W., Theologis, A., and Ecker, J.R. (2003). Empirical analysis of transcriptional activity in the *Arabidopsis* genome. Science 302, 842-846.

Yanagisawa, S. (2001). The transcriptional activation domain of the plant-specific Dof1 factor functions in plant, animal, and yeast cells. Plant Cell Physiol 42, 813-822.

Ye, X.S., Xu, G., Pu, R.T., Fincher, R.R., McGuire, S.L., Osmani, A.H., and Osmani, S.A. (1995). The NIMA protein kinase is hyperphosphorylated and activated downstream of p34cdc2/cyclin B: coordination of two mitosis promoting kinases. The EMBO journal 14, 986-994.

Yoshimura, Y., Tanaka, H., Nozaki, M., Yomogida, K., Yasunaga, T., and Nishimune, Y. (2001). Nested genomic structure of haploid germ cell specific haspin gene. Gene 267, 49-54.

Zeitlin, S.G., Shelby, R.D., and Sullivan, K.F. (2001). CENP-A is phosphorylated by Aurora B kinase and plays an unexpected role in completion of cytokinesis. J Cell Biol 155, 1147-1157.

Zhang, J.Z. (2003). Evolution by gene duplication: an update. Trends in Ecology & Evolution 18, 292-298.

Zhang, Y., and Reinberg, D. (2001). Transcription regulation by histone methylation: interplay between different covalent modifications of the core histone tails. Genes Dev 15, 2343-2360.

Zhou, D.X. (1999). Regulatory mechanism of plant gene transcription by GT-elements and GT-factors. Trends Plant Sci 4, 210-214.

Publications in connection with the submitted dissertation

Houben, A., Demidov, D., Caperta, A.D., Karimi, R., Agueci, F., and Vlasenko, L. (2007). Phosphorylation of histone H3 in plants-A dynamic affair. Biochim Biophys Acta.

Caperta, A.D., Rosa, M., Delgado, M., Karimi, R., Demidov, D., Viegas, W., and Houben, A. (2008). Distribution patterns of phosphorylated Thr 3 and Thr 32 of histone H3 in plant mitosis and meiosis. Cytogenet Genome Res **122,** 73-79.

Demidov, D., Hesse, S., Tewes, A., Rutten, T., Fuchs, J., Karimi Ashtiyani, R., Lein, S., Fischer, A., Reuter, G., Houben, A (in press). Aurora1 phosphorylation activity on histone H3 and its cross talk with other post-translational histone modifications in Arabidopsis

Frau Raheleh Karimi Ashtiyani

Corrensstraße 3

06466 Gatersleben

Eidesstattliche Erklärung

Hiermit erkläre ich, dass diese Arbeit von mir bisher weder der Mathematisch-Naturwissenschaftlich-Technischen Fakultät der Martin-Luther-Universität Halle-Wittenberg noch einer anderen wissenschaftlichen Einrichtung zum Zweck der Promotion eingereicht wurde.

Ich erkläre ferner, dass ich diese Arbeit selbständig und nur unter Zuhilfenahme der angegebenen Hilfsmittel und Literatur angefertigt habe.

Gatersleben, den ....   _____

                                                 Raheleh Karimi Ashtiyani

CURRICULUM VITAE

Name   Raheleh Karimi Ashtiyani
Birth   16 / 09 / 1979 in Tehran, Iran
Nationality   Iranian
Marital Status   Married
Contact information   "Chromosome structure and function" group
                                Institute of Plant Genetics and Crop Plant Research (IPK)
                                Corrensstraße 3
                                06466 Gatersleben, Germany
                                phone: 0049 (0) 39482 5477
                                FAX: 0049 (0) 39482 5137
                                e-mail: karimi@ipk-gatersleben.de

ACADEMIC QUALIFICATIONS

2002-2004   **M.Sc. in Agricutural Engineering-plants breeding**, Razi University, Iran.

1997-2001   **B.Sc. in Agricultural Engineering-Agronomy and plants breeding,** Tehran University, Iran

1993–1997   **Diploma** of theoretical secondary education studies, Tehran, Iran

EMPLOYMENT HISTORY / RESEARCH EXPERIENCE

Since January 2006   PhD. Student, Chromosome Structure and Function group, Department of Cytogenetic, Institute of Plant Genetics and Crop Plant Research (IPK), Germany, Supervisor Dr. A. Houben

2004 –2006   Junior Scientist, Laboratory of Physiology and Proteomics, ABRII, Iran. Research topic: "Identification of salt responsive proteins in rice anther and ovary". Supervisor Dr. Gh. Hosseini Salekdeh

2002 – 2004   M. Sc. research work in the Lab of Physiology and Proteomics, ABRII, Iran. Research topic: "Leaves and roots proteome analysis of Durum wheat under salt stress". Supervisor Dr. Gh. Hosseini Salekdeh